



ΕΘΝΙΚΟ ΜΕΤΣΟΒΙΟ ΠΟΛΥΤΕΧΝΕΙΟ

Εργαστήριο Ατμοκινητήρων & Λεβήτων

Τομέας Θερμότητας της Σχολής Μηχανολόγων Μηχανικών

ΔΙΠΛΩΜΑΤΙΚΗ ΕΡΓΑΣΙΑ

«Modeling of a combined heat and power plant unit fueled with biomass for coupling with an aluminum production process»

Του Φοιτητή

Χυσέني Σαντίκ

Επιβλέπων

Καρέλλας Σωτήριος, Αναπληρωτής Καθηγητής,
Σχολή Μηχανολόγων Μηχανικών, ΕΜΠ

Αθήνα, Οκτώβριος 2017

Ευχαριστίες

Αρχικά, θα ήθελα να ευχαριστήσω τον επιβλέποντα καθηγητή μου κύριο Σωτήριο Καρέλλα για την εμπιστοσύνη του και για την ευκαιρία που μου έδωσε να ασχοληθώ με ένα πολύ ενδιαφέρον θέμα, καθώς και για την καθοδήγησή του σε όλη τη διάρκεια της εκπόνησης της εργασίας. Επίσης, θα ήθελα να ευχαριστήσω τον Δημήτριο Γκριμέκη και τον κύριο Άγγελο Δουκέλη, για τις χρήσιμες υποδείξεις και την βοήθειά τους καθ' όλη τη διάρκεια της εργασίας. Τέλος, θα ήθελα να ευχαριστήσω την οικογένειά μου και τους φίλους μου για τη στήριξη σε όλο το διάστημα εκπόνησης της εργασίας και γενικότερα σε όλη τη διάρκεια των σπουδών μου.

Abstract

In this thesis, the importance of biomass as a renewable fuel was presented, together with processes which promote the use of biomass fuels in Combined Heat and Power plants, as well as the upgrade, in terms of chemical and thermodynamic properties, these processes offer.

In the first chapter, the use of biomass, globally, as well as in the European region is presented. The use of biomass is an inseparable part of heat and power generation for the European Union and its efforts to reduce the Green House Gas Emissions. In this chapter some typical and some rather peculiar types of biomass are presented, as well as three pretreatment technologies applied for the quality improvement of biomass fuels.

In the second chapter, various steam cycles are presented, together with various boiler technologies, some of which are state of the art. Following the presentation of the steam cycles and the boiler technologies, the different types of real time control on different components of the cycle are shown. In further note, three commercial softwares are and their equations for the simulation of steam cycles are presented. Lastly, the model created in the commercial software named GateCycle, of the combined cycle power plant coupled with the Aluminum plant is explained.

In the third chapter, the modified biomass fueled cogeneration power plant is presented and explained, together with all of the GateCycle components that are used for the modelling of the plant. Following, the inputs of all the case studies regarding the heat, full and part loads, of the combined heat and power plant are presented, along with the results of these case studies, showed in the form of tables and charts.

In the fourth chapter, the improved combined heat and power plant is presented, in which the case studies comprise of the four different biomass fuels and the operating pressure and live steam temperature. In this chapter, the variation of the electrical and overall energetic and exergetic efficiencies depending on the temperature and the operating pressure of the steam are presented, as well as a comparison of the four biomass fuels, dried and pretreated. In addition, the cooling capacity of the improved plans are presented, together with part load operation of the power plant with the best fuel.

Finally, in chapter five, the conclusions of this study are summarized, including some ideas for further study.

Περίληψη

Σε αυτή τη διπλωματική, παρουσιάζεται σημασία της βιομάζας ως ανανεώσιμη πηγή ενέργειας, οι διαδικασίες οι οποίες προάγουν την χρήση βιομάζας σε μονάδες συμπαραγωγής, όπως επίσης την αναβάθμιση σε χημικές και θερμοδυναμικές ιδιότητες αυτές οι διαδικασίες προσφέρουν.

Στο πρώτο κεφάλαιο, είναι παρουσιάζεται η χρήση της βιομάζας σε παγκόσμιο αλλά και ευρωπαϊκό επίπεδο. Η χρήση της βιομάζας είναι άρρηκτα συνδεδεμένη με την παραγωγή θερμότητας και ηλεκτρικής ενέργειας της Ευρωπαϊκής Ένωσης, στην προσπάθειά της να ελαττώσει την εκπομπή ρύπων που επιβαρύνουν το φαινόμενο του θερμοκηπίου. Σε αυτό το κεφάλαιο παρουσιάζονται κάποιες χαρακτηριστικές αλλά και ιδιαίτερες μορφές βιομάζας, καθώς και τρεις τρόποι προεπεξεργασίας που χρησιμοποιούνται για την βελτίωση των χαρακτηριστικών των καυσίμων βιομάζας.

Στο δεύτερο κεφάλαιο, παρουσιάζονται διάφοροι κύκλοι ατμού, μαζί με ποικίλες τεχνολογίες λέβητα, κάποιες από τις οποίες είναι οι πλέον σύγχρονες. Στην συνέχεια απεικονίζονται διάφοροι τύποι ελέγχου σε διαφορετικά κομμάτια των κύκλων. Έπειτα παρουσιάζονται τρία εμπορικά λογισμικά και οι εξισώσεις που χρησιμοποιούν για την προσομοίωση των κύκλων ατμών. Τέλος, αναλύεται το μοντέλο συνδυασμένου κύκλου που συνεργάζεται με τον Αλουμίνιο Ελλάδος, που κατασκευάστηκε στο εμπορικό λογισμικό GateCycle.

Στο τρίτο κεφάλαιο, παρουσιάζεται και αναλύεται το τροποποιημένο μοντέλο συμπαραγωγής με βιομάζα, μαζί με όλα τα εξαρτήματα του GateCycle που χρησιμοποιούνται για τον σχεδιασμό του μοντέλου. Στην συνέχεια, παρουσιάζονται οι παραδοχές που έγιναν για τις προσομοιώσεις, οι οποίες αφορούν την το ολικό και το μερικό φορτίο του μοντέλου συμπαραγωγής, μαζί με τα αποτελέσματα αυτών των προσομοιώσεων, που απεικονίζονται με την μορφή πινάκων και διαγραμμάτων.

Στο τέταρτο κεφάλαιο, παρουσιάζεται το βελτιωμένο μοντέλο συμπαραγωγής, στο οποίο οι προσομοιώσεις γίνονται με τέσσερα διαφορετικά καύσιμα βιομάζας, διάφορες πιέσεις λειτουργίας και θερμοκρασίες ατμού. Σε αυτό το κεφάλαιο, παρουσιάζεται η μεταβολή των ηλεκτρικών και ολικών ενεργειακών και εξεργειακών βαθμών απόδοσης ανάλογα με την θερμοκρασία και την πίεση λειτουργίας, καθώς και η σύγκριση των τεσσάρων καυσίμων βιομάζας, ξηρών και προεπεξεργασμένων. Επιπλέον, παρουσιάζεται η ψυκτική ικανότητα των βελτιωμένων μοντέλων, μαζί με μερικό φορτίο λειτουργίας του μοντέλου με το καλύτερο καύσιμο.

Τέλος, στο πέμπτο κεφάλαιο, συνοψίζονται τα αποτελέσματα αυτής της εργασίας και παρατίθενται ιδέες για περαιτέρω έρευνα.

Nomenclature

\dot{C}	Molar flow kmol/s
c	Molar concentration, mol
C_p	Specific heat capacity at constant pressure, kJ/kg K
e	Specific exergy kJ/kg
\dot{E}	Exergy flow, kJ/s
Ex	Exergy, kJ/kg
F	Force, n
h	Specific enthalpy, kJ/kg
\dot{m}	Mass flow, kg/s
P	Mechanical power, kJ/s
Q	Heat Flow, kJ/s
R	Severity Factor
p	Pressure, bar
u	Velocity, m/s
w	Moisture
s	Specific entropy, kJ/kg K
T	Temperature, °C
t	Time, s
z	Axial Direction, m

Greek Letters

Γ	Mass exchange rate between phases
ε	Desired moisture
η	Efficiency
ρ	Density, kg/m ³
χ	Steam Dryness Factor

Subscripts

0	Reference state
AUX	Auxiliary
B	Fuel
ch	Chemical
D	Steam
el	Electrical

ex	Exergetic
Fri	Friction
G	Generator
g	Gaseous
gra	Gravitational
ik	Interface between wall and phase
kin	Kinetic
l	Liquid
ST	Steam Turbine
th	Thermal
wall,k	Interface between wall and phase

Abbreviations

BFB	Bubbling Fluidized Bed
BOP	Balance of Plant
BSG	Brewery Spent Grain
CHP	Combined Heat and Power
CFB	Circulating Fluidized Bed
COP	Coefficient of performance
DT	Dry Torrefaction
ECC	Ejector compression cycle
EFB	Empty Fruit Bunch
FLB	Fluidized Bed
GHG	Greenhouse Gases
HTC	Hydrothermal Carbonization
HHV	Higher Heating Value
LHV	Lower Heating Value
PF	Pulverized Fuel
SC	Supercritical
USC	Ultra - Supercritical
WT	Wet Torrefaction

Contents

Ευχαριστίες.....	2
Abstract	3
Περίληψη.....	4
Nomenclature.....	5
List of Figures.....	10
List of tables.....	14
1. INTRODUCTION	16
1.1 World and EU Energy Mixture	17
1.2 Biomass characterization	19
1.3 Types of biomass	20
1.3.1 Brewery Spent Grain	21
1.3.2 Wood Pellets.....	21
1.3.3 Spruce Bark.....	22
1.3.4 Oil Palm Empty Fruit Bunches.....	22
1.3.5 Sunflower Husk Pellets.....	23
1.3.6 Corn Stover	23
1.4 Pretreatment technologies	24
1.4.1 Steam explosion	24
1.4.2 Dry Torrefaction	25
1.4.3 Hydrothermal Carbonization (Wet Torrefaction).....	27
1.5 Combined Heat and Power Plants with Biomass as fuel	28
2. Steam Power and Heat Cycles	30
2.1 Boiler Technologies	33
2.2 Steam Power Plants Control	34
2.2.1 Fuel Flow Control.....	35
2.2.2 Feedwater Control.....	36
2.2.3 Steam pressure Control.....	37
2.2.4 Steam Temperature Control	37
2.2.5 Air Flow Control.....	38
2.2.6 Furnace pressure control	38
2.3 Modelling of power plants.....	39
2.3.1 Advanced Process Simulator - Apros.....	39

2.3.2	Aspen Plus Dynamics.....	41
2.3.3	GateCycle.....	42
2.4	Cogeneration Plant for Aluminum of Greece.....	44
3.	Modified CHP Plant.....	47
3.1	Presentation of the GateCycle components.....	48
3.1.1	Fluidized Bed Boiler – FLB.....	49
3.1.2	Economizer.....	52
3.1.3	Superheater.....	53
3.1.4	Steam Turbine.....	54
3.1.5	Condenser.....	56
3.1.6	Heat Exchanger.....	57
3.1.7	Deaerator.....	58
3.1.8	Flash Tank.....	59
3.1.9	Pump.....	60
3.1.10	Splitter.....	61
3.1.11	Mixer.....	62
3.1.12	Temperature Control Mixer.....	63
3.2	Inputs of the Modified Biomass CHP Plant.....	64
3.3	Results of the Modified Biomass CHP Power Plant.....	70
3.3.1	Results of the Raw Spruce Simulation.....	70
3.3.2	Results of the Raw Empty Fruit Bunch Simulation.....	77
3.3.3	Results of the Torrefied Spruce Simulation.....	81
3.3.4	Results of the Torrefied EFB Simulation.....	85
4.	Improved CHP Plant.....	89
4.1	Results of the Improved Biomass CHP Plant – Dried Fuels.....	91
4.2	Results of the Improved Biomass CHP Plant – Pretreated Fuels.....	111
4.3	Comparison of the four biomass fuels, Part Load Operation of the best fuel and Cooling Power Output.....	131
5.	Conclusions and Further Research.....	140

List of Figures

Figure 1: Energy share of energy production by fuels[3].....	17
Figure 2: Renewables Energy share in EU-28[6]Table 1.2 - 1	18
Figure 3: Flow and T – s diagram of backpressure plant based on the Rankine cycle.....	30
Figure 4: Principal combustion technologies for biomass	31
Figure 5: Depiction of the parameters being controlled	35
Figure 6: Three element feedwater control in steam drum boilers. FT = Flow transmitter, LT = Level Transmitter, LIC = Level Indication and automatic control, s = set point, M = Motor[52].	36
Figure 7: Depiction of spray cooling steam temperature control. IT = Temperature transmitter, TIC = Temperature indication and control, s = Set point[52].	38
Figure 8: Cogeneration Power Plant beside the Aluminum of Greece Plant.....	45
Figure 9: Cogeneration Power Plant model in GateCycle	45
Figure 10: Schematic of the Cogeneration Power Plant beside the Aluminum of Greece Plant.....	46
Figure 11: Biomass fueled power plant	47
Figure 12: Schematic of the Biomass fueled power plant	48
Figure 13: Fluidized Bed Boiler icon.....	49
Figure 14: Boiler - General input window	49
Figure 15: Boiler - Fuel input window	50
Figure 16: Boiler – Design input window	50
Figure 17: Boiler – Combustion window.....	51
Figure 18: Economizer icon.....	52
Figure 19: Economizer – General Input Window	52
Figure 20: Superheater icon.....	53
Figure 21: Superheater – General Input Window.....	53
Figure 22: Steam Turbine icon	54
Figure 23: Steam Turbine – General Input Window	54
Figure 24: Steam Turbine – Pressure Input Window	55
Figure 25: Steam Turbine – Limits and Losses Windows	55
Figure 26: Condenser icon	56
Figure 27: Condenser – General Input Window	56
Figure 28: Heat Exchanger icon	57
Figure 29: Heat Exchanger – General Input Window.....	57
Figure 30: Deaerator icon	58
Figure 31: Deaerator – General Input Window	58
Figure 32: Flash Tank icon.....	59
Figure 33: Flash Tank – General Input Window	59
Figure 34: Pump icon	60
Figure 35: Pump – General Input Window	60
Figure 36: Splitter icon.....	61
Figure 37: Splitter – General Input Window	61
Figure 38: Mixer icon	62
Figure 39: Mixer General Input Window	62
Figure 40: Temperature Control Mixer icon	63
Figure 41: Temperature Control Mixer – General Input Icon.....	63

Figure 42: Overall Energetic and Exergetic Efficiencies for the Raw Spruce simulation	74
Figure 43: Electrical Energetic and Exergetic Efficiencies for the Raw Spruce simulation	75
Figure 44: Biomass CHP Power Plant Sankey Diagram for the Raw Spruce simulation	75
Figure 45: Biomass CHP Power Plant Grassmann Diagram for the Raw Spruce simulation.....	76
Figure 46: Overall Energetic and Exergetic Efficiencies for the Raw EFB simulation.....	78
Figure 47: Electrical Energetic and Exergetic Efficiencies for the Raw EFB simulation	79
Figure 48: Biomass CHP Power Plant Sankey Diagram for the Raw EFB simulation.....	79
Figure 49: Biomass CHP Power Plant Grassmann Diagram for the Raw EFB simulation.....	80
Figure 50: Overall Energetic and Exergetic Efficiencies for the Torrefied Spruce simulation	82
Figure 51: Electrical Energetic and Exergetic Efficiencies for the Torrefied Spruce simulation	82
Figure 52: Biomass CHP Power Plant Sankey Diagram for the Torrefied Spruce simulation	83
Figure 53: Biomass CHP Power Plant Grassmann Diagram for the Torrefied Spruce simulation.....	83
Figure 54: Overall Energetic and Exergetic Efficiencies for the Torrefied EFB simulation	86
Figure 55: Electrical Energetic and Exergetic Efficiencies for the Torrefied EFB simulation	86
Figure 56: Biomass CHP Power Plant Sankey Diagram for the Torrefied EFB simulation	87
Figure 57: Biomass CHP Power Plant Grassmann Diagram for the Torrefied EFB simulation.....	87
Figure 58: Improved CHP plant model for the non-pretreated fuels	89
Figure 59: Schematic of the Improved CHP plant model for the non-pretreated fuels	90
Figure 60: Overall Energetic and Exergetic Efficiencies for the Dry Spruce Simulation of the Improved Model (160 bar)	93
Figure 61: Electrical Energetic and Exergetic Efficiencies for the Dry Spruce Simulation of the Improved Model (160 bar)	93
Figure 62: Overall Energetic and Exergetic Efficiencies for the Dry Spruce Simulation of the Improved Model (180 bar)	94
Figure 63: Electrical Energetic and Exergetic Efficiencies for the Dry Spruce Simulation of the Improved Model (180 bar)	95
Figure 64: Overall Energetic and Exergetic Efficiencies for the Dry Spruce Simulation of the Improved Model (200 bar)	96
Figure 65: Electrical Energetic and Exergetic Efficiencies for the Dry Spruce Simulation of the Improved Model (200 bar)	96
Figure 66: Overall Energetic and Exergetic Efficiencies for the Dry Spruce Simulation of the Improved Model (220 bar)	97
Figure 67: Electrical Energetic and Exergetic Efficiencies for the Dry Spruce Simulation of the Improved Model (220 bar)	98
Figure 68: Overall Energetic and Exergetic Efficiencies for the Dry Spruce Simulation of the Improved Model (600 °C)	100
Figure 69: Electrical Energetic and Exergetic Efficiencies for the Dry Spruce Simulation of the Improved Model (600 °C)	100
Figure 70: Overall Energetic and Exergetic Efficiencies for the Dry EFB Simulation of the Improved Model (160 bar).....	102
Figure 71: Electrical Energetic and Exergetic Efficiencies for the Dry EFB Simulation of the Improved Model (160 bar)	103
Figure 72: Overall Energetic and Exergetic Efficiencies for the Dry EFB Simulation of the Improved Model (180 bar).....	104

Figure 73: Electrical Energetic and Exergetic Efficiencies for the Dry EFB Simulation of the Improved Model (180 bar)	104
Figure 74: Overall Energetic and Exergetic Efficiencies for the Dry EFB Simulation of the Improved Model (200 bar).....	105
Figure 75: Electrical Energetic and Exergetic Efficiencies for the Dry EFB Simulation of the Improved Model (200 bar)	106
Figure 76: Overall Energetic and Exergetic Efficiencies for the Dry EFB Simulation of the Improved Model (220 bar).....	107
Figure 77: Electrical Energetic and Exergetic Efficiencies for the Dry EFB Simulation of the Improved Model (220 bar)	107
Figure 78: Overall Energetic and Exergetic Efficiencies for the Dry EFB Simulation of the Improved Model (600 °C)	109
Figure 79: Electrical Energetic and Exergetic Efficiencies for the Dry EFB Simulation of the Improved Model (600 °C).....	110
Figure 80: Improved CHP plant model for the pretreated fuels.....	111
Figure 81: Schematic of the Improved CHP plant model for the pretreated fue	111
Figure 82: Overall Energetic and Exergetic Efficiencies for the Torrefied Spruce Simulation of the Improved Model (160 bar).....	113
Figure 83: Electrical Energetic and Exergetic Efficiencies for the Torrefied Spruce Simulation of the Improved Model (160 bar).....	114
Figure 84: Overall Energetic and Exergetic Efficiencies for the Torrefied Spruce Simulation of the Improved Model (180 bar).....	115
Figure 85: Electrical Energetic and Exergetic Efficiencies for the Torrefied Spruce Simulation of the Improved Model (180 bar).....	115
Figure 86: Overall Energetic and Exergetic Efficiencies for the Torrefied Spruce Simulation of the Improved Model (200 bar).....	116
Figure 87: Electrical Energetic and Exergetic Efficiencies for the Torrefied Spruce Simulation of the Improved Model (200 bar).....	117
Figure 88: Overall Energetic and Exergetic Efficiencies for the Torrefied Spruce Simulation of the Improved Model (220 bar).....	118
Figure 89: Electrical Energetic and Exergetic Efficiencies for the Torrefied Spruce Simulation of the Improved Model (220 bar).....	118
Figure 90: Overall Energetic and Exergetic Efficiencies for the Torrefied Spruce Simulation of the Improved Model (600 °C)	120
Figure 91: Electrical Energetic and Exergetic Efficiencies for the Torrefied Spruce Simulation of the Improved Model (600 °C)	121
Figure 92: Overall Energetic and Exergetic Efficiencies for the Torrefied EFBs Simulation of the Improved Model (160 bar)	123
Figure 93: Electrical Energetic and Exergetic Efficiencies for the Torrefied EFBs Simulation of the Improved Model (160 bar).....	123
Figure 94: Overall Energetic and Exergetic Efficiencies for the Torrefied EFBs Simulation of the Improved Model (180 bar)	124
Figure 95: Electrical Energetic and Exergetic Efficiencies for the Torrefied EFBs Simulation of the Improved Model (180 bar).....	125

Figure 96: Overall Energetic and Exergetic Efficiencies for the Torrefied EFBs Simulation of the Improved Model (200 bar)	126
Figure 97: Electrical Energetic and Exergetic Efficiencies for the Torrefied EFBs Simulation of the Improved Model (200 bar).....	126
Figure 98: Overall Energetic and Exergetic Efficiencies for the Torrefied EFBs Simulation of the Improved Model (220 bar)	127
Figure 99: Electrical Energetic and Exergetic Efficiencies for the Torrefied EFBs Simulation of the Improved Model (220 bar).....	128
Figure 100: Overall Energetic and Exergetic Efficiencies for the Torrefied EFBs Simulation of the Improved Model (600 °C)	130
Figure 101: Electrical Energetic and Exergetic Efficiencies for the Torrefied EFBs Simulation of the Improved Model (600 °C)	130
Figure 102: Comparison of the overall energetic and exergetic efficiencies of the four biomass fuels (dried and pretreated)	132
Figure 103: Comparison of the electrical energetic and exergetic efficiencies of the four biomass fuels (dried and pretreated)	132
Figure 104: Energetic and Exergetic Overall efficiencies for the full and part load operation of the torrefied Spruce	133
Figure 105: Energetic and Exergetic Electrical efficiencies for the full and part load operation of the torrefied Spruce	134
Figure 106: Biomass CHP Power Plant Sankey Diagram for the Torrefied Spruce simulation	134
Figure 107: Biomass CHP Power Plant Grassmann Diagram for the Raw EFB simulation	135
Figure 108: Electrical, Thermal and Overall efficiencies depending to the mass flow	135
Figure 109: Variation of the COP of the ECC system with the heat source inlet temperature for chilled water outlet temperature of 10 °C[54]	136
Figure 110: COP variation with the hot water inlet and chilled water outlet temperatures for the absorption chiller[54].....	137

List of tables

Table 1: Moisture content, gross calorific value, net calorific value, bulk density and energy density of biomass fuels[9]	20
Table 2: Advantages and Limitations of Different Types of Torrefaction Reactors.....	26
Table 3: Characteristics of hydrochars and biochar from Norway spruce on a same solid yield basis[48]	28
Table 4: Various CHP plants in European countries.....	29
Table 5: Advantages and disadvantages of steam turbines	33
Table 6: Boiler technologies characteristics	34
Table 7: Inputs of the Biomass CHP Plant with Raw Spruce as fuel.....	64
Table 8: Raw Spruce Chemical Composition.....	67
Table 9: Inputs of the Biomass CHP Plant with Raw EFB as fuel.....	67
Table 10: Raw EFB Chemical Composition.....	68
Table 11: Inputs of the Biomass CHP Plant with Torrefied Spruce as fuel	68
Table 12: Torrefied Spruce Chemical Composition.....	69
Table 13: Inputs of the Biomass CHP Plant with Torrefied EFB as fuel.....	69
Table 14: Torrefied EFB Chemical Composition.....	69
Table 15: Thermodynamic Cycle Properties for the Raw Spruce simulation.....	73
Table 16: Total Energetic and Exergetic Efficiency Values for the Raw Spruce simulation	74
Table 17: Electrical Energetic and Exergetic Efficiency Values for the Raw Spruce simulation.....	74
Table 18: Cycle Thermodynamic Properties for the Raw EFB simulation.....	77
Table 19: Total Energetic and Exergetic Efficiency Values for the Raw EFB simulation	78
Table 20: Electrical Energetic and Exergetic Efficiency Values for the Raw EFB simulation.....	78
Table 21: Cycle Thermodynamic Properties for the Torrefied Spruce simulation	81
Table 22: Total Energetic and Exergetic Efficiency Values for the Torrefied Spruce simulation	81
Table 23: Electrical Energetic and Exergetic Efficiency Values for the Torrefied Spruce simulation	81
Table 24: Cycle Thermodynamic Properties for the Torrefied EFB simulation.....	85
Table 25: Total Energetic and Exergetic Efficiency Values for the Torrefied EFB simulation	85
Table 26: Electrical Energetic and Exergetic Efficiency Values for the Torrefied EFB simulation.....	85
Table 27: Dry Spruce Chemical Composition	92
Table 28: Dry Spruce Improved Model Simulation Outputs for 160 bar	92
Table 29: Dry Spruce Improved Model Simulation Outputs for 180 bar	94
Table 30: Dry Spruce Improved Model Simulation Outputs for 200 bar	95
Table 31: Dry Spruce Improved Model Simulation Outputs for 220 bar	97
Table 32: Dry Spruce Improved Model Simulation Outputs for 230 bar (Supercritical).....	98
Table 33: Dry Spruce Improved Model Simulation Outputs for 600 °C.....	99
Table 34: Dry Spruce Chemical Composition	101
Table 35: Dry EFB Improved Model Simulation Outputs for 160 bar	102
Table 36: Dry EFB Improved Model Simulation Outputs for 180 bar	103
Table 37: Dry EFB Improved Model Simulation Outputs for 200 bar	105
Table 38: Dry EFB Improved Model Simulation Outputs for 220 bar	106
Table 39: Dry EFB Improved Model Simulation Outputs for 230 bar (Supercritical).....	108
Table 40: Dry EFB Improved Model Simulation Outputs for 600 °C.....	109
Table 41: Torrefied Spruce Chemical Composition.....	112
Table 42: Wet Torrefied Spruce Improved Model Simulation Outputs for 160 bar	113

Table 43: Wet Torrefied Spruce Improved Model Simulation Outputs for 180 bar	114
Table 44: Wet Torrefied Spruce Improved Model Simulation Outputs for 200 bar	116
Table 45: Wet Torrefied Spruce Improved Model Simulation Outputs for 220 bar	117
Table 46: Wet Torrefied Spruce Improved Model Simulation Outputs for 230 bar (Supercritical)	119
Table 47: Wet Torrefied Spruce Improved Model Simulation Outputs for 600 °C.....	120
Table 48: Torrefied EFBs Chemical Composition	122
Table 49: Torrefied EFBs Improved Model Simulation Outputs for 160 bar	122
Table 50: Torrefied EFBs Improved Model Simulation Outputs for 180 bar	124
Table 51: Torrefied EFBs Improved Model Simulation Outputs for 200 bar	125
Table 52: Torrefied EFBs Improved Model Simulation Outputs for 220 bar	127
Table 53: Torrefied EFBs Improved Model Simulation Outputs for 230 bar (Supercritical).....	128
Table 54: Torrefied EFB Improved Model Simulation Outputs for 600 °C.....	129
Table 55: Cooling Power Output for the Dry Spruce with COP = 0.763.....	137
Table 56: Cooling Power Output for the Dry EFBs with COP = 0.763	138
Table 57: Cooling Power Output for the Torrefied Spruce with COP = 0.3168	138
Table 58: Cooling Power Output for the Torrefied EFBs with COP = 0.3168.....	139

1.INTRODUCTION

World energy consumption has always been one of the key factors concerning the development of modern day societies. Since the industrial revolution in late 18th century erupted, energy and thus fossil fuel consumption has been on an exponential rise. The use of fossil fuels, of course has been a huge contributor to the establishment of the Western civilization since then, but as the years passed, even more countries have been improving their infrastructure in terms of energy production. In conjunction with the extravagant energy consumption in the West, there have been many concerns and expostulation regarding the environmental impacts of energy power plants. As the whole world is experiencing an economic and demographic growth, energy consumption, and thus the negative environmental implications will only be on the rise.

Greenhouse gas emissions (GHG's), especially carbon dioxide, are imposing the greatest threat for the environment, as it is often alleged that they are connected to climate change. According to the European Commission's Energy Statistical pocketbook [1], the GHG's of the EU-28 and member states in 1995 were a staggering 5399.3 million ton CO₂ equivalent, while by the year 2014 these emissions were reduced by 19.2 % with the GHG's of 1995 as a reference. The reduction of the aforementioned emissions was the result of legal legislations in association with the pressure from various environmental conservancies. These legislations required the reduction of the percentage of fossil fuels consumed for energy production. In the year 2007 the 2020 climate and energy package was introduced by the European commission, a binding legislation with three key targets. These targets are the 20 % cut of GHG's from 1990 levels, 20 % EU energy originating from Renewables and 20 % improvement in energy efficiency.

In conformity with the 2020 climate and energy package, the amount of renewable energy production has increased significantly in the past few years, with frontrunners central and northern European state members. The renewable energy production has mainly been relied to wind and solar energy, with many wind farms and solar panel installations being introduced. However the electricity production based on these renewables, depends on weather conditions, which vary depending on the season and daytime. Therefore, their power level is ever changing and their intermittent power generation leads to load fluctuations, leading to ripples in the balance of the electrical grid. Due to these cons, interest in the use of solid biomass and biofuels in general has been greatly increased.

Biomass is a carbon dioxide neutral fuel in the long term, as they absorb the same amount of carbon dioxide growing, as they produce when they are combusted. As opposed to wind and solar energy, biomass is dependent free by weather conditions and seasonal variations. It can be used in a co-firing burner configuration, in biogas, ethanol or biodiesel generation and most importantly, it has the significant advantage of being able to serve as a source of base load power[1]. In addition, coal to biomass conversions, enable generators to use coal existing assets and infrastructure to produce renewable energy. Something that cannot be stated for other renewable energy sources. Biomass will be a key factor to the increase of the renewable's percentage in Europe's energy mixture.

1.1 World and EU Energy Mixture

Consumption of energy from all sources is on the rise on a global scale, a fact that arises concerns about energy security, effects of fossil fuel emissions on the environment and the aggravation of global warming. These concerns, in association with sustained high oil prices, expand the support for use of non-fossil renewable energy sources and nuclear power, as well as natural gas, which is the least carbon intensive fossil fuel. Although the use of renewable energy sources has been significantly boosted in the last years, fossil fuels still comprise around 80 % of the total energy share worldwide[2]. Leading the race for energy production is petroleum and its products with solid fuels featuring in the second place.

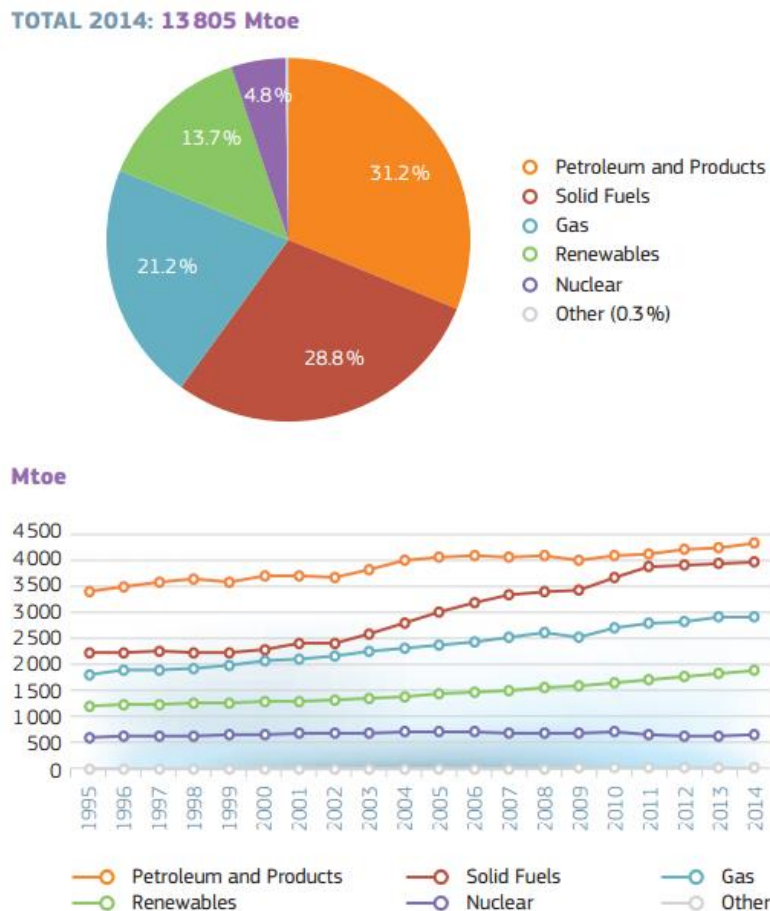


Figure 1: Energy share of energy production by fuels[3]

As shown in the figure above the use of fossil fuels has been on the rise since 1995, but that can be said for renewables as well. Especially since 2006, energy production by renewable sources has been booming. This proves the fact that even more countries are promoting energy producers to install renewables, by means of funding and guarantees.

The European Union has been a frontrunner in the installation and promotion of renewable energy plants, as one of its top priorities is the creation of resilient Energy Union with a forward-looking climate policy, which is capable of delivering the adopted 2020, 2030 climate, energy targets, and the EU's longer-term climate objectives. In order to achieve these goals, Europe has to decarbonize its energy supply, integrate the fragmented national energy markets into a smooth functioning and coherent European system, and set up a framework that allows the effective coordination of national efforts. Renewable energy sources are the key factor for this transition, because of their ability to mitigate GHG's, their ability to lower environmental pressures associated with the conventional energy production and reduce the reliance on fossil fuels. The EU-wide share of renewable energy rose from 14.3 % in 2012 to almost 16% in 2014[4]. Heat and cooling kept being the dominant renewable energy sources market sector in EU, while coal was the most substituted fuel by renewables across EU in 2013 and 2014.

Although the European Union has made great efforts to shift their energy production to a more environmental friendly agenda, its dependency on fossil fuels remains at a significant level. In 2014, the average EU-28 energy dependency was 53.4 %, a share that has been steadily increasing over the last two decades[5]. A key asset to curtail this downward cycle are renewables, including bioenergy, which should have a top priority since coal can be easily replaced by solid biomass, without drastic alterations in existing infrastructure. Despite this ability, the European Commission strategy has not given bioenergy, a top priority role in renewables. One can identify this strategy by the share of renewables in the EU-28.

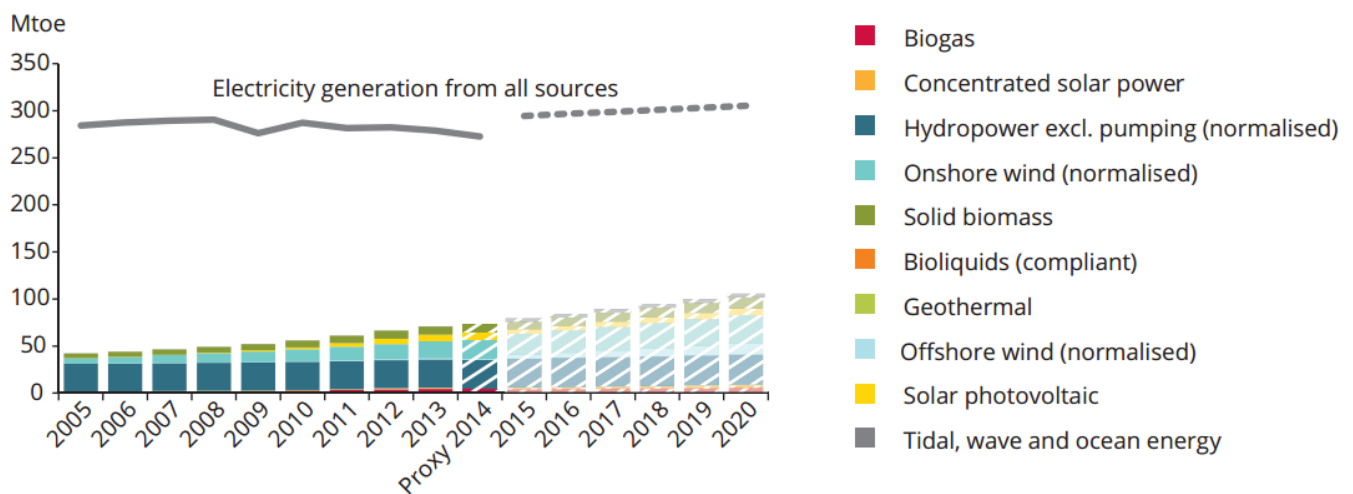


Figure 2: Renewables Energy share in EU-28[6]

As shown in figure 2, hydropower and wind power have been the dominant form of renewable energy in Europe, with hydropower having a stable production percentage, while wind power has been steadily growing. Solar photovoltaics had a blooming period during 2011 and 2013, but their growth seems to be diminishing in the last years, while bioenergy including solid biomass and biogas are on the increase since 2005. Bioenergy is now the most common form of renewable energy in the EU[7].

Bioenergy's contribution to the EU's 2020 and 2030 objectives is crucial. Sustainable biomass use for heating, cooling and electricity production can result in a number of energy, economic, employment and environmental benefits. Biomass can also contribute to the EU Energy security, as far as the majority of biomass demand is met through domestically produced raw material. Biomass represents at present 2/3 of the renewable energy and 10% of the total energy consumed in Europe, with solid biomass being the largest source of renewable energy in EU[7].

1.2 Biomass characterization

Biomass includes all non-fossilized and biodegradable organic material originating from plants, animals and microorganisms. This also includes products, by-products, residues and waste from agriculture, forestry and related industries as well as the non-fossilized and biodegradable organic fractions of industrial and municipal wastes. Biomass also includes gases and liquids recovered from the decomposition of non-fossilized and biodegradable organic material[8].

Biomass can be converted into useful energy or energy carriers by both thermochemical and biochemical conversion technologies. The characteristics and quality of solid biomass as a fuel vary widely, depending mainly on the kind of biomass and the pre-treatment technologies applied. Moisture content, ash content, ash-sintering temperatures, lower and higher heating value (LHV and HHV accordingly), particle dimensions, bulk and energy density are some of the characteristics reviewed for biomass fuels, as these factors will contribute to the selection of the appropriate combustion technology. These physical properties have different effects to storage as well. Moisture content determines storage durability and dry matter losses, self-ignition and plant design as well, while ash content is connected to dust emissions, ash utilization or disposal. Bulk density is the key factor concerning the fuel logistics such as storage, transport and handling, while the heating value and the particle density are factors that influence the combustion technology and operational safety[9]. Further down, some physical characteristics of various biomass fuels are shown.

Table 1: Moisture content, lower heating value, higher heating value, bulk density and energy density of biomass fuels[9]

	Moisture content [wt% w.b.]	LHV [MJ/kg d.b.]	HHV [MJ/kg w.b.]	Bulk Density [kg w.b./m ³]	Energy Density [MJ/m ³]
Wood pellets	10.0	19.8	16.4	600.0	9840.0
Woodchips - hardwood	50.0	19.8	8.0	450.0	3600.0
Woodchips - softwood	50.0	19.8	8.0	350.0	2800.0
Bark	50.0	20.2	8.2	320.0	2620.0
Sawdust	50.0	19.8	8.0	240.0	1920.0
Straw(winter wheat)	15.0	18.7	14.5	120.0	1740.0
Olive residues(from 2-phase production)	63.0	21.5	6.1	1130.0	6890.0

Biomass can be derived by energy crops, which are plants cultivated for the purpose of producing thermal energy, electricity or biofuel such as biodiesel and bioethanol[10]. Energy crops can be classified in four categories according to the biofuels they produce. First-class crops derive mostly from food crops, such as sugar cane and corn. United States and Brazil are the most dominant producers of ethanol, holding a tremendous 87.5 % of world ethanol production. The United States use a significant portion of their corn production in order to produce ethanol, while Brazil uses sugar cane as a raw material for its production[11]. Although these kinds of crops are useful concerning the production of high-level biofuels, their use as aliment poses the necessity of alternatives as imperative. Alternatives emerge from second-class crops, which as opposed to the first class, are not food crops or they are residues by the agricultural production. They comprise mostly by crops of lignocellulosic cultivations, which are used for energy storage by means of liquid or gas biofuels. Third-class crops produce biofuels by cultivations of increased field yield, such as microalgae, and lastly fourth-class crops are those classified as cultivations of zero or below zero carbon emissions[10].

1.3 Types of biomass

As mentioned above there are quite a few types and crops of biomass. Their cultivation is based on the climatic characteristics of each region, soil quality, as well as the topography of each region. That is the reason why, different kinds of crops thrive on different areas of the world. Some of them are fit to be used as solid biomass, such as wood from Finland’s forests, while others are mainly used for biogas production, such as sugar cane in Brazil. Some types of biomass are presented below:

1.3.1 Brewery Spent Grain

Brewery Spent Grain (BSG) is a residual by-product from one of the first steps in the brewing process in solubilizing the malt and cereal grains to ensure adequate extraction of the wort[12]. It is the most significant by-product in the total brewing process, accounting for roughly 85 % of total by-products, accounting for 30 % - 60 % of the biochemical oxygen demand and suspended solids from a typical brewery[13].

BSG is considered as a lignocellulosic material, rich in protein and fibre, which account for around 20 % and 70 % of its composition, respectively. BSG is a high value material because of its hemicellulose, lignin and high protein content, but challenges are associated with using it as feedstock due to the existence of a complex outer layer, making it difficult to separate and convert, and the high moisture content (80 % - 85 %), making it susceptible to microbial growth and spoilage in just over a week[14].

Although BSG is the main by-product of the brewing process, it has received little attention as marketable commodity, and its disposal often poses an environmental threat. Up until now, the main application of BSG has been as an animal feed, mainly for cattle, due to its high content of protein and fibre. Although, due to its relatively low cost and high nutritive value, BSG has been evaluated for the manufacture of flakes, whole-wheat bread, biscuits and aperitif snacks for human nutrition. Last but not least, BSG has been recommended for use in energy production, either through direct combustion or by fermentation to produce biogas[15]. Most studies have been focused solely upon the production of biogas and especially bioethanol, by means of anaerobic fermentation, because of the sugars that are released[16]. Recently, a study was performed by the University of Ljubljana, in which biogas batch reactors were bioaugmented with various microorganisms, in order to improve anaerobic digestion efficiency of BSG[17].

1.3.2 Wood Pellets

Utilization of woody biomass for heat and power production has been mainly restricted to timber, sawdust, wood chips and wood pellets. Wood pellets are compressed, cylindrical, sometimes quadratic grains, with a diameter depending on the use, industrial or non-industrial, made from wood materials that are condensed under heat and pressure. Pelletizing makes certain of having a uniform fuel and a low content of moisture (2 % - 8 %) and ash (about 0.5 %)[18].

The quality of pellets is determined by the end user's requirements on the heating system and the handling properties. The dimensions of the pellets, both diameter and length, are important factors with respect to combustion. Experience has shown that thinner pellets allow a more uniform combustion rate, especially in small furnaces. Transport efficiency is dependent on the bulk density of pellets, while mechanical strength is a very important quality factor at many levels. Organic dust may constitute a health risk for those handling the fuel, as dust explosion is a great problem connected with the handling and transporting of fuel[19].

Storage is, as well, a very important factor, considering that biomass fuels in general, have a relatively low energy density, so the design of the storage facilities is quite important in order to keep fuel costs low. Several problems arise, connected to storage, such as biological and biochemical degradation, while pellets must be kept in a moisture-free location, because, when exposed to water, pellets get damp, swell and disintegrate[20]. Wood pellets are suitable for heating family houses, farms and block buildings, with equipment designed especially for the combustion of pellets[9].

1.3.3 Spruce Bark

Norway spruce (*Picea abies*) is one of the most abundant and economically important tree species in the boreal hemisphere, and it is mainly used for sawn timber and pulp. Although, spruce bark has a lot of potential in being used as a renewable source of biomass. The techno-economical potential of bark is high, as the technology of biorefinery concepts are constantly developing, so bark can be first utilized as a source of high value extracts, and then be combusted.

The Norway spruce bark of butt and middle logs from the first commercial thinnings may provide a feasible source for higher-value chemicals in biorefinery production[21]. Spruce bark has high concentrations of several polyphenolic compounds, including stilbenes, lignin, flavonoids and tannins. These phenolic metabolites have multiple biological activities, such as protection against environmental stresses, antifungal and antimicrobial functions, and antifeedant activity, all presumed to be vital for tree resistance[22].

1.3.4 Oil Palm Empty Fruit Bunches

Empty fruit bunch (EFB) from oil palm is one of the potential biomass, to produce biofuels like bio-oil due to its abundant supply and favorable physicochemical characteristics. Oil palm (*Elais guineensis*) is currently one of the leading perennial oleaginous food crops grown widely in many tropical regions of Southeast Asia with abundant rainfall and sunlight, mainly for the production of edible cooking oil. EFBs are waste residue generated from palm oil industries after harvesting fresh fruit bunches from oil palm trees and separating the fruit from the bunch. It is estimated, that for every ton of palm oil produced from a fresh fruit bunch, approximately 1 ton of EFBs is generated[23].

They are a brown bunch with non-uniform shape and low bulk density, with length and width varying from 17 – 30 cm long and 25 – 35 cm wide. Due to the biological growth of fruit bunches, coupled with the preceding steam sterilization process in the palm oil production lines, this by-product has a significantly high content of moisture, accounting for over 60 % of its total weight, so its combustion has been quite limited[24]. EFBs are a source of a variety of nutrients, such as Phosphorus (P), Potassium (K) and Magnesium (Mg), with the result of being a very useful organic matter. Due to these characteristics, it is widely used as a substrate for mushroom cultivation and as organic mulch as well as supplementary

fertilizer of oil palm plantations[25]. Apart from non-energetic purposes, EFBs can be utilized as a source for the production of bio-oil.

Bio-oil is a dark brown, polar high density and viscous organic fluid, containing a mixture of oxygenated compounds such as levoglucosan, carboxylic acids, alcohols, esters, ketones, aldehydes and benzenoids[26]. Due to EFBs' high moisture and ash content (10 % -13 %), and lower energy content compared to some other types of biomass feedstock, there has been a large amount of experimental studies focusing on the energetic utilization of EFBs. Although EFBs have not been in the spotlight, their high content of cellulose and lignin[27] makes them a perfect candidate for future utilization.

1.3.5 Sunflower Husk Pellets

Sunflower (*Helianthus annuus* L.) is one of the most important oil crops and its oil can be used for food and bioenergy. Sunflower husk pellets are made of the scales of sunflower nuts. They are a by-product of sunflower oil extraction process and can be found in big quantities in sunflower oil factories. Their HHV is close to the HHV of wood pellets, being 17 MJ/kg – 17.6 MJ/kg, with some cases achieving 18 MJ/kg. Their ash content is on the level of 2.6 % - 3 %, their sulfur content may be slightly higher than 0.2 %, exceeding the accepted limit for wood pellets. Their most significant disadvantages are their high content of dust and their low bulk density, which make their transportation economically unworthy[28]

Sunflower husk pellets are cheaper compared to wood pellets, although they are a rather rare raw material for European countries, with the highest volumes being exported to Poland and Ukraine. But recent years have shown that the demand of sunflower husk pellets has been on the rise, although the supply cannot satisfy it.

1.3.6 Corn Stover

Corn stover is a broad term, which describes all of the above ground biomass from the crop except the grain. It consists of an agricultural residue that is left over after the corn has been harvested. Stover is comprised of structural components including stalks (50 %), leaves (22%), husks (13%) and cobs(15%)[29]. It holds the third place concerning the production of cereal crop, only following wheat and rice. Corn stover has a huge availability, especially in the USA, which exceeds on-farm demand[30], so it is a great source of renewable energy producing biomass. It is classified as lignocellulosic, as it is mostly composed of cellulose, hemicelluloses and lignin and it is considered as the largest source of agricultural residue available for use in cellulosic biofuel production in the US[31].

In addition, the large amounts of starch present in corn makes it a valuable feedstock for ethanol production. Two thirds of production cost of corn ethanol is the market value of corn grain[32] which is an internationally traded commodity and can be stored and transported over a long distance economically. On the other hand, long distance transport of corn stover is not economically feasible, and

storage is another issue, which can cause biomass loss, reduce feedstock quality, and increase biofuel production cost[33].

1.4 Pretreatment technologies

Biomass has the potential to become a major global energy source, with the ability to make a substantial contribution to the sustainable future energy demand[34]. Biomass can be considered as organic matter, able to produce energy carrier sources, otherwise known as biofuels. There are a number of different bioenergy routes (processes) that can be applied to convert raw biomass feedstocks into final energy and chemical products, which are typically divided into two main categories: thermochemical and biochemical routes. Each different route typically consists of a series of conversion steps that transform the raw biomass feedstock into an energy carrier such as heat, electricity or liquid or gas-based biofuel[34].

The preferred bioenergy conversion route often depends on a variety of factors such as specific feedstock and the quantity available, the desired form of the energy product, the current availability of the processing technology, environmental standards and the economic conditions. However, in most cases, it is ultimately the form in which the energy is required that is the main governing factor, followed by the availability and quantity of biomass feedstocks[35]. Although biomass has the potential to produce both cleaner-burning and more sustainable sources of fuels, there are disadvantages associated with the use of biomass feedstocks. For instance, their low energy density and heterogeneity in physical nature make handling, transport and storage more complex and more expensive than fossil fuels[36].

Furthermore, there is a high degree of variation in the chemical composition, moisture and alkali content across different biomass feedstocks. This requires some form of pretreatment in order to meet the requirements for quality and homogeneity for the successful application of many conversion technologies. Biomass upgrading and pretreatment protocols are therefore key steps required for the efficient conversion of biomass into energy products and can significantly affect both the efficiency and choice of methodology of the subsequent energy process. The primary goal of pretreatment is to overcome the recalcitrant nature of the feedstock and to modify its structure, making the feedstock more amenable for conversion into a final product[37]. Except that, energy densification is a primary goal as well, since the pretreatment improves the LHV, so the transportation of the biomass fuel, for each gigajoule transported, becomes cheaper.

1.4.1 Steam explosion

Steam explosion or steam pretreatment is the most widely employed and extensively studied physicochemical pretreatment for lignocellulosic biomass[38]. It is a hydrothermal pretreatment, in which the biomass is subjected to pressurized steam, with pressures between 0.7 and 4.8 MPa, and

temperatures of about 160 – 240°C, for a period of time ranging from seconds to several minutes, and then suddenly depressurized. This pretreatment combines mechanical forces and chemical effects due to hydrolysis of acetyl groups present in hemicellulose. Autohydrolysis takes place when high temperatures promote the formation of acetic acid from the acetyl groups, while water as well can also act as an acid at high temperatures. The mechanical effects are caused because the pressure is suddenly reduced and fibers are separated owing to the explosive decompression. In combination with the partial hemicellulose hydrolysis and solubilization, the lignin is redistributed and to some extent removed from the material[39].

The most important factors affecting the effectiveness of steam explosion are particle size, temperature, residence time and the combined effect of both temperature (T) and time (t), which is described by the severity factor (R_0) [$R_0 = t \cdot e^{[T-100/14.75]}$] being the optimal conditions for maximum sugar yield a severity factor between 3.0 and 4.5[40]. Steam explosion, can be effectively enhanced by addition of H₂SO₄, CO₂ or SO₂ as a catalyst. The use of acid catalyst increases the recovery of hemicellulose sugars, decreases the production of inhibitory compounds and improve the enzymatic hydrolysis on the solid residue[41].

Steam explosion has several advantages compared to other pretreatment technologies, such as that it is an attractive process due to the limited use of chemicals, it does not result in excessive dilution of the resulting sugars and it requires low energy input with no recycling or environmental cost, compared to other pretreatment technologies. Although, steam explosion has several disadvantages, such as the incomplete destruction of lignin – carbohydrate matrix resulting in the risk of condensation and precipitation of soluble lignin components making the biomass less digestible, destruction of a portion of the xylan in hemicellulose and possible generation of fermentation inhibitors at higher temperatures, and the need to wash the hydrolysate, which may decrease overall saccharification yields by 20 – 25% initial dry matter due to removal of soluble sugars.

1.4.2 Dry Torrefaction

Dry torrefaction (DT) is a biomass pretreatment process that is considered the least severe form of thermochemical processing[37]. It is a low temperature process (200 – 300 °C) that takes place in the absence of oxygen, usually at atmospheric pressure at nitrogen atmosphere, for a duration of approximately 1 hour or less[42]. The process yields a solid product, biochar, that has improved combustion properties with an increased energy density than the original untreated biomass. Dry torrefaction induces changes in the biomass due to the thermal decomposition of hemicellulose and the partial depolymerisation of lignin and cellulose, which as a result produces a torrefied biomass with a higher carbon content, but a lower overall mass and a higher calorific value[43].

Additionally, torrefied biomass is hydrophobic, resistant to biological decomposition, has improved grindability and when pulverized it displays more uniform and smaller particle sizes, properties

which indicate better fuel characteristics for combustion and gasification purposes, similar to coal[44]. Furthermore, dry torrefaction pretreatment significantly removes oxygen from biomass and increases the heating value. Below are shown some different types of torrefaction reactors with their advantages and disadvantages.

Table 2: Advantages and Limitations of Different Types of Torrefaction Reactors

Reactor Type	Advantages	Disadvantages
Rotary drum	<ul style="list-style-type: none"> • Proven relatively simple equipment • Low pressure drop • Possibility of both direct and indirect heating 	<ul style="list-style-type: none"> • Lower heat transfer (specially in indirect heating) • Difficult to measure and control temperature • Less plug flow compared with other reactors • Bigger system size • Necessary proper drum sealing • Difficult in scaling up the system
Moving bed	<ul style="list-style-type: none"> • Simple reactor and its construction • Very good heat transfer • High bed density 	<ul style="list-style-type: none"> • Significant pressure drop • Difficult to control temperature
Screw type	<ul style="list-style-type: none"> • Possibility for plug flow • Mature technology for torrefaction 	<ul style="list-style-type: none"> • Indirect heating only • Higher possibility of hot spots • Lower heat transfer rate • Scale up problem • Requires shaft sealing
Multiple heart furnace	<ul style="list-style-type: none"> • Proven equipment design • Higher possibility of scale up • Close to plug flow • Good temperature and residence time control • Possibility of adding fines 	<ul style="list-style-type: none"> • Lower heat transfer rate compared with other direct reactors • Limited volumetric capacity • Relatively larger reactors • Require shaft sealing
Fluidized bed	<ul style="list-style-type: none"> • Excellent heat transfer rate • Easily scalable 	<ul style="list-style-type: none"> • Requires smaller particle size • Necessary to have additional gas equipment to supply fluidizing fluids • Possibility of attrition (fines formation) • Difficult to get pug flow

1.4.3 Hydrothermal Carbonization (Wet Torrefaction)

Hydrothermal carbonization (HTC) or wet torrefaction is a pretreatment process for lignocellulosic biomass where the biomass is treated with hot compressed water. The solid product of HTC is hydrochar, which is friable, hydrophobic and has increased energy densification compared to the raw biomass[45]. HTC is a method that has attracted a great deal of attention because it uses water, which is inherently present in green biomass, non-toxic, environmentally benign, and inexpensive medium.

Typical HTC of biomass is achieved in water at elevated temperatures (180 – 250 °C) under saturated pressured (2 – 10 MPa) for several hours[46]. Besides the solid product, this process, being exothermic, generates gas and aqueous chemicals. The mechanisms involved in the HTC of biomass generally differ the mechanisms of dry torrefaction, due to the presence of compressed water. A hydrolysis process mechanism is followed which cleaves the ester and ether bonds between molecules and in so doing, the activation energies for the polymerization reactions of the biomass polymers decrease. Consequently, the degradation of hemicellulose during HTC is higher than the dry torrefaction process[47].

Wet torrefaction is considered to be less toxic and more environmentally friendly compared to its counterparts, as the only input streams are the biomass itself, water and an inert gas. In addition, the fuel properties, including energy density of the torrefied product are superior to those obtained with DT. WT does not require a pre-drying of the raw biomass, making this form of pretreatment economically attractive. This implies a wider range of biomass feedstocks (including aquatic based biomass for example) may be suitable for WT pretreatment and ultimately the solid fuels produced have increased calorific value, improved grindability and pelletability, as well as a lower ash content[48]. Although, WT possesses some advantages over DT, it is not problem-free.

There are still some engineering challenges remaining for this technology. Since WT is carried out in an active medium and at relatively high temperatures and pressures, the major concern is the reactor material, which must, not only work at elevated pressures, but also withstand corrosion.

Another problem relates to the feedstock impurities, which are normally present at high percentage in biomass wastes and residues. If they are converted to inorganic salts during WT, these may cause some problems by precipitating, depositing and clogging the reactor.

Lastly, an important issue is the energy consumption needed for the heating of large amounts of water, which may account up to 20 % of the energy of the hydrochar. Below, some characteristics of biochar and hydrochar by Norway spruce are shown.

Table 3: Characteristics of hydrochars and biochar from Norway spruce on a same solid yield basis[48]

Characteristics	Hydrochar		Biochar
	WT 210°C	WT 222°C	DT 275°C
	30 min	5 min	60 min
Solid yield (%)	74.1	73.8	74.0
Higher Heating Value (MJ/kg)	22.4	22.6	22.1
Energy yield (%)	80.3	80.7	79.8
Proximate Analysis (wt% dry basis)			
Ash	0.1	0.1	0.2
Volatile Matter	82.6	81.5	75.7
Fixed Carbon	17.4	18.4	24.2
Ultimate analysis (wt% dry and ash free)			
C	55.2	55.7	55.4
H	6	6.1	5.7
N	0.1	0.1	0.1
O	38.7	38.1	38.8

1.5 Combined Heat and Power Plants with Biomass as fuel

The development of energy generation technologies is now focused on systems that are characterized by a high efficiency of energy conversion from fuels into useful energy that provide reduced emissions of pollutants into the atmosphere. In addition, it is essential to ensure energy security, in particular through the use of local energy sources in distributed power and heat generation systems. A very important issue now is also the reduction of dioxide emissions into the atmosphere by the power generation sector as stated by the global, but in particular by the European agenda[49].

Combined Heat and Power (CHP) configurations, either centralized or decentralized, are now deemed as one the most efficient technologies for energy saving. CHPs can be established in block buildings such as hospitals, or educational institutions, in towns, or big industries with high demand of heat energy. CHP technologies have many advantages compared to only power stations. They have an increased energy conversion efficiency amounting up to 80 %, reduced emissions, especially for CO₂, significant savings of economical sources since the power and heat are provided in affordable prices and they promote the decentralized configurations. Furthermore, having decentralized units ensures stability of energy and heat supply, while the variety of these units will enable the electricity and heat power market to offer competitive prices.

In the current stage, micro-CHP (power less than 100 kW) systems are merging on the market, with a promising prospect for the near future. With the introduction of more and more stringent environmental legislations and the increasing urgency to address climate change, renewable energy resources play a crucial role in replacing fossil fuels that power traditional CHP systems. Biomass has already been used extensively within Europe for heat and power generation with various technologies being developed for energy conversion in biomass-fueled CHP systems. Some of Europe's CHP systems are demonstrated below.

Table 4: Various CHP plants in European countries

Name	Location	Operator	Configuration	Fuel
Dél-Nyírségi	Hungary	Veolia Energy Hungary	1 X 20MW CHP	Wood
Hebbag	Switzerland	EKT Holding AG	630 kW CHP	Wood waste
Imavere	Estonia	AS Graanul Invest	1 X 10 MW CHP	Wood, Bark
Pfaffenhofen	Germany	Babcock & Wilcox Vølund	26.7 MWth 6 MWel	Wood, Wood saw waste
Roost	Luxemburg	Kiowatt SA	1 X 2.7 MW CHP	Wood
BMHKW Odenwald	Germany	Biomasseheizkraftwerk Odenwald GmbH	1 X 7.5 MW CHP	Scrap Wood, Straw, Forestry Wood

2. Steam Power and Heat Cycles

Conventional steam power plants are configurations based on the Rankine cycle, for the production of electricity and heat, through the combustion of a fuel in a steam boiler. A typical conventional steam power plant is a subcritical unit, in which the live steam parameters are 160 – 180 bar and 535 – 565 °C[50]. In order to increase the net efficiency of the plant and decrease the pollution and fuel consumption, the combustion process of steam boilers must be improved and the steam parameters increased. If the steam parameters are increased over 221 bar, but they remain below 250 bar and 593°C, the power plant is called a supercritical power plant (SC). In ultra-supercritical (USC) power plants, the pressure and temperature are higher than 250 bar and 593°C.

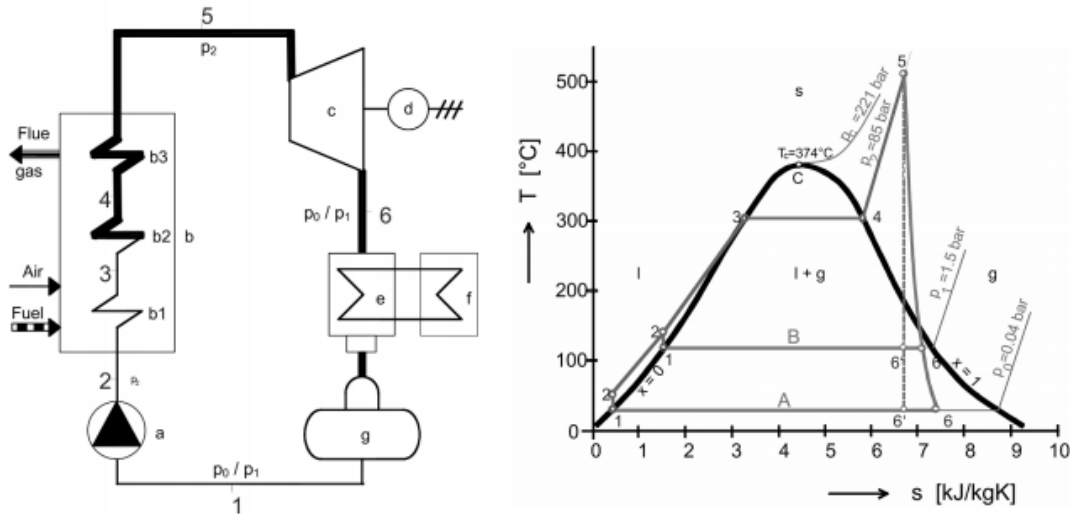


Figure 3: Flow and $T-s$ diagram of backpressure plant based on the Rankine cycle

There are various combustion systems for biomass fuels, but those in industrial application are three: Fixed Bed Combustion, Fluidized Bed Combustion and Pulverized Fuel Combustion. These furnaces are generally equipped with mechanical and pneumatic fuel-feeding systems. Moreover, modern industrial combustion plants are equipped with process control systems supporting fully automatic system operation. The basic principles of these three technologies are shown in the figure below.

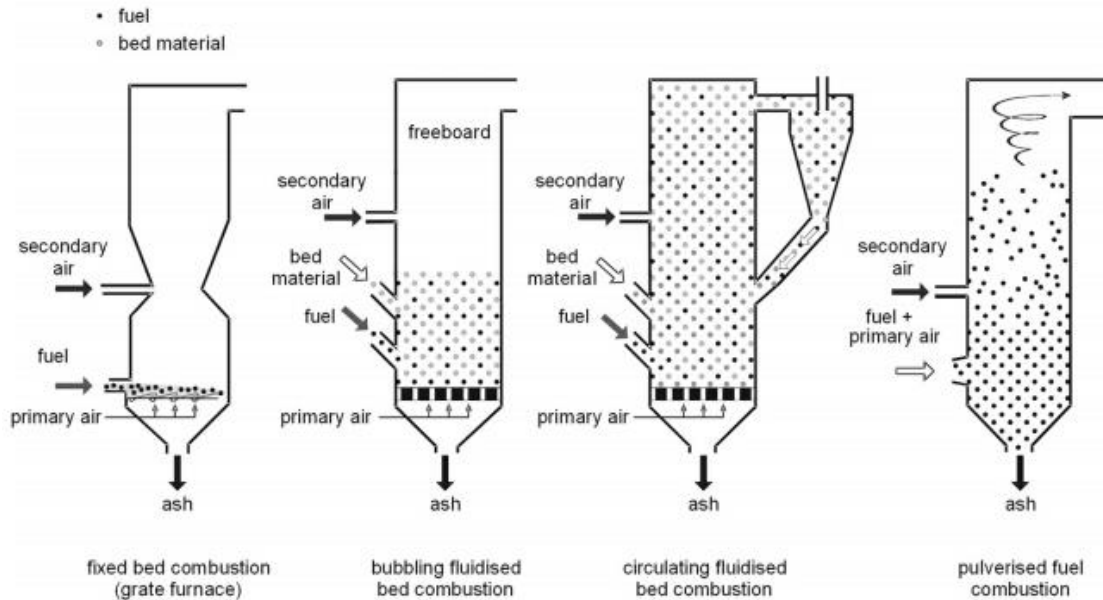


Figure 4: Principal combustion technologies for biomass

Fixed bed combustion systems include grate furnaces and underfeed stokers. Primary air passes through a fixed bed, in which drying, gasification and charcoal combustion take place. The combustible gases produced are burned after secondary air addition has taken place, usually in a combustion zone separated from the fuel bed.

Within a fluidized bed furnace, biomass fuel is burned in a self-mixing suspension of gas and solid-bed material into which combustion air enters from below. Depending on the fluidization velocity, bubbling fluidized bed (BFB) and circulating fluidized bed (CFB) combustion can be distinguished.

Pulverized fuel (PF) combustion is suitable for fuels available as small particles (average diameter smaller than 2mm). A mixture of fuel and primary combustion air is injected into the combustion chamber. Combustion takes place while the fuel is in suspension and gas burnout is achieved after secondary air addition.

Heat generated in a combustion process is used to produce high-pressure steam in a boiler, with typical pressure and temperature values as mentioned above. The steam is expanded to a lower pressure through the expansion engine and delivers mechanical power to drive an electricity generator. Large turbines in power stations are built as multistage expansion machines with up to more than 20 stages and live pressures of up to about 250 bar (for USC configurations), and with backpressures of less than 0.1 bar[9]. In such multistage turbines, with high-pressure ratios between inlet and outlet steam, high efficiencies of up to 40 % are achieved. For industrial applications and for small power stations based on biomass, typical live steam pressures of 70 – 80 bar and typical live steam temperatures of 400 – 500°C enable efficiencies of 20 – 30 %. Steam plants are based on the Rankine cycle, as mentioned above, with

water as the working medium. For practical applications, three design types and operational modes of steam plants can be distinguished:

- Back pressure plants with utilization of the total waste heat from the condensation of the steam. In such plants, the backpressure of the turbine corresponds the temperature needed for the heat utilization, i. e. typically close to or greater than 1 bar and 100°C.
- Condensing plants for power production without heat utilization. The backpressure and the corresponding temperature are as low as possible to achieve maximum electrical efficiency, hence the temperature is close to ambient temperature while the backpressure is significantly below 0.1 bar corresponding to 46°C.
- Extraction plants, used as extraction condensing plants or extraction backpressure plants, for power production with variable heat output. Such a plant enables a variable extraction of steam at an intermediate pressure and temperature level for heat utilization, with the remaining steam being utilized to drive an additional low-pressure section of the turbine in condensing mode. It combines the advantages of backpressure and condensing plants but exhibits higher complexity. With this kind of plant, except its flexibility, superheated steam can be utilized for various processes, for example superheated steam used in Aluminum plants.

CHP production, or co-generation, is performed by back pressure plants and by extraction plants. Condensing plants exclude heat utilization and are thus for dedicated power production. Reasonable efficiencies of condensing plants demand medium or large scale power plants ranging from at 24 MW_e to more than 500 MW_e, since smaller applications achieve only poor electrical efficiencies. Backpressure steam turbines with utilization of the total waste heat from the condensation of the steam are typically in the range of 0.5 – 5 MW_e, while extraction turbines are typical applications of greater than 5 MW_e. There are several advantages and disadvantages considering biomass combustion Combined Heat and Power plants. These are presented below.

Table 5: Advantages and disadvantages of steam turbines

Advantages	Disadvantages
Mature, proven technology	Only limited efficiencies are reached in small, decentralized plants due to investment and technology limitations
Broad power range available	High specific investment for low power ranges
Separation between fuel and thermal cycle, enabling the use of fuel containing ash and contaminants	High operation costs for small and medium plants
High pressures and temperatures can be applied enabling high efficiencies for large plants	Low part-load efficiencies
Co-firing of fossil fuels and biomass is possible to enable high efficiency	Variations in fuel quality lead to variation of steam and power production
	Superheater temperature (and therefore efficiency) can be limited due to high temperature corrosion and fouling, especially due to alkali metals, chlorine and sulphur
	High quality steam is necessary

2.1 Boiler Technologies

The thermodynamic efficiency of the Rankine steam cycle increases if temperature and pressure of the superheated live steam entering the turbine are raised. When steam pressure and superheat temperature are increased above 221 bar and 540 °C the steam becomes supercritical (SC). In supercritical conditions, heated water does not produce a two phase mixture of liquid and steam as in subcritical steam, but instead it changes directly from liquid to steam. The boiler is classified as ultra-supercritical (USC) when the main and reheat steam temperatures exceed 580 °C. In subcritical once-through boilers superheat pressure is around 180 bar and temperature is around 540 °C. The operating ranges of subcritical, supercritical and ultra-supercritical boilers are illustrated below.

Table 6: Boiler technologies characteristics

	Steam Pressure [bar]	Steam Temperature [°C]	Plant Efficiency [%]
Subcritical	<221	<565	33-39
Supercritical (SC)	221-250	540-580	38-42
Ultrasupercritical	>250	>580	>42

Efficiency of a USC plant can be as high as 45 % when efficiency of subcritical plant is around 35 %. A potential 50 % efficiency is foreseen for advanced USC technology with the availability of proper boiler materials, providing steam parameters of 300 bar and 700 °C or even 760 °C. USC technology is a cost effective option to reduce emissions of generated electricity. As the efficiency of the plant is increased, less fuel is burned per unit of electricity generated. Since coal-fired power plants are under pressure due to ever-tightening emission restrictions, USC technology provides one solution to this problem[51].

Increasing steam pressures and temperatures pose new challenges for the materials used in the boiler. Conventional boiler materials are not able to last long, and the damage of exposure would happen quickly in USC conditions. Nickel alloys are usually used in USC boilers and steam turbines. Research is focusing on the development of new steels for boiler tubes and on high alloy steels that are resistant to corrosion and thermal cycling, a feature absolutely necessary to current plants, which operate in transitional states and not in nominal capacity.

2.2 Steam Power Plants Control

Control engineering is applied to steam power plants in order to produce desired thermal output of the boiler and desired power output of the plant, as well as to operate the boiler at lowest cost for fuel and other boiler inputs, consistent with high levels of safety and full boiler design life. In addition, the produced live steam must have the correct temperature and pressure, and the produced electricity must have the correct voltage and frequency. The control system must ensure a safe start up, shutdown, monitor online operation, detect unsafe conditions and take appropriate actions for safe operation. These objectives are achieved in steam power plants by applying a coordinative control strategy between the steam boiler, turbine and generator without overloading the components[52]. The coordinative control strategy combines the controls of the fuel power, generator power, turbine power, steam pressure and temperature, air control, feedwater control and furnace pressure control.

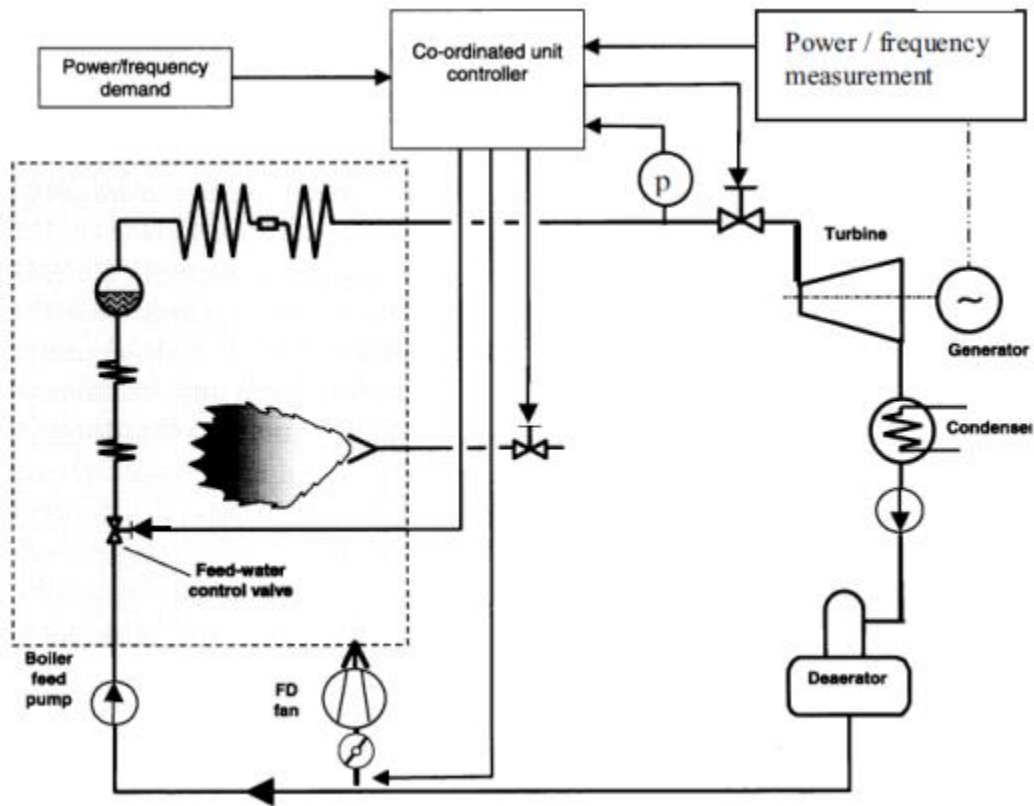


Figure 5: Depiction of the parameters being controlled

2.2.1 Fuel Flow Control

Fuel flow into the furnace is determined by the block control as a function of power output set point. Usually a simple linear or quadratic function between the load and coal flow is designed. The fuel composition, heat value and moisture content depend on the type of the fuel and plants utilize different types of fuels. Therefore, the fuel flow set point is adjusted with heat value correction. Heat value correction is based on the enthalpy difference between water at the inlet of the boiler and steam at the outlet of the boiler. Designed enthalpy difference is compared with measured enthalpy difference and the coal heat value is corrected according to the enthalpy deviation. Thereby the changing fuel content can be considered in the fuel feed control.

2.2.2 Feedwater Control

In once-through boilers the control of the water-steam balance is based on measurements of feedwater flow, steam mass flow and temperatures. The feedwater flow set point is a function of the power set point and it is typically adjusted with enthalpy correction. Enthalpy correction is based on the desired enthalpy of the steam after the evaporator. Steam enthalpy after the evaporator is calculated as a function of temperature and pressure, which are measured from the process. Calculated enthalpy is compared with the design enthalpy which is also a function of the power set point. The deviation of these two leads to a correction in the feedwater flow.

Feedwater flow and pressure can be controlled either with control valve or with feed water pump. In addition, combination between these two can be used. Nowadays control with feedwater pump is implemented with a frequency converter which provides a fast and accurate control. Control with a control valve is a cheaper option, but disadvantage is the pressure loss that it produces. The sensitivity of feedwater control is dependent on the ratio of water volume in the steam drum and the overall water volume in the boiler: the smaller the volume ratio is, the more sensitive the system is[53].

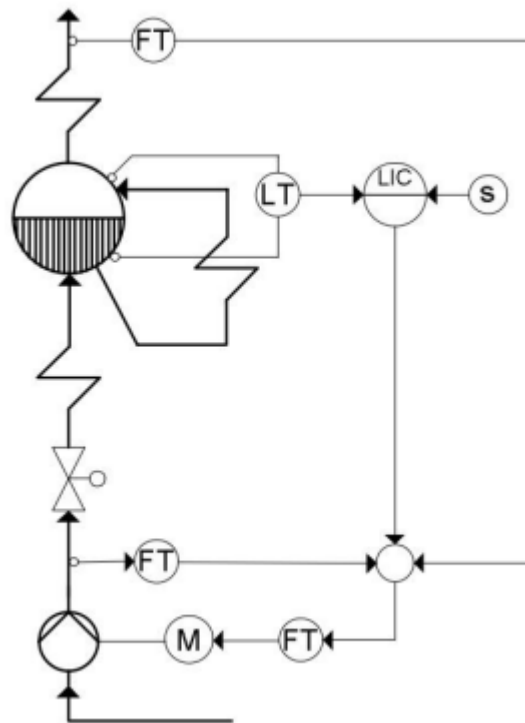


Figure 6: Three element feedwater control in steam drum boilers. FT = Flow transmitter, LT = Level Transmitter, LIC = Level Indication and automatic control, s = set point, M = Motor[52].

2.2.3 Steam pressure Control

Power plants can be operated in either fixed pressure or sliding pressure control mode. The fixed pressure stands for keeping the live steam pressure constant at all levels of power output. Thus, the enthalpy drop in the turbine is constant and the power output of the plant is adjusted by the live steam mass flow rate. The fixed pressure control method can follow two different modes, one for the boiler and one for the turbine. In the boiler follow mode, the live steam pressure is kept constant by fuel feeding, as the main steam valve of the steam boiler adjusts the power output of the plant. In boiler follow mode, if the power output of the plant is increased, the main steam valve is opened, which decreases the live steam pressure. Thus, the fuel feeding is increased in order to compensate the pressure decrease accordingly. On the other hand, in the turbine follow mode the live steam pressure is kept constant by the main steam valve of steam boiler, as the power output is adjusted by fuel feeding. If the power output is increased, the fuel feeding is increased, which raises the live steam pressure. Thus, the main steam valve is opened accordingly[52].

In natural sliding pressure mode, turbine control valve is constantly in fully open position, and the power output of the unit is controlled with fuel feed to the furnace. In modified or throttled sliding pressure mode, the turbine control valve is slightly throttled, so that fast limited load changes can be executed by adjusting the valve position. In sliding pressure mode, both in the natural and modified modes, steam pressure varies as function of load and a certain variant pressure correspond the power produced by the turbine. As the turbine power, boiler thermal power and feedwater flow increase also the steam pressure rises. Therefore, the steam pressure is not directly controlled but it slides as a function of the power. The turbine power is controlled by adjusting the fuel flow into the boiler[53].

2.2.4 Steam Temperature Control

To maximize the efficiency of the power plant, the temperature of the superheated steam is designed as high as possible. Function of steam temperature control is to keep steam temperature in its set point value to prevent exceeding of maximum material temperatures and too fast temperature transients. Also, the turbine has its own restrictions considering steam temperature and transient rate of the temperature.

The temperature of superheated steam is controlled by various methods. Spray cooling of the steam consists of the most common method as it provides the easiest implementation, cost efficiency and simplicity. The spray cooling water is usually taken after the feedwater pump and its amount is controlled by the temperature of the steam before and after the superheater and the power set point. Spray cooling is achieved through Attemperators. In addition to water, steam of lower temperature can be used as a cooling medium[53].

Another method for the temperature control is the by-passing of flue gases. Through this method, flue gases are redirected in the furnace, leading it to cool down, worsen the heat transfer based on radiation, but improving heat transfer through convection. Lastly, a heat exchanger between superheaters

could be used, in order to draw heat from the steam and cool it down, although this method is way more expensive than the previously mentioned methods.

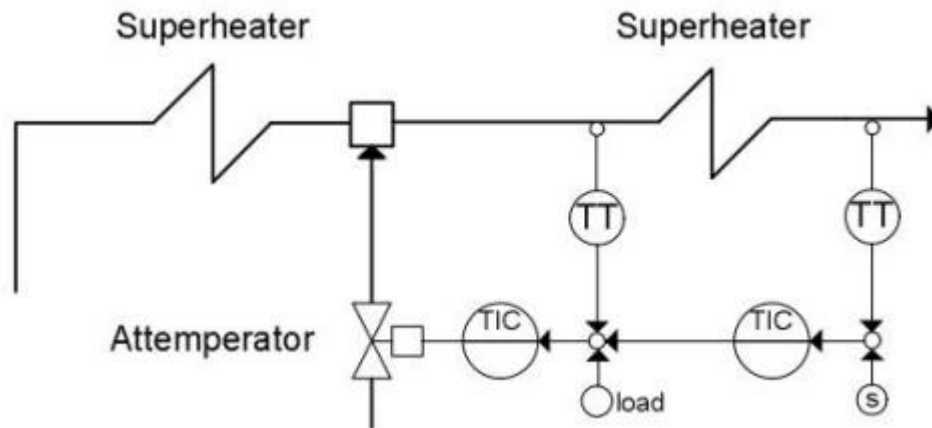


Figure 7: Depiction of spray cooling steam temperature control. IT = Temperature transmitter, TIC = Temperature indication and control, s = Set point[52].

2.2.5 Air Flow Control

Air-fuel ratio is kept at desired level by controlling the amount of combustion air in the furnace. The combustion will be incomplete, if there is not enough air in the furnace. On the other hand excess air in the furnace produces flue gas losses, and nitrogen oxide emissions will increase. The main control criteria in combustion air control are the fuel flow to the boiler and the concentration of oxygen in the flue gas. In practice air flow is controlled according to boiler load set point and in parallel with the fuel flow control. Also, there can be a feedforward from the fuel flow to the air flow control, so disturbances can be predicted before they can be seen in the boiler load. Because the mass flow of the solid fuel cannot be measured accurately, oxygen (O_2) correction is used to correct the amount of combustion air in the furnace. Oxygen analysis of the flue gas is forwarded as a feedback to the air flow controller. O_2 -correction is used as a fine adjustment in the combustion air control[53].

2.2.6 Furnace pressure control

Furnace pressure is a key component for the plant, as combustion quality is dependent on stable pressure inside the furnace. An induced draft fan controls furnace pressure, with its speed, inlet guide vanes or blade angles are adjusted accordingly to the desired pressure. Furthermore, the pressure

inside the furnace is designed to be lower than the ambient pressure, in order to ensure that no leakage occurs from the furnace[53].

2.3 Modelling of power plants

A dynamic simulation tool is especially useful for power systems, especially decentralized ones, such as biomass fueled CHP's, because they must be able to operate in transient mode for most of the time. Due to technological and economic reasons, the plant is operated in thermal-load following mode and the thermal load depends on highly fluctuating demand for process heat, either due to the heating of houses or industrial heat loads. The need for a dynamic simulation tool also comes from the necessity of designing a fast response control system, in case the calorific value of the biomass fuel is bound to change continuously due to the varying composition of the feedstock. Finally, a possibility is the use of such a tool for cogeneration plants operated in electric-load following mode. The control requirements might become challenging for the turbine island operation of such plants, if there are strong and fast variations of the electrical demand.

This could be the case in the future, if such plants are adopted in the remote agricultural areas of developing countries. Dynamic models of small power output systems are not only useful to capture and predict the unsteady behavior of the plant, but may also be used to study real-time control strategies. In the future this kind of dynamic models could be embedded in the so-called model-predictive controllers, where the dynamics of the plant is canceled out by the inverted model of the plant to obtain (in theory) a perfect controller.

Furthermore, dynamic simulation tools are necessary for the design engineering of a power plant and the estimation of its future operation. Through such a tool, the dimensioning of all the components, such as heat exchangers, steam turbines, pipes, fans, condensers, extractions etc. can be simulated and through a preliminary analysis, an exergetic and economic optimization can be achieved. Lastly, dynamic process simulation can be used for operator training: the plant simulator can be used to allow operators to test emergency and unconventional procedures and help them understand how to set the best control parameters for obtaining the best economical and technical performance of the plant.

2.3.1 Advanced Process Simulator - Apros

Apros is a commercial software package developed, designed for the modelling of various industrial processes including their automation and electrical components. It has been developed by Fortum and VTT Technical Research Centre of Finland since 1986. It provides a wide variety of specialized component libraries and solution techniques for the dynamic simulation of power plants. Apros uses two kinds of thermal hydraulics modules, providing the user with more options. These are the homogenous flow model, and the heterogeneous flow model.

- Homogeneous flow model

The one-dimensional homogeneous flow model (also known as three-equation or mixture flow model) is based on the one-dimensional conservation equations of the mixture. This flow model is suited for single-phase flow components including either water or steam such as superheater, reheater, turbine sections and economizers. In case of two-phase flow components such as evaporator and condenser, the water and steam in this model have same velocity, pressure and temperature. The partial differential equations are discretized with respect to space and time and the non-linear terms are linearized.

Mass Balance Equation:

$$\frac{\partial \rho}{\partial t} + \frac{\partial(\rho u)}{\partial z} = 0 \quad (1)$$

Momentum Balance Equation:

$$\frac{\partial(\rho u)}{\partial t} + \frac{\partial(\rho u^2)}{\partial z} + \frac{\partial p}{\partial z} = F_{gra} + F_{wall} \quad (2)$$

Energy Balance Equation:

$$\frac{\partial(\rho h_0)}{\partial t} + \frac{\partial(\rho u h_0)}{\partial z} = \frac{\partial p}{\partial t} + Q_{wall} \quad (3)$$

In the above equations, the symbols ρ and u denote to the density and longitudinal velocity of fluid, respectively. The symbol t represents time, z represents the axial direction, F_{gra} is the gravitational acceleration force, F_{wall} and Q_{wall} represent the friction force and the heat flow through walls. The total enthalpy (stagnation enthalpy) h_0 is the static enthalpy including the kinetic energy of the flow.

- Heterogeneous flow model

The heterogeneous flow model (also known as two-phase, six equation or Euler–Euler flow model) is suited for two-phase flow water/steam components, where there is a slip between phases. The solution of the heterogeneous flow model is based on the one-dimensional conservation equations of mass, momentum, and energy for each phase (water and steam).

Mass Balance Equation:

$$\frac{\partial(\chi_k \rho_k)}{\partial t} + \frac{\partial(\chi_k \rho_k u_k)}{\partial z} = \Gamma_k \quad (4)$$

Momentum Balance Equation:

$$\frac{\partial(\chi_k \rho_k u_k)}{\partial t} + \frac{\partial(\chi_k \rho_k u_k^2)}{\partial z} + \chi_k \frac{\partial p}{\partial z} = \Gamma_k u_{ik} + \chi_k F_{gra,k} + F_{wall,k} + F_{ik} + F_{va} + F_{fl} + \Delta p_{pu} \quad (5)$$

Energy Balance Equation:

$$\frac{\partial(\chi_k \rho_k h_{0,k})}{\partial t} + \frac{\partial(\chi_k \rho_k u_k h_{0,k})}{\partial z} = \chi_k \frac{\partial p}{\partial t} + \Gamma_k h_{0,ik} + F_{ik} u_{ik} + Q_{wall,k} + Q_{ik} \quad (6)$$

The subscript k denotes to l = liquid or g = gas. The subscript ik refers to the interface between two phases and the subscript wall, k represents the interface between one phase and the wall. The term Γ is the mass exchange rate between the phases (i.e. water and steam), while the term χ stands for the steam dryness fraction. The interfacial heat transfer Q_{ik} is separately calculated for gas and liquid phase. The wall heat transfer $Q_{wall,k}$ is determined according to the heat transfer zone. The interfacial friction F_{ik} (so-called the friction between the liquid and gas phases) is obtained as a weighted average of the different correlations depending on the flow regimes. The three last terms of equation (5) correspond to friction created by valves, from pipe configurations and the rise of pressure by the pumps respectively. In equation (6), as in the homogenous flow, the enthalpy h_0 includes the kinetic energy $h_{kin} = u^2/2$ as well.

2.3.2 Aspen Plus Dynamics

Aspen Plus Dynamics was developed originally as a joint effort between the United States Department of Energy and Massachusetts Institute of Technology under the name of Advanced System for Process Engineering (ASPEN). Compared to Apros, Aspen Plus Dynamics has only the homogenous flow model. The thermal hydraulics modules are described through the use of three major principles: conservation of mass, conservation of momentum and conservation of energy.

Mass Balance Equation:

$$\frac{\partial c}{\partial t} + \frac{1}{A} \frac{\partial \dot{c}}{\partial z} = 0 \quad (7)$$

Momentum Balance Equation:

$$\frac{\partial(\rho u)}{\partial t} + \frac{1}{A} \frac{\partial(\dot{m}u)}{\partial z} + \frac{\partial p}{\partial z} = F_{gra} + F_{fri} \quad (8)$$

Energy Balance Equation:

$$\frac{\partial(\rho h)}{\partial t} + \frac{1}{A} \frac{\partial(\dot{m}h)}{\partial z} = Q_{wall} \quad (9)$$

Here z and t are the axial position and time as well, ρ and u denote to the density and the vertical velocity, C is the molar concentration, \dot{C} and \dot{m} represents the molar and mass flow rate, respectively. The term Q_{wall} describes the heat flow from fluid to surroundings through walls. The terms F_{gra} and F_{fri} are the gravitational acceleration and the friction forces per unit fluid volume.

2.3.3 GateCycle

GateCycle is a commercial simulation tool used for design and performance evaluation of thermal power plant systems for both new and operating projects. The software combines an intuitive, graphical user interface with detailed analytical models for the thermodynamic, heat-transfer and fluid-mechanical processes within power plants. GateCycle can accurately predict the performance of combined cycle plants, simple cycle plants, conventional Rankine cycle plants co-generation systems, and many other energy systems, such as gas turbines fueled by biomass-derived syngas.

GateCycle would generally not be used as a pre-screening tool, as it is a complex piece of software that requires experience to use; however, it can be used for pre-feasibility all the way to plant acceptance. Since the tool is used to evaluate power and heat generation, renewable energy resource simulation would be limited to biomass, landfill gas, and waste-to-energy.

In the design mode of the software, the user specifies the performance attributes that are required, and the software identifies the equipment to match the performance criteria. The tool also works in the opposite way, where the user defines operational conditions, and the tool calculates the corresponding “as-built” performance. GateCycle provides both simple and in-depth analyses within the interface, allowing it to provide results for any situation needed. As described previously, the software has the capability to model equipment “as built”, meaning you can still be designing the plant.

GateCycle models are extremely flexible, allowing an indefinite number of calculation cases to cover variations in design parameters, as well as plant performance (if the plant is under “off-design” conditions)[28].

This software is capable of analyzing the efficiency of every power system that can be built from the individual components its tool window offers. The Toolbox contains equipment modules such as: Turbines (Gas and Steam), Heat Exchangers (Economizers, Superheaters, Boilers, Condensers, Preheaters), Pumps, Pipes, Valves etc. In order to create a model in GateCycle, the user chooses the desired equipment icons from the toolbox, places them in the model sheet and connects them. The software performs some logical checks in order to ensure that the connections are right.

In order to commence the calculations with GateCycle, the required properties must be inserted, in order for the design and operation conditions for each equipment icon and the whole model to be defined. There are two categories of properties, the system properties and the equipment properties.

The system properties can be accessed through the Properties Editor. The system properties include specific values for the control of the calculations. Some of these properties are the number of iterations and the convergence criterion so that the calculation can converge in a single value without oscillations, as well as steam-water properties libraries, generator losses, ambient pressure and temperature and power losses of type BOP (Balance of Plant).

The equipment properties are accessible through the Properties window of each equipment icon, by double clicking it. For every simulation of GateCycle, only some properties are required as inputs, while the others are not altered from the default value. The parameters in the Properties window define the calculation methods that will be used for the simulation of the cycle and the analysis of the steam cycle.

After the model is completed, the Run button can be pressed. As soon as the button is pressed the software follows the below mentioned steps:

- The software reads all of the connection and equipment icons properties from the model diagram and its libraries.
- It analyzes the connection properties in order to define the order of which the calculations will be performed for the equipment icons. This procedure ensures that every equipment icon is part of the calculations and the chosen order allows the iterations to be quick and efficient.
- It reads again the system and equipment icons properties from its libraries.
- It checks whether the input properties are right.
- It defines all of the parameters that the user has not defined.
- It locates all of the pressure and flow values inside the system and makes sure that the set configuration is consistent throughout the model and for the whole duration of the iterations.
- It analyzes the system's efficiency, calling the proper routine for the calculation of each component, one at a time, with the order defined above. After the routine returns its values, the results of each equipment icon are linked with all of the other equipment icons connected with the now calculated component. An iteration is complete when the above procedure is completed for every equipment component.
- Then the software checks if the results for each one of the equipment components fits with the values of the previous iteration, with the abovementioned convergence criterion.
- The simulation is complete when there is a mass and energy balance for each of the components, as well as for the whole system.

A typical GateCycle simulation converges with 2 to 40 iterations, according to the complexity of the model, the convergence criterion and the accuracy and suitability of the initial values in the libraries for the given simulation.

2.4 Cogeneration Plant for Aluminum of Greece

Next to the factory of Aluminum of Greece a cogeneration, high efficiency, power plant for electricity and thermal power was built in 2008. Its nominal power amounts to 334 MWel and it operates on natural gas. Its outputs are thermal power, which is used for the production of Alumina as well electricity, which is provided to the national grid. The plant consists of the below components:

- Two gas turbines of nominal power of 125 MW each, with natural gas combustion chambers of 33.33% efficiency. After some improvements, their nominal power amounts now to 135 MW each.
- A steam turbine of nominal power of 84 MW with a minimum operating power of 5.6 MW.
- A condenser with pressure of 0.5172 bar and temperature of 82 °C, using seawater for the condensation of the outlet steam from the steam turbine.
- Two heat recovery steam boilers, with the purpose of creating enough steam for the production of electricity with the steam turbine and the needs of the Aluminum Plant. These needs consist of 156.85 tn/hr of 68 bar and 480 °C steam, 27.75 tn/hr of 68 bar and 290 °C steam and lastly 40.6 tn/hr of 15 bar and 290 °C steam.
- An auxiliary boiler of binary fuel combustion, capable of creating 100 tn/hr of 63 bar and 485 °C steam, with an efficiency of 94% with natural gas as a fuel, which operates only when both of the gas turbines are off, feeding only one of the production lines of the Aluminum plant.
- A natural gas preheating system, which warms it up from 15 °C to 70 °C, with the concentrates returning from the Aluminum plant.

On a daily basis, the gas turbines operate on an alternating schedule, at nearly maximum power. Because of that, the steam turbine operates at 10 MW, namely a much lower power output than the nominal. As it is stated above, the main purpose of this power plant is feeding the Aluminum plant with steam of high and intermediate pressure. This means that these two plants are directly connected, which means that the power plant must be operational constantly and as planned.



Figure 8: Cogen Power Plant beside the Aluminum of Greece Plant

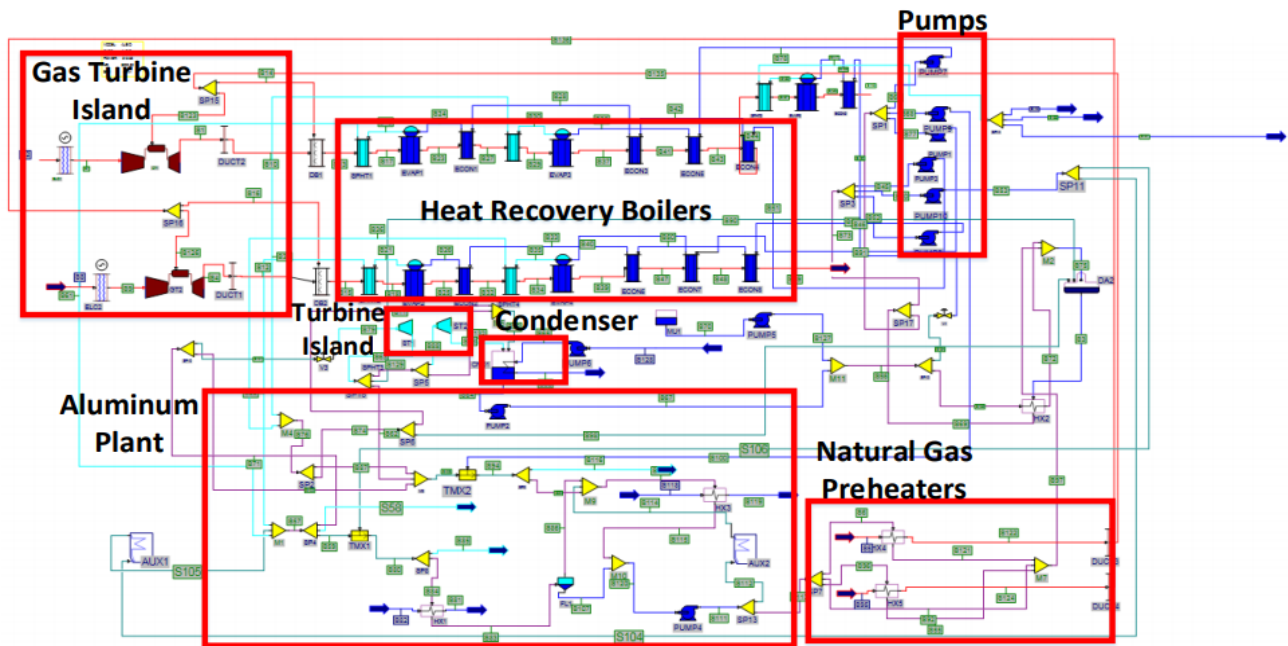


Figure 9: Cogen Power Plant model in GateCycle

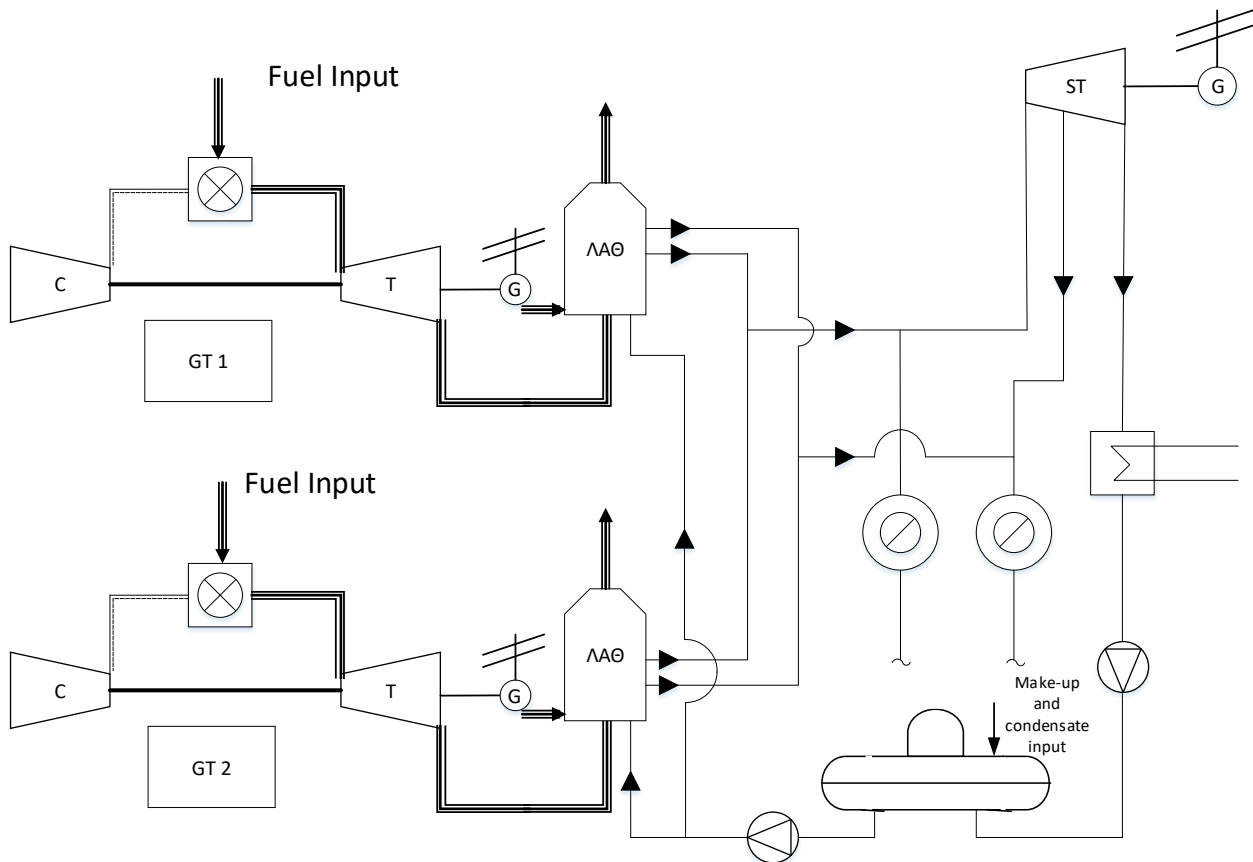


Figure 10: Schematic of the Cogeneration Power Plant beside the Aluminum of Greece Plant

As it is shown in the figures 9 and 10, the model of the power plant is quite complex, because of the many parameters that have to be taken into account. For example, that heat recovery steam boilers are modeled as a series of economizers (deep blue icons), evaporators (deep blue icons with a light blue top) and superheaters (light blue icons). In addition to that, just before the gas turbines, two electrical chillers are installed in order to ensure the maximum available power output from them.

There are also two auxiliary boilers, in order to simulate a state of emergency steam flow demand. The number of pumps, splitters and mixers is high due to the need of ultimate control of the steam flows. The thermal needs of the Aluminum plant are quite specific so the model is full of control equipment and temperature control mixers.

3.Modified CHP Plant

One of the two purposes of this thesis was to build a new configuration of power plant, which produces the same amount of steam for the Aluminum plant and electricity solely from the steam turbine. This means that the new power plant has now no gas turbines, thus no heat recovery steam boilers, but instead a fluidized bed boiler with four different types of biomass fuel, namely Empty Fruit Bunch (EFB), Spruce wood, torrefied Empty Fruit Bunch and torrefied Spruce wood.

The fluidized bed boiler will produce as much heat power as needed for the different scenarios of heat demand, having the electricity production at a stable level, in order to compensate for the loss of the two gas turbines. These scenarios take place a few days of the year because of maintenance regulations.

So, as it is mentioned above, the usual operation of the power plant consists of 156.85 tn/hr of 68 bar and 480 °C steam, 27.75 tn/hr of 68 bar and 290 °C steam and 40.6 tn/hr of 15 bar and 290 °C steam for 342 days a year. The second scenario consists of 80.55 tn/hr of 68 bar and 480 °C steam, 27.75 tn/hr of 68 bar and 290 °C steam and 40 tn/hr of 15 bar and 290 °C steam for 9 days a year. Lastly, the third scenario consists of 53.15 tn/hr of 68 bar and 480 °C steam, 27.75 tn/hr of 68 bar and 290 °C steam and 40 tn/hr of 15 bar and 290 °C steam for 14 days a year.

The model was highly modified, but the part of the thermal needs modelling remained intact, since the main purpose of both power plants is to fulfill the needs of the Aluminum plant. The new model of the power plant is presented below:

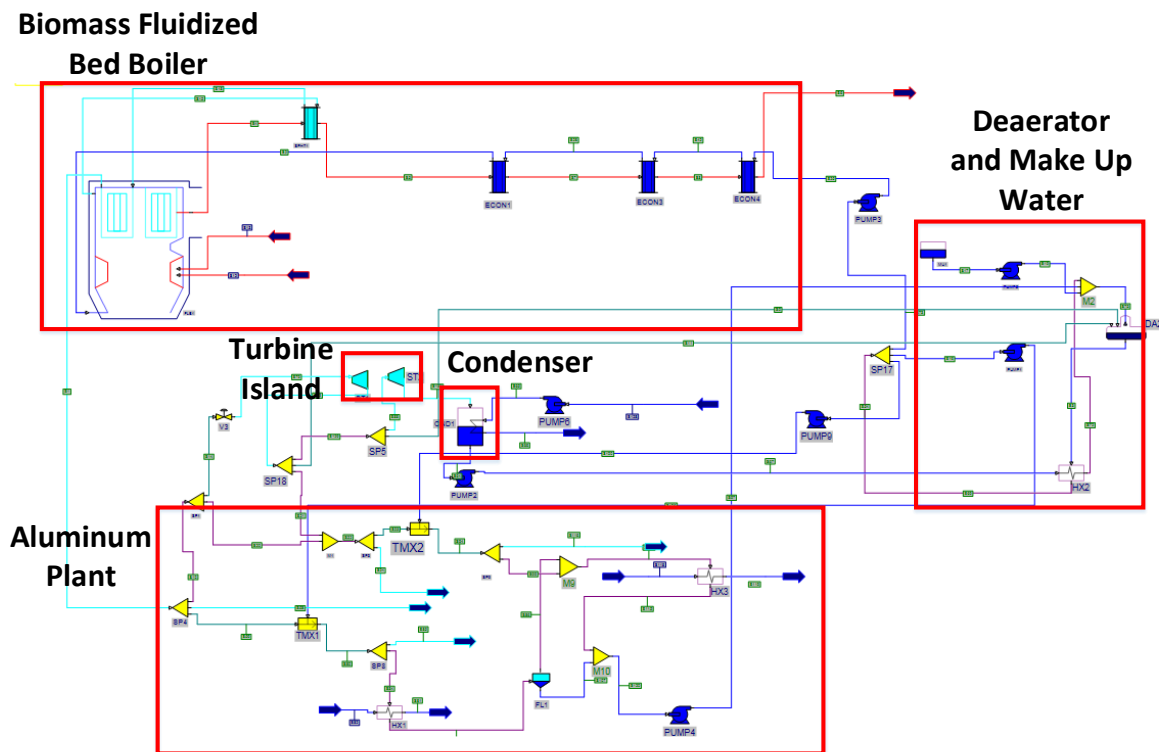


Figure 11: Biomass fueled power plant

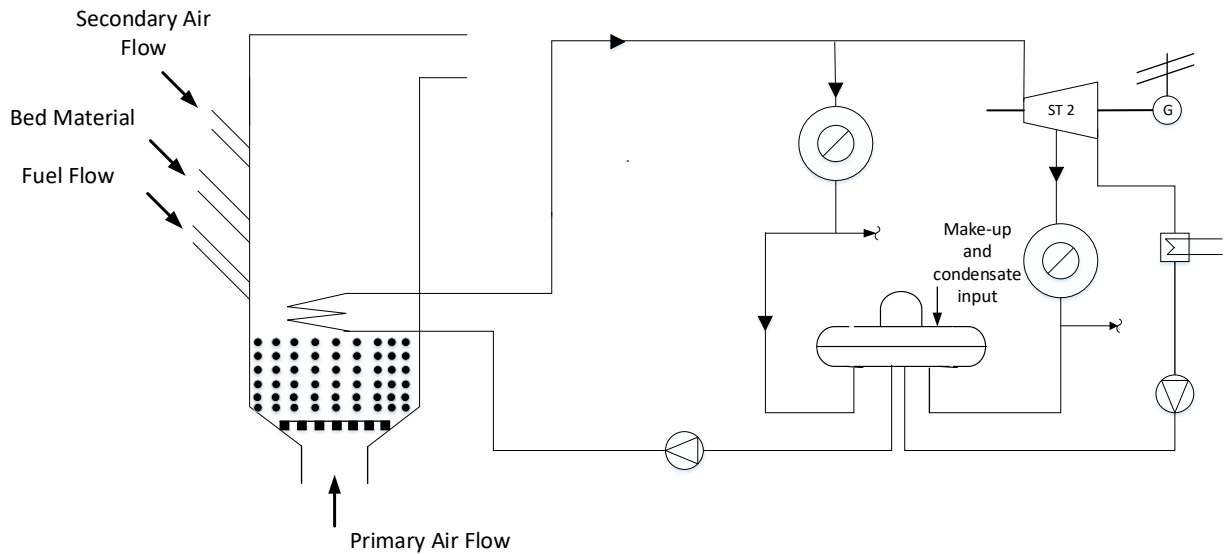


Figure 12: Schematic of the Biomass fueled power plant

As it is shown in figure 11, the model is now less complex because of the fluidized bed boiler component, which includes libraries for a superheater and an evaporator module. So only three economizer and one superheater component are needed in order to model the heat, the exhaust gases from the gas turbines, generate. In addition, the preheating system of the natural gas is unnecessary, since this CHP plant will be fueled with biomass. The preheating system is shown in figure 9 at the bottom right corner, modeled as two heat exchangers. Except the preheating system, the auxiliary boilers are also unnecessary, since the fluidized bed boiler can provide any excess heat, should it be required.

Although most of the configuration was modified, the turbine island and the heat demand parts were intact, since they are directly connected with the Aluminum plant. As one can see, not only steam is required by the Aluminum plant, but also heat transferred with two heat exchangers as shown in figure 11.

3.1 Presentation of the GateCycle components

Below, all of the components' properties windows will be shown, in order to clarify the inputs required for the model, as well as to prove that it works well and its outputs are the desired ones. Every component, as mentioned above, can receive inputs by the user or operate with default values. Although the input values are really easy to insert, each component must be in compliance with the components connected with it. Namely, the user must insert values that allow the software to start its calculations smoothly, otherwise the software will not run due to errors or it will perform calculations without converging.

3.1.1 Fluidized Bed Boiler – FLB

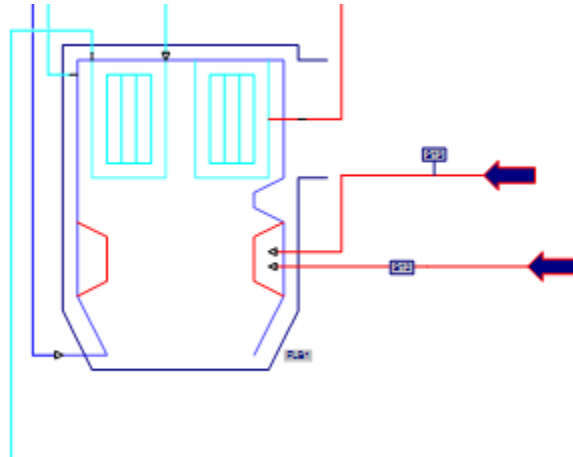


Figure 13: Fluidized Bed Boiler icon

Fluidized Bed Boiler

UOM Report Help Steam

ID: Description:

Boiler Load Method: tonm/hr

Specify Fuel Mix by:

Fuels	Fuel Mix (Mass):
Solid: <input type="text" value="Settings"/>	<input type="text" value="1.0000"/>
Gas: <input type="text" value="Settings"/>	<input type="text" value="0.00000"/>
Oil: <input type="text" value="Settings"/>	<input type="text" value="0.00000"/>

BFW Damping Factor:

Run Off Design Do Not Overwrite

Exit the window after saving all data

Figure 14: Boiler - General input window

The inputs on this window consist of the total water mass flow passing through the boiler, as well as the fuel mix inserted to it. In our model the fraction of the solid fuel is 1, meaning that the boilers operates only with solid fuels such as biomass.

Boiler-Solid Fuel Settings

UOM Define Help Steam

ID: Description:

Ultimate Analysis Method: Heating Value Method: kJ/kg

Ultimate Analysis by Weight:		Proximate Analysis by Weight:	
Carbon (C):	0.55756	Volatile Matter:	0.38919
Hydrogen (H):	0.054299	Fixed Carbon:	0.59245
Oxygen (O):	0.38376	Ash:	0.018360
Nitrogen (N):	0.0036675	Water:	0.00000
Sulfur (S):	0.00071312		

Pulverizer Specific Power Consumption: kJ/kg

Fuel Inlet Temperature: C

Exit the window after saving all data

Figure 15: Boiler - Fuel input window

In the fuel input window, the user defines either the ultimate analysis by weight or the proximate analysis by weight of the fuel, as well as the fuel inlet temperature and its Lower Heating Value (LHV). The analysis of the fuel together with its LHV can be as received, moisture free or moisture and ash free. The user can open the fuel input window by clicking the “Settings” button, as shown in figure 15.

Boiler-Design

UOM Define Help Steam

ID: Description:

Water Walls Design Method:

Superheater Design Method:
 C

Reheater Design Method:
 C

Exit the window after saving all data

Figure 16: Boiler – Design input window

In the Boiler-Design window, the user inserts the desired temperature of the superheated steam exiting the boiler, as well as the quality of the steam and the temperature of the reheated steam, should there be one. In case the boiler has no reheating steam as input, only the “Water Walls Design Method” and the “Superheater Design Method” are shown in this window.

The last input window for the FLB is the combustion window, in which the user defines the excess air required for the combustion of the fuel, as well as the temperature of the exhaust gases from this component. Since this component cannot simulate a whole fluidized boiler by itself, some additional components of economizers and superheaters are required. These exhaust gases pass through the additional components, cooling off each time they offer their heat to the water or steam flow. The exhaust gases temperature of the FLB is a key factor for the calculations of the cycle.

Fluidized Bed Boiler-Combustion			
UOM	Define	Help	Steam
ID :	FLB1	Description:	Fluidized Bed Boiler
Combustion Controls:			
Fraction Excess Air	▼	0.70000	Fraction
Flue Gas Exit Temperature:		727.00	C
Primary Combustion Air:			
Weight Fraction of Coal Input:		0.00000	
Weight Fraction of Oil Input:		0.00000	
Weight Fraction of Gas Input:		0.00000	
Combustion in Upper Bed :		0.050000	Fraction of total LHV Load
		OK	Cancel
Exit the window after saving all data			

Figure 17: Boiler – Combustion window

3.1.2 Economizer

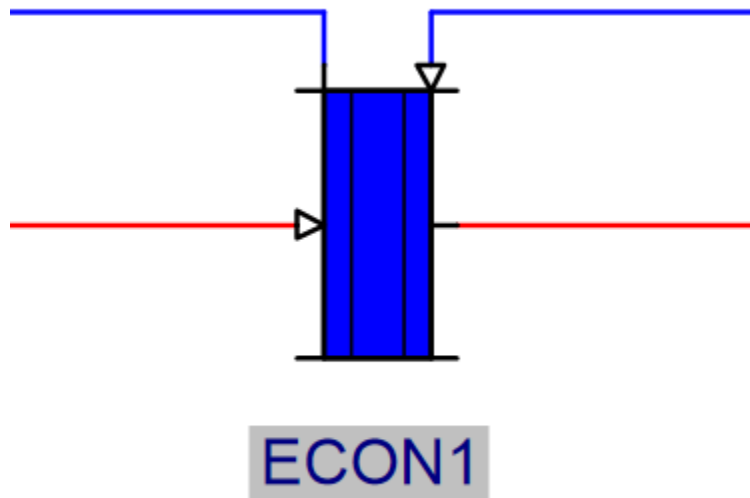


Figure 18: Economizer icon

The screenshot shows the 'Economizer' dialog box. At the top, there is a menu bar with 'UOM', 'Report', 'Help', and 'Steam'. Below the menu bar, the 'ID' field is set to 'ECON1' and the 'Description' field is set to 'Economizer'. The 'Method' dropdown menu is set to 'Water Outlet Temperature' and the value is '280.00 C'. The 'Sizing' dropdown menu is set to 'Specify HT Coeff' and the value is '0.045426 kJ/sec-m²-K'. There is a checkbox for 'Check For Minimum Exit Gas Temperature' which is unchecked. There are two checkboxes for 'Run Off Design' and 'Do Not Overwrite', both of which are unchecked. On the right side, there is a grid of buttons: 'Flows...', 'Configuration', 'Tolerances...', 'Losses...', 'Correlations', 'Limits...', and 'Perf. Factors...'. At the bottom, there are 'OK' and 'Cancel' buttons. A footer note says 'Exit the window after saving all data'.

Figure 19: Economizer – General Input Window

The inputs of the economizer are shown in the above figure. There are different methods one can use for the economizer, such as the surface area, the cold stream's outlet temperature, the hot stream's outlet temperature etc. One can also change the heat transfer coefficient of the economizer, as well as other properties by clicking the buttons on the bottom right of this window. For our simulation, the "Water Outlet Temperature" method is used.

3.1.3 Superheater

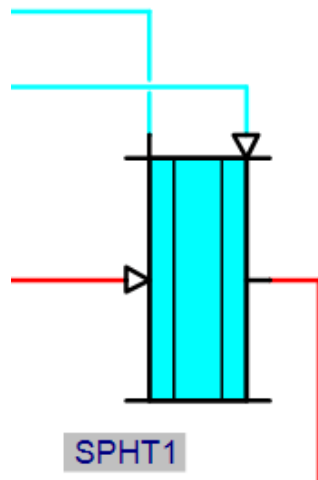


Figure 20: Superheater icon

Figure 21: Superheater – General Input Window

As shown, the input window of the superheater is almost identical to that of the economizer. The only difference lies at the temperature control input. This superheater is the one just before the default superheater of the LFB. It is the first module the exhaust gases from the FLB are inserted to.

3.1.4 Steam Turbine

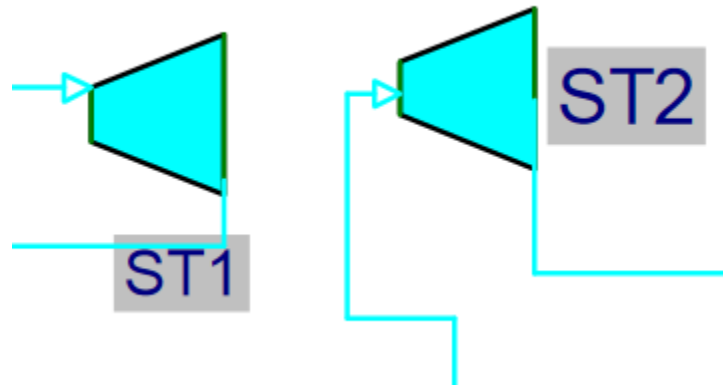


Figure 22: Steam Turbine icon

The screenshot shows the 'Steam Turbine' configuration window. It has a menu bar with 'UOM', 'Report', and 'Help'. The 'Description' field is 'Steam Turbine'. There are checkboxes for 'Bypass Steam Turbine' (unchecked), 'Include Power in System Results' (checked), 'Demand Control Calculations' (unchecked), 'Exhaust Loss' (unchecked), 'Run Off-Design' (unchecked), and 'Do Not Overwrite' (unchecked). The 'Design Point Efficiency Method' is set to 'Isentropic Expansion Efficiency' with a value of 0.93000. The 'Rotational Speed' is set to 3600. There are buttons for 'Inlet/Exit P', 'SCC', 'Limits/Losses', 'Flows...', and 'Tolerances...'. At the bottom, there are 'OK' and 'Cancel' buttons. A status bar at the bottom says 'Exit the window after saving all data'.

Figure 23: Steam Turbine – General Input Window

As shown in the figure above, the inputs the user has to insert is the isentropic efficiency of the turbine, its control valves and lastly, its the rotational speed.

	bar	Stream ID
Inlet	68.000	S79
Inlet or Control Valve DP:	0.020000 fraction	
Bowl	66.640	
Expansion Line End	15.000	
Outlet	15.000	S63

Figure 24: Steam Turbine – Pressure Input Window

In this window, the user specifies the method with which the steam turbine will operate. In our simulation the inlet pressure of the steam turbine is given by the inlet steam flow. So the “Throttle Pressure Set Upstream” Method is used here. The outlet pressure is specified either by inserting a pressure drop inside the steam turbine or by specifying the outlet pressure.

Figure 25: Steam Turbine – Limits and Losses Windows

Using this window, the user can specify the limits of the steam turbine's operation. As seen above, the parameters defining the limits of the operation are the Gearbox losses, the minimum exit quality of the steam, the maximum inlet temperature of the steam and the performance factor of the turbine.

3.1.5 Condenser

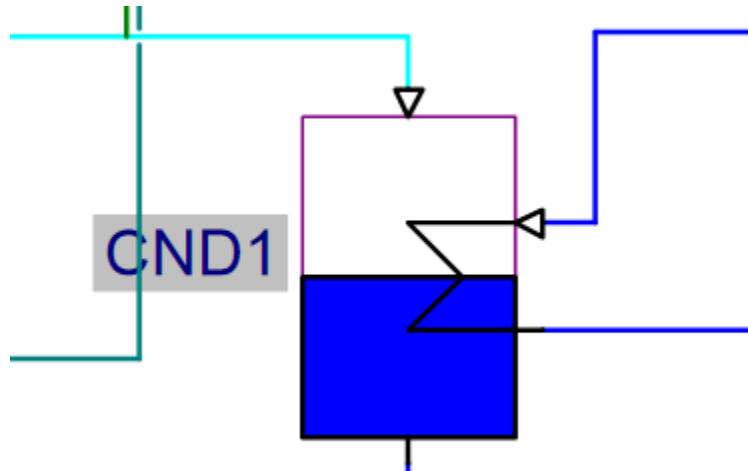


Figure 26: Condenser icon

Condenser	
UOM	Report Help Steam
ID :	CND1 Description: Condenser
Method:	Desired Pressure 0.050000 bar
Design Cooling Water Method:	Input Cooling Water Data Cooling
Design Heat Transfer Coefficient U Method:	User Input Values for U 0.016183 kJ/sec-m ² -K
Cooling Water Pressure Drop:	No Pressure Drop
<input type="checkbox"/> Run Off Design	Flows... HEI 9 Inputs Tolerances Other Inputs
<input type="checkbox"/> Do Not Overwrite	OK Cancel
Exit the window after saving all data	

Figure 27: Condenser – General Input Window

In this window, the user specifies the operating pressure of the condenser, which is of course the outlet pressure of the steam turbine. The user can also specify the design method of the cooling water, by either choosing a specific temperature rise of the cooling water or by having these parameters specified by the cooling water stream. In addition, the heat transfer coefficient can be altered, but in all of the case studies, the default value is kept constant.

3.1.6 Heat Exchanger

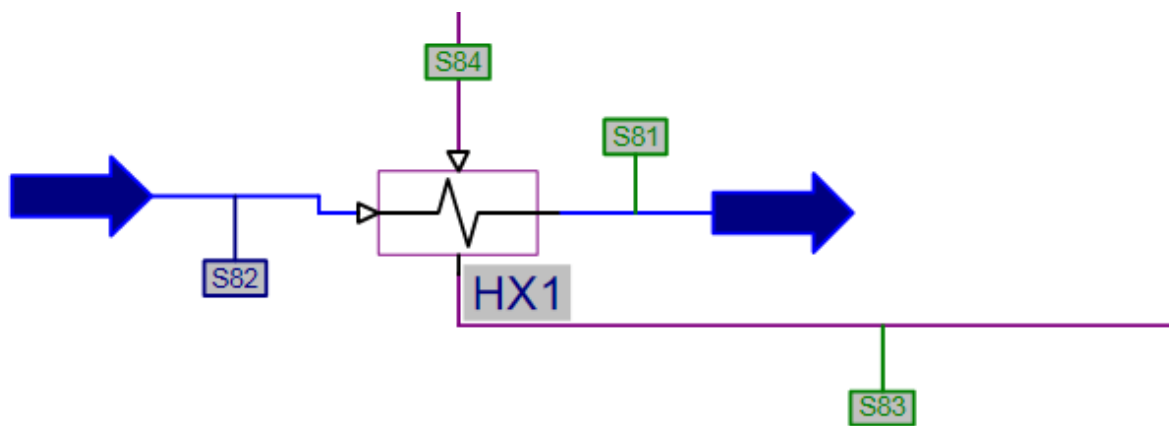


Figure 28: Heat Exchanger icon

General Heat Exchanger	
UOM	Report Help Steam
ID :	HX4 Description: Heatexchanger
Calculational Method:	Hot Side Outlet Temperature 90.000 C
Heat Transfer Coefficient Method:	Overall Heat Transfer Coefficient 0.045426 kJ/sec-m ² -K
Hot Side Inlet Stream:	S6 <input checked="" type="checkbox"/> Disable Phase Change Warnings
Cold Side Inlet Stream:	S30 <input checked="" type="checkbox"/> Disable Phase Change Warnings
Second Specification:	No Second Method
<input type="checkbox"/> Run Off Design <input type="checkbox"/> Do Not Overwrite	
<input type="button" value="OK"/> <input type="button" value="Cancel"/>	
Exit the window after saving all data	

Figure 29: Heat Exchanger – General Input Window

The heat exchanger input window provides many methods with which the user can specify how heat is transferred by one stream to another. Some of them are: the specification of the hot stream outlet temperature, the specification of the cold stream outlet temperature, the effectiveness of the heat exchanger, its surface area etc. For this component, the default heat transfer coefficient is applied as well, while there is no second method applied due to the fact that the streams and their thermodynamic properties must be strictly defined. Most of the times, the software cannot run due to the errors the two methods create.

3.1.7 Deaerator

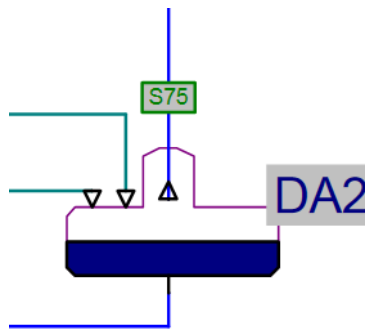


Figure 30: Deaerator icon

Deaerator			
UOM	Report	Help	Steam
ID :	DA2	Description:	Deaerator
Deaerator Operating method:			Steam IDs:
Floating P Operation: demand pegging steam if < min P			Main : S11
Vent Method:			Aux : S9
Specified vent mass flow rate			0.00000 tonm/hr
Pegging Steam Control Method:			Maximum Flow:
Control Main Steam Flow to Max., then Control Aux Steam Flow			0.00000 tonm/hr
Operating Pressure:	Desired 4.0000	Minimum 4.0000	Maximum 10.000 bar
Exit BFW Subcooling:	0.00000		13.889 C
<input type="checkbox"/> Equalize Inlet Pressures		<input checked="" type="checkbox"/> Disable Warning When P > Max. P	
Floating Pressure Damping Factor:			0.50000
<input type="checkbox"/> Demand Flow			Tolerances...
			Flows...
			OK Cancel
Exit the window after saving all data			

Figure 31: Deaerator – General Input Window

In the general input window of the deaerator many options are provided, according to the desired operation of the deaerator. The most significant ones, are the minimum and maximum operating pressures of the deaerator, as well as that demand of steam flow from extractions in the steam turbine, to ensure enough heat is provided for the deaeration.

3.1.8 Flash Tank

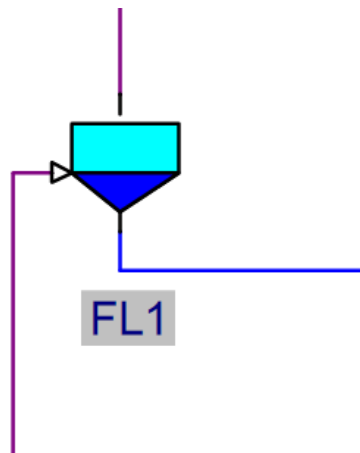


Figure 32: Flash Tank icon

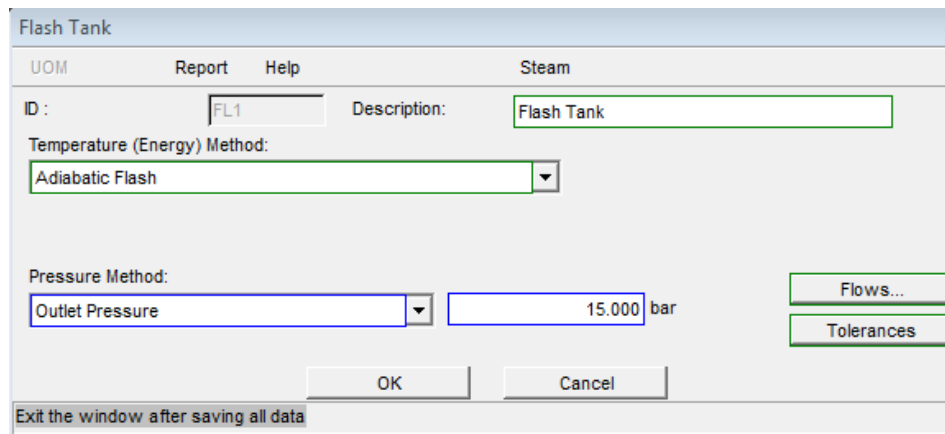
A screenshot of the 'Flash Tank' software window. The window has a title bar 'Flash Tank' and a menu bar with 'UOM', 'Report', 'Help', and 'Steam'. The 'ID' field contains 'FL1' and the 'Description' field contains 'Flash Tank'. The 'Temperature (Energy) Method' is set to 'Adiabatic Flash'. The 'Pressure Method' is set to 'Outlet Pressure' with a value of '15.000 bar'. There are buttons for 'Flows...' and 'Tolerances'. At the bottom are 'OK' and 'Cancel' buttons. A status bar at the very bottom says 'Exit the window after saving all data'.

Figure 33: Flash Tank – General Input Window

In the general input window, the user specifies the pressure of the flash tank, or the pressure drop in it. As for the temperature method, the user has many options, some of which are: the one used above where the flash tank is an adiabatic one, a dew point flash tank, the specification of the exit quality of the outlet steam, the water outlet temperature etc.

3.1.9 Pump

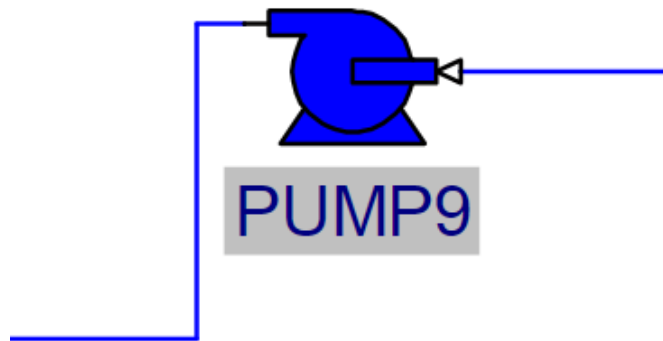


Figure 34: Pump icon

Pump

UOM Report Help Steam

ID : Description:

Control Valve Exit Pressure:

Pump Exit Pressure :
 bar

Pump Efficiency:

Variable Speed

Include Power in System Auxiliaries

Run Off Design

Do Not Overwrite

Exit the window after saving all data

Figure 35: Pump – General Input Window

The inputs of the pumps are quite simple since the user only needs to specify the outlet pressure and the isentropic efficiency of the pump. Of course, the pump component offers more options, such as Head input, Pump Curve Fit or a pressure difference between the inlet and the outlet.

3.1.10 Splitter

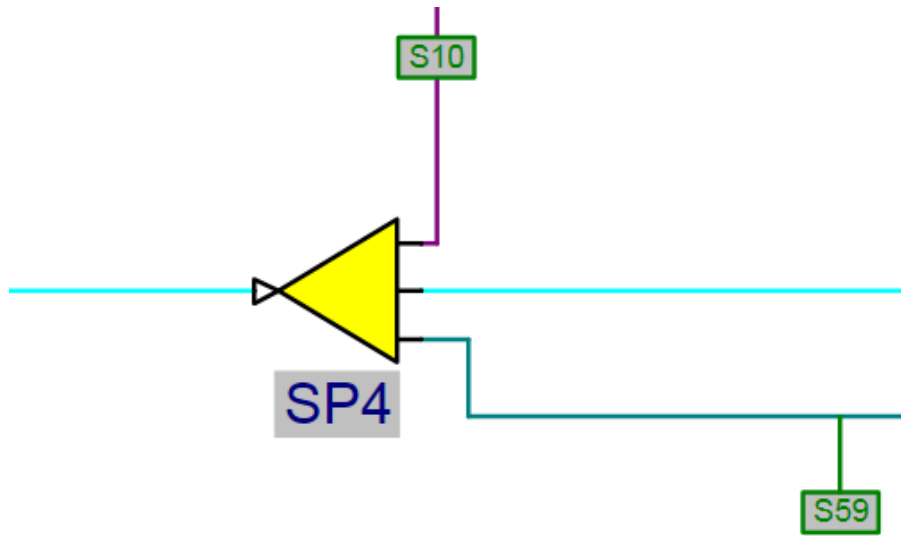


Figure 36: Splitter icon

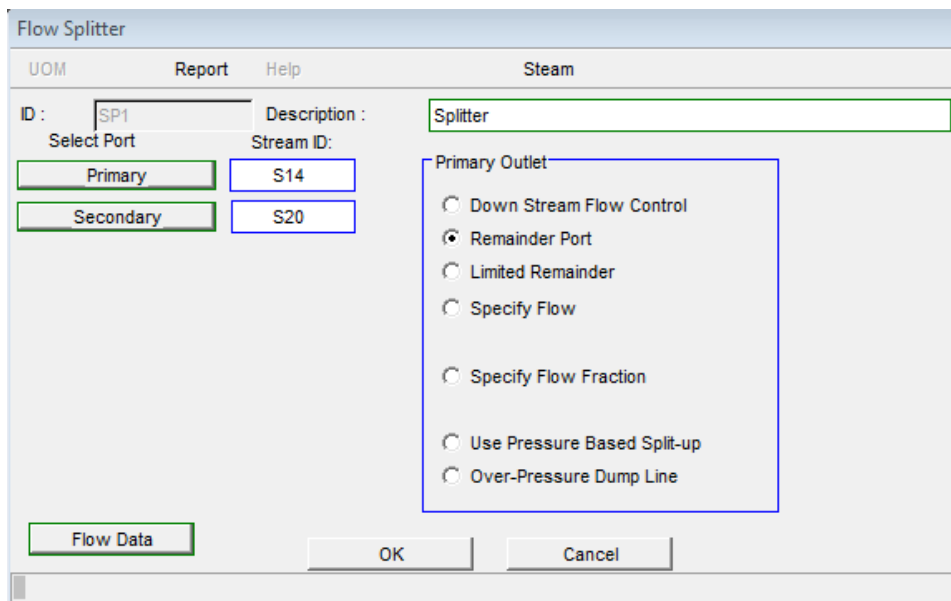


Figure 37: Splitter – General Input Window

The splitter is the component which splits a certain stream of water or steam into 2 or more different streams. It is important that all of the streams created respect the mass flow balance. For example the user cannot specify three streams with three values that the inlet flow cannot provide. One of them must be specified as a remainder port. In addition, not all three streams can be controlled by downstream conditions, because there might not be enough flow to satisfy these conditions. Splitters are really useful in GateCycle but the user should choose its inputs with caution, in order to avoid any errors.

3.1.11 Mixer

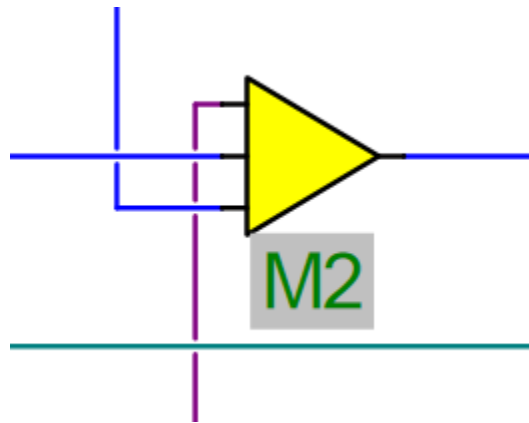


Figure 38: Mixer icon

The screenshot shows the 'Flow Mixer' dialog box. At the top, there are menu options: 'UOM', 'Report', 'Help', and 'Steam'. The 'ID' field contains 'M1'. The 'Description' field contains 'Mixer'. There are two checkboxes: 'Equalize Inlet Pressure' (unchecked) and 'Demand Flow' (checked). At the bottom right, there are two buttons: 'Demand' and 'Flows'. At the bottom center, there are 'OK' and 'Cancel' buttons. A footer message reads 'Exit the window after saving all data'.

Figure 39: Mixer General Input Window

The mixer component usually does not need any inputs except some instances, in which the user can specify the inlet pressures are equalized and there is a demand of specific flows. The mixer can mix either pure one phase streams or steam and water. When the user specifies a flow demand, this means that the connected splitters or other components of the model must operate with downstream flow conditions.

3.1.12 Temperature Control Mixer

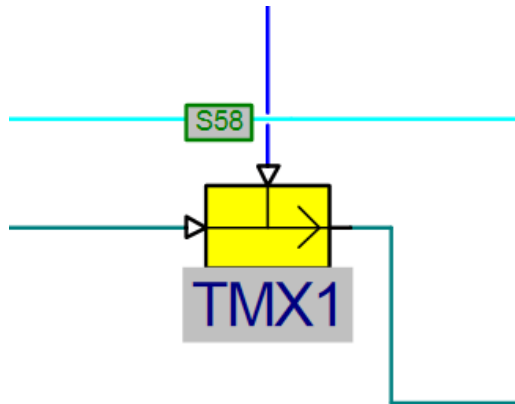


Figure 40: Temperature Control Mixer icon

TMIX/Attemperator	
UOM	Report Help Steam
ID :	TMX2 Description : Temperature Control Mixer
Temperature Control Method:	
Outlet Temperature	280.00 C
Pressure Control:	
Outlet Pressure	15.000 bar
<input checked="" type="checkbox"/> Demand Outlet Flow	270.00 tonm/hr
Control Flow Damping Factor	0.50000
<input type="checkbox"/> Include DownStream Component in Macro Loop	
<input type="checkbox"/> Disable Warning when not Achieving Temperature Control	
<input type="checkbox"/> Equalize Inlet Pressures	
<input type="button" value="Limits..."/> <input type="button" value="Flows..."/> <input type="button" value="Tolerances"/>	
<input type="button" value="OK"/> <input type="button" value="Cancel"/>	
Exit the window after saving all data	

Figure 41: Temperature Control Mixer – General Input Icon

The temperature control mixer component can either operate as a control mixer for two streams of the same phase, or as an atemperator. This component provides some really useful functions, such as the the outlet pressure of the mixed stream, except its temperature. This component is used to provide the Aluminum plant with the desired temperature and pressure of the steam flow.

3.2 Inputs of the Modified Biomass CHP Plant

On the below tables all of the inputs, both for the system and the components will be presented in order to show the desired operation of the plant. These inputs were chosen as the best ones after the simulation of nearly twenty different sets of inputs. The main purpose of this CHP plant is to have at all times an electrical gross power output of 84 MW and to satisfy the thermal needs of the Aluminum plant, for all the above mentioned scenarios.

In addition, the temperature of the exhaust gases was one of the key factors of the simulation. Their temperature should be as low as possible, taking into account the acid dew point. However the biomass fuels used for the boiler have a really low percentage of sulfur, which makes them one of the safest and nearly SO₂ free fuels.

The first simulation that will be presented is the one with Raw Spruce as fuel:

Table 7: Inputs of the Biomass CHP Plant with Raw Spruce as fuel

Fluidized Bed Boiler		
Fuel Type	Raw Spruce	
Lower Heating Value	7433	kJ/kg
Fraction Excess Air	0.7	
Flue Gas Exit Temperature	445	°C
Water Mass Flow 1st Scenario	236.22	kg/s
Water Mass Flow 2nd Scenario	212.52	kg/s
Water Mass Flow 3rd Scenario	204.04	kg/s
Live Steam Tempreature	480	°C

Superheater		
Steam Outlet Temperature	380	°C
Heat transfer Coefficient	0.045426	W/m ² K

Third Economizer		
Water Outlet Temperature	280	°C
Heat transfer Coefficient	0.045426	W/m ² K

Second Economizer		
Water Outlet Temperature	225	°C
Heat transfer Coefficient	0.045426	W/m ² K

First Economizer		
Water Outlet Temperature	150	°C
Heat transfer Coefficient	0.045426	W/m ² K

First Stage Turbine		
Isentropic Expansion Efficiency	0.7975	
Outlet Pressure	15	bar

Second Stage Turbine		
Isentropic Expansion Efficiency	0.81995	
Outlet Pressure	0.5179	bar

Condenser		
Desired Pressure	0.5179	bar
Heat Transfer Coefficient	0.016183	W/m ² K

Low Pressure Control Temperature Mixer		
Outlet Temperature	188.2	°C
Outlet Pressure	8.5	bar

Low Pressure Control Temperature Mixer		
Outlet Temperature	188.2	°C
Outlet Pressure	8.5	bar
Steam Mass Flow	75	kg/s

High Pressure Control Temperature Mixer		
Outlet Temperature	290	°C
Outlet Pressure	68	bar
Steam Mass Flow	51.39	kg/s

Deaerator		
Minimum Operating Pressure	1.8	bar
Maximum Operating Pressure	10	bar
Floating P Operation Method	Steam Demand	

Pumps		
Feeding Water Pump		
Exit Pressure	68	bar
Isentropic Efficiency	0.75	
Condensate Pump		
Exit Pressure	16.5	bar
Isentropic Efficiency	0.75	
Cooling Water Pump		
Exit Pressure	30.735	bar
Isentropic Efficiency	0.75	

Heat Exchangers		
Heat Exchanger 1		
Hot Side Outlet Temperature	270	°C
Heat Transfer Coefficient	0.00025794	W/m ² K
Heat Exchanger 2		
Cold Side Outlet Temperature	105	°C
Heat Transfer Coefficient	0.00025794	W/m ² K
Heat Exchanger 3		
Hot Side Outlet Temperature	152	°C
Heat Transfer Coefficient	0.00025794	W/m ² K

Table 8: Raw Spruce Chemical Composition

Raw Spruce Wood (As Received)	
Moisture Content	57.20%
Ash Content	0.78%
Carbon	23.43%
Hydrogen	2.28%
Nitrogen	0.15%
Sulphur	0.03%
Oxygen	16.12%
Lower Heating Value (LHV) [kJ/kg]	7433
Higher Heating Value (HHV) [kJ/kg]	9043

The only new inputs in this model are specified in the first four components, namely the fluidized bed boiler, the superheater and the three economizers. The other components' inputs remain the same because of the fact that these values are connected to the Aluminum plant.

The method with which the FLB is operating, is called "Calculate Fuel Flow, Match Water Wall Flow" which means that the FLB provides enough heat in order so that the water flow inserted in it, exits with the design thermodynamic parameters. The water mass flow was calculated considering the steam demands from the Aluminum plant and the power output of the turbine.

In addition, the flue gas exit temperature from the FLB has a value which allows the superheater and the economizers to raise the temperature of the water flow as specified. The values of the exit temperatures from the economizers and the superheater are the outcome of many combinations, until the model provides a good efficiency and, as low as possible, flue gas temperature.

Since all of the four different biomass fuels, are used in the same model, only those parameters that are altered will be provided below. Any parameters that are not shown once again remain the same, since the goal is to compare these fuels with one another. Altering any further parameters would mean trying to compare different configurations of plants.

Table 9: Inputs of the Biomass CHP Plant with Raw EFB as fuel

Fluidized Bed Boiler		
Fuel Type	Raw EFB	
Lower Heating Value	5380	kJ/kg
Fraction Excess Air	0.3	
Flue Gas Exit Temperature	408	°C
Water Mass Flow 1st Scenario	236.22	kg/s
Water Mass Flow 2nd Scenario	212.50	kg/s
Water Mass Flow 3rd Scenario	204.00	kg/s
Live Steam Temperature	480	°C

Table 10: Raw EFB Chemical Composition

Empty Fruit Bunch (As Received)	
Moisture Content	57.20%
Ash Content	2.19%
Carbon	19.49%
Hydrogen	2.34%
Nitrogen	0.19%
Sulphur	0.02%
Oxygen	18.58%
Lower Heating Value (LHV) [kJ/kg]	5380
Higher Heating Value (HHV) [kJ/kg]	7280

As it can be observed except the chemical composition and the LHV of the fuels, the fraction excess air and the flue gas temperature of the EFB are lower. The lower flue gas temperature of the EFB is derived from the fact that it has a lower adiabatic flame temperature than the raw spruce. Although these two fuels have the same amount of water content, EFBs are worse of a fuel than wood.

Following these two fuels, the below presented inputs consist of the same fuels as well but with the exception that they are now pretreated. This simulation will provide us with the information of how pretreatment technologies improve the properties of a fuel. Of course pretreatment technologies provide fuels which are almost moisture free (3 – 7%, although in the simulations they are considered moisture free due to minimal alterations in the results), a factor that alone improves the properties and the LHV of a fuel.

Table 11: Inputs of the Biomass CHP Plant with Torrefied Spruce as fuel

Fluidized Bed Boiler		
Fuel Type	Torrefied Spruce	
Lower Heating Value	22600	kJ/kg
Fraction Excess Air	0.7	
Flue Gas Exit Temperature	718	°C
Water Mass Flow 1st Scenario	236.22	kg/s
Water Mass Flow 2nd Scenario	212.49	kg/s
Water Mass Flow 3rd Scenario	204.00	kg/s
Live Steam Temperature	480	°C

Table 12: Torrefied Spruce Chemical Composition

Wet Torrefied Spruce Wood (Dry - Ash Free)	
Moisture Content	-
Ash Content	-
Carbon	55.70%
Hydrogen	6.10%
Nitrogen	0.10%
Sulphur	0.00%
Oxygen	38.10%
Lower Heating Value (LHV) [kJ/kg]	22600
Higher Heating Value (HHV) [kJ/kg]	-

Table 13: Inputs of the Biomass CHP Plant with Torrefied EFB as fuel

Fluidized Bed Boiler		
Fuel Type	Torrefied EFB	
Lower Heating Value	19450	kJ/kg
Fraction Excess Air	0.7	
Flue Gas Exit Temperature	804	°C
Water Mass Flow 1st Scenario	236.22	kg/s
Water Mass Flow 2nd Scenario	212.49	kg/s
Water Mass Flow 3rd Scenario	204.00	kg/s
Live Steam Temperature	480	°C

Table 14: Torrefied EFB Chemical Composition

Torrefied EFB (Dry – Ash Free)	
Moisture Content	-
Ash Content	-
Carbon	51.14%
Hydrogen	4.38%
Nitrogen	1.27%
Sulphur	0.02%
Oxygen	43.19%
Lower Heating Value (LHV) [kJ/kg]	19450
Higher Heating Value (HHV) [kJ/kg]	-

3.3 Results of the Modified Biomass CHP Power Plant

3.3.1 Results of the Raw Spruce Simulation

As mentioned above, three simulations took place, each for each one of the steam demand scenarios from the Aluminum plant. The purpose of the simulation was to extract information for the electrical energetic and exergetic efficiency of the CHP power plant, the energetic and the exergetic overall efficiency, as well as the boiler power output, the fuel consumption, the auxiliary losses, the thermal energy output and the flue gas temperature.

The below tables and figures will provide the information for the value of each of these efficiencies, as well as values for the heat and electricity produced. Lastly, both Sankey and Grassman diagrams will be provided.

Before any tables and figures are shown, the equations with which these thermodynamic values are obtained. As a note before the presentation of the values, it must be stated that, all of the values, except the total energetic and the exergetic efficiencies and those parameters relevant to them, are given as outputs by GateCycle. The exergetic values are calculated by the user, with the below presented equations.

Energetic thermodynamic parameters equations:

$$P_{elgross} = (P_{ST1} + P_{ST2})\eta_G \quad (10)$$

$$P_{elnet} = (P_{ST1} + P_{ST2})\eta_G - P_{AUX} \quad (11)$$

$$Q_{FLB} = \dot{m}_B LHV \quad (12)$$

$$Q_{th} = \dot{m}_{S58}(h_{S58} - h_{MU}) + \dot{m}_{S24}(h_{S24} - h_{MU}) + \dot{m}_{S85}(h_{S85} - h_{MU}) + \dot{m}_{S84}(h_{S84} - h_{S83}) + \dot{m}_{S116}(h_{S116} - h_{MU}) + \dot{m}_{S109}(h_{S109} - h_{S115}) \quad (13)$$

$$a = \frac{P_{elnet}}{Q_{th}} \quad (14)$$

$$\eta_{elnet} = \frac{P_{elnet}}{Q_{FLB}} \quad (15)$$

$$\eta_{elgross} = \frac{P_{elgross}}{Q_{FLB}} \quad (16)$$

$$\eta_{net} = \frac{P_{elnet} + Q_{th}}{Q_{FLB}} \quad (17)$$

$$\eta_{gross} = \frac{P_{elgross} + Q_{th}}{Q_{FLB}} \quad (18)$$

$$Q_{thideal} = \dot{m}_{S58}(h_{S58} - h_{MU}) + \dot{m}_{S24}(h_{S24} - h_{MU}) + \dot{m}_{S85}(h_{S85} - h_{MU}) + \dot{m}_{S84}(h_{S84} - h_{S83}) + \dot{m}_{S116}(h_{S116} - h_{MU}) + \dot{m}_{S109}(h_{S109} - h_{S115}) + \dot{m}_{S59}(h_{S59} - h_{S80}) + \dot{m}_{S23}(h_{S23} - h_{S94}) \quad (19)$$

$$\eta_{netideal} = \frac{P_{elnet} + Q_{thideal}}{Q_{FLB}} \quad (20)$$

$$\eta_{grossideal} = \frac{P_{elgross} + Q_{thideal}}{Q_{FLB}} \quad (21)$$

The above equations present the thermodynamic parameters of the simulation and how they are calculated. It is explained below what each of these parameters represent.

- P_{ST} is the mechanical power generated by the steam turbine
- $P_{elgross}$ is the total electrical power the generated without taking into account any auxiliary losses
- P_{elnet} is the electrical power offered to the grid by the power plant
- Q_{FLB} is the total thermal output of the fluidized bed boiler
- Q_{th} is the total thermal power offered to the Aluminum plant
- \dot{m}_{SXX} is the mass flow of each stream of steam offered to the Aluminum plant, or the stream of steam offering heat to the Aluminum plant via a heat exchanger
- h_{SXX} is the enthalpy of each of the above mentioned streams
- h_{MU} is the enthalpy of the make up water. The make up water is provided at certain pressure and temperature of 1.0342 bar and 15.56 °C, resulting in an enthalpy of 65.38 kJ/kgK.
- α is the power to heat ratio
- η_{elnet} is the net electrical efficiency of the cycle

- $\eta_{elgross}$ is the gross electrical efficiency of the cycle
- η_{net} is the net total efficiency of the cycle, taking into account the thermal power offered to the Aluminum plant
- η_{gross} is the gross total efficiency of the cycle, taking into account the thermal power offered to the Aluminum plant
- $Q_{thideal}$ is the thermal output the CHP power plant could offer to the Aluminum plant, if the temperature control mixers were heat exchangers, and could control the temperature of the steam without mixing cold water and steam
- $\eta_{netideal}$ is the net total efficiency of the cycle, taking into account the “ideal” thermal power that could be offered to the Aluminum plant
- $\eta_{grossideal}$ is the gross total efficiency of the cycle, taking into account the “ideal” thermal power that could be offered to the Aluminum plant

Fuel exergy equations:

$$\varphi_{dry} = 1.0437 + 0.1882 \frac{m_{H_2,f}}{m_{C,f}} + 0.0610 \frac{m_{O_2,f}}{m_{C,f}} + 0.0404 \frac{m_{N_2,f}}{m_{C,f}} \quad (21)$$

$$Ex_{ch} = [(LHV) + 2442w]\varphi_{dry} + 9417\left(\frac{m_{S,f}}{100}\right) \quad (22)$$

Where $m_{H_2,f}$, $m_{C,f}$, $m_{O_2,f}$, $m_{N_2,f}$, $m_{S,f}$, w is the ultimate analysis of the biomass fuel.

Stream exergy equation:

$$\dot{E} = \dot{m}((h - h_0) - T_0(s - s_0)) \quad (23)$$

$$\dot{E}_{th} = \dot{m}_{S58}(e_{S58} - e_{MU}) + \dot{m}_{S24}(e_{S24} - e_{MU}) + \dot{m}_{S85}(e_{S85} - e_{MU}) + \dot{m}_{S84}(e_{S84} - e_{S83}) + \dot{m}_{S116}(e_{S116} - e_{MU}) + \dot{m}_{S109}(e_{S109} - e_{S115}) + \dot{m}_{S59}(e_{S59} - e_{S80}) + \dot{m}_{S23}(e_{S23} - e_{S94}) \quad (24)$$

$$\dot{E}_{el} = P_{el} \quad (25)$$

$$\eta_{el\text{exnet}} = \frac{\dot{E}_{el\text{net}}}{\dot{m}_B Ex_{ch}} \quad (26)$$

$$\eta_{el\text{exgross}} = \frac{\dot{E}_{el\text{gross}}}{\dot{m}_B Ex_{ch}} \quad (27)$$

$$\eta_{ex\text{net}} = \frac{\dot{E}_{el\text{net}} + \dot{E}_{th}}{\dot{m}_B Ex_{ch}} \quad (28)$$

$$\eta_{ex\text{gross}} = \frac{\dot{E}_{el\text{gross}} + \dot{E}_{th}}{\dot{m}_B Ex_{ch}} \quad (29)$$

This equation is used for every stream mentined above, with constant values of T_0 and s_0 .

$$T_0 = 288.15 \text{ K (15 } ^\circ\text{C)}$$

$$s_0 = 0.23 \text{ kJ/kg K}$$

Table 15: Thermodynamic Cycle Properties for the Raw Spruce simulation

Operation	Nominal	S1	S2	Unit
Boiler Thermal Output	782.2	703.7	675.6	MW
Gross Power Output	83.6	83.4	83.3	MW
Net Power Output	62.0	62.0	62.0	MW
Thermal Power Output	448.8	378.3	353.2	MW
Water Mass Flow	236.2	212.5	204.0	kg/s
Flue Gas Mass Flow	709.0	637.9	612.4	kg/s
Fuel Mass Flow	105.2	94.7	90.9	kg/s
Power to Heat Ratio α	18.6%	22.0%	23.6%	

Table 16: Total Energetic and Exergetic Efficiency Values for the Raw Spruce simulation

Operation	Nominal	S1	S2
Total Power	100.0%	74.1%	69.2%
η_{net}	65.3%	62.6%	61.5%
η_{gross}	68.1%	65.6%	64.6%
$\eta_{netideal}$	70.3%	68.1%	67.2%
$\eta_{grossideal}$	73.0%	71.1%	70.3%
η_{exnet}	33.8%	34.5%	34.7%
$\eta_{exgross}$	35.9%	36.8%	37.1%

Table 17: Electrical Energetic and Exergetic Efficiency Values for the Raw Spruce simulation

Operation	Nominal	S1	S2
Total Power	100.0%	74.1%	69.2%
η_{elnet}	7.9%	8.8%	9.2%
$\eta_{elgross}$	10.7%	11.5%	11.9%
η_{elxnet}	6.0%	6.7%	7.0%
$\eta_{elxgross}$	8.1%	9.0%	9.4%

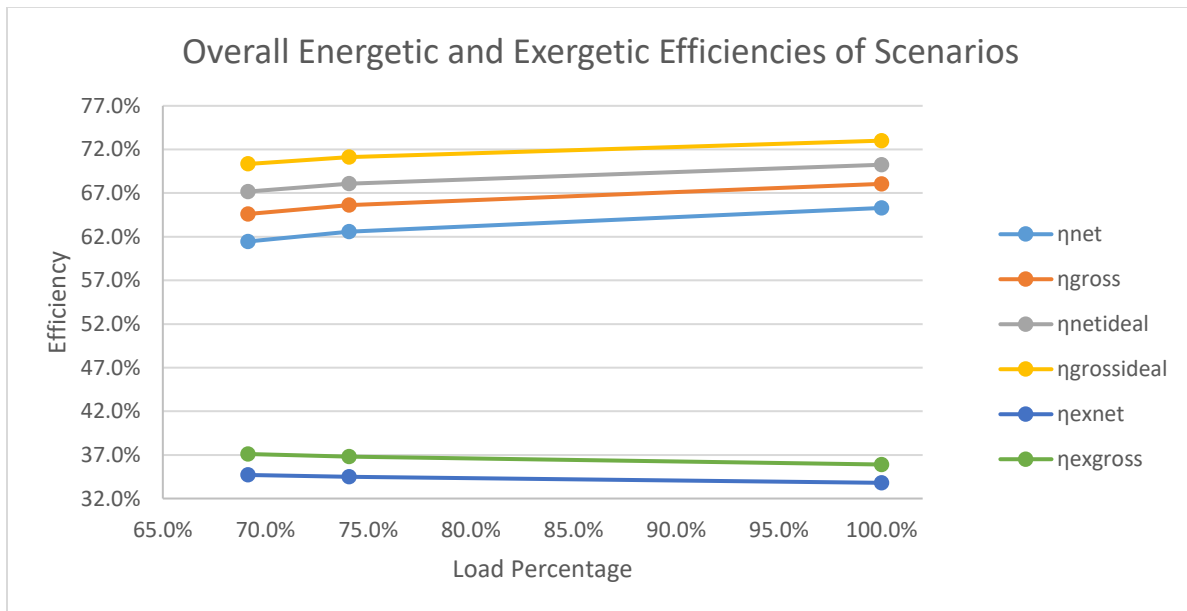


Figure 42: Overall Energetic and Exergetic Efficiencies for the Raw Spruce simulation

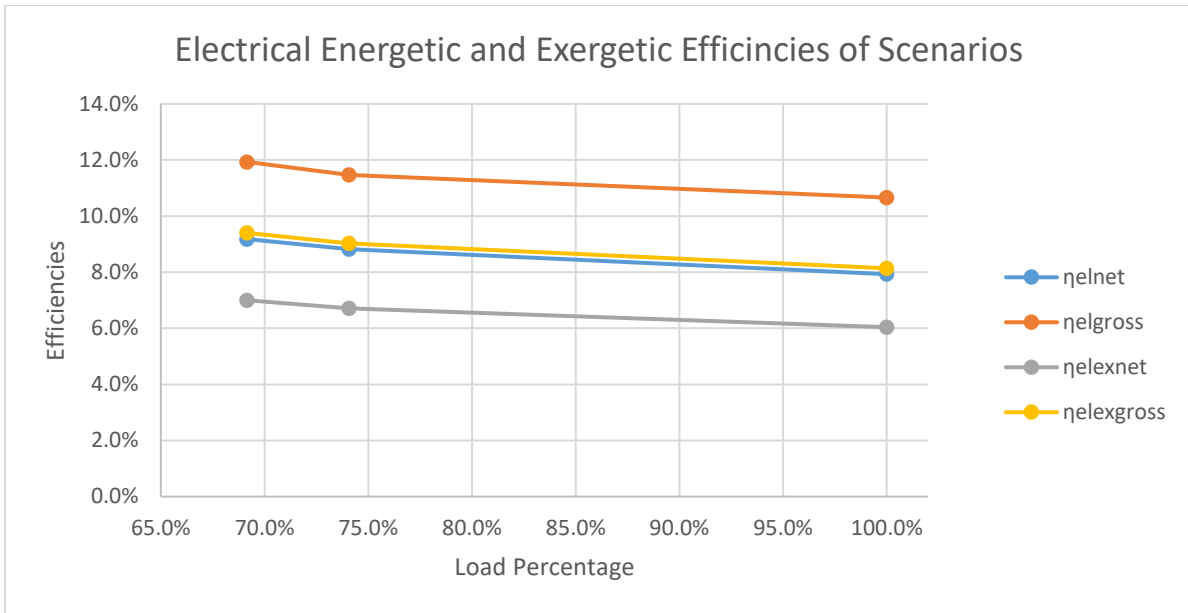


Figure 43: Electrical Energetic and Exergetic Efficiencies for the Raw Spruce simulation

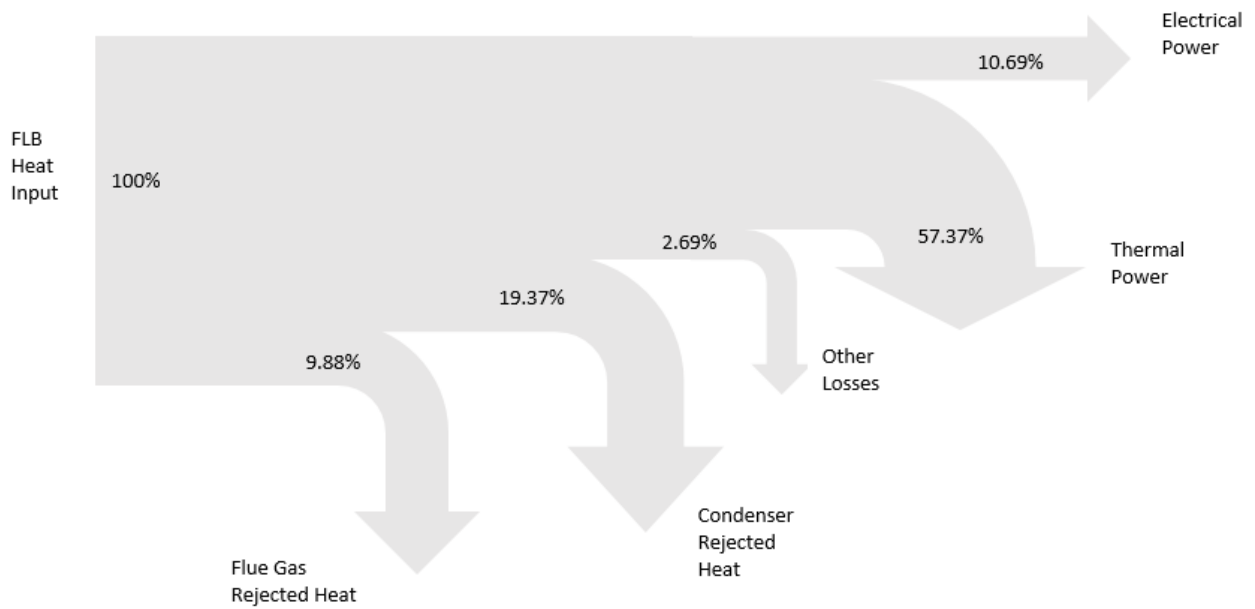


Figure 44: Biomass CHP Power Plant Sankey Diagram for the Raw Spruce simulation

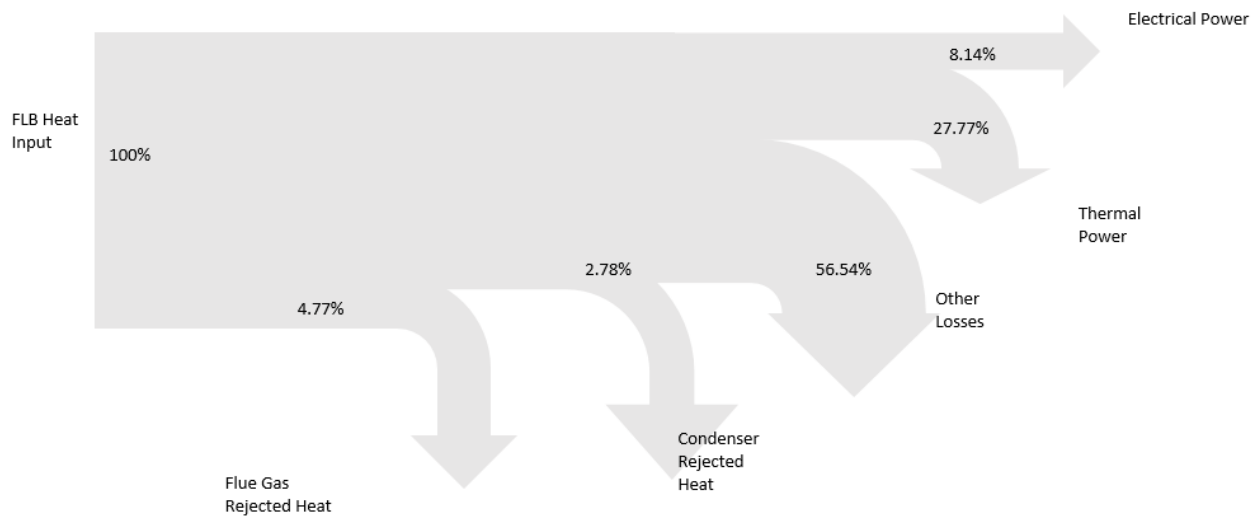


Figure 45: Biomass CHP Power Plant Grassmann Diagram for the Raw Spruce simulation

As it can be seen by the tables 16 and 17, as well as the figures 42 and 43, the overall efficiency of the CHP plant at maximum operational heat output is 65%, meaning it is lower than most CHP plants around the world, but that can be attributed to the configuration of the Heat Part of the model. This CHP plant has a main purpose of satisfying the steam needs the Aluminum plant has, so taking into account the complexity of that part of the model, this efficiency is quite satisfying. One interesting fact is that the “ideal” efficiencies, which are explained above, are quite higher than the normal ones. This means that a possible change to the configuration of the model is implementing a heat exchanger, instead of having an attenuator.

As expected, when the power plant operates at part load, the total efficiency drops, while the electrical efficiency rises, since the electricity production of the plant remains constant through any part load operations.

The total exergetic efficiency of the CHP power plant is quite lower than the energetic, which is to be expected since a big part of the input exergy into the cycle is degraded because it is offered to the Aluminum plant as heat and it is not transformed into useful work. As opposed to the total exergetic efficiency, the exergetic electrical efficiency is lower than the energetic one, but by a lower margin.

Due to the fact that the biomass fuel has a really high moisture content, when calculating the fuel chemical exergy, it results in a significantly higher exergetic LHV. The chemical exergy of the raw spruce wood with the abovementioned chemical analysis is 9753 kJ/kg, as opposed to the LHV which is 7433 kJ/kg.

The Sankey diagram provides information of how the energy input of the plant is distributed, showing that a significant part of it is rejected to the environment via the condenser, while the heat rejected by the flue gases is a big part as well, meaning there should be improvements regarding the utilization of that heat. Since biomass fuels have a quite low percentage of sulfur, an improvement would be the utilization of the latent heat of the moisture of the fuel. The amount of moisture in the flue gases is high due to the high moisture content of the raw spruce wood. Using a condensing heat exchanger, this latent heat, amounting to MW’s, could provide district heat.

Lastly, the Grassmann diagram provides the information of the exergy input. As it can be seen, more than half of the input is destroyed into the boiler. So after the boiler the cycle can only utilize less than half of the input exergy, which is then degraded through the streams that provide heat to the Aluminum plant.

As one can see, the exergetic efficiency is connected to the power to heat ratio, since whenever this ratio rises, so do the exergetic efficiencies. This occurs due to the fact that the energy and the exergy of electricity are the same, which means there is less destruction of the exergy when a cycle produces solely electricity. So part load operation results in higher exergetic efficiencies.

One more thing one can note, is that that the auxiliary power consumption of the plant is really high, constituting 25.6% of the gross electricity production. This is attributed as well, to the configuration of the heat part of the model which was not altered from the initial model of the Combined Cycle power plant. The whole model consists of six high duty pumps, which operate constantly, with high pressure ratios and most importantly high mass flows. One more attribute of the pumps, which makes them really high sinks of electrical power, is their low isentropic efficiency of 0.75.

3.3.2 Results of the Raw Empty Fruit Bunch Simulation

Table 18: Cycle Thermodynamic Properties for the Raw EFB simulation

Operation	Nominal	S1	S2	Unit
Boiler Thermal Output	807.6	726.5	697.4	MW
Gross Power Output	83.6	83.3	83.2	MW
Net Power Output	62.0	62.0	62.0	MW
Thermal Power Output	448.8	378.3	353.2	MW
Water Mass Flow	236.2	212.5	204.0	kg/s
Flue Gas Mass Flow	812.2	730.6	701.4	kg/s
Fuel Mass Flow	150.1	135.0	129.6	kg/s
Power to Heat Ratio α	18.6%	22.0%	23.6%	

Table 19: Total Energetic and Exergetic Efficiency Values for the Raw EFB simulation

Operation	Nominal	S1	S2
Total Power	100.0%	74.1%	69.2%
η_{net}	63.3%	60.6%	59.5%
η_{gross}	65.9%	63.6%	62.6%
$\eta_{netideal}$	68.0%	66.0%	65.1%
$\eta_{grossideal}$	70.7%	68.9%	68.1%
η_{exnet}	30.6%	31.2%	31.4%
$\eta_{exgross}$	32.5%	33.2%	33.6%

Table 20: Electrical Energetic and Exergetic Efficiency Values for the Raw EFB simulation

Operation	Nominal	S1	S2
Total Power	100.0%	74.1%	69.2%
η_{elnet}	7.7%	8.5%	8.9%
$\eta_{elgross}$	10.3%	11.5%	11.9%
η_{elxnet}	5.5%	6.1%	6.3%
$\eta_{elxgross}$	7.4%	8.2%	8.5%

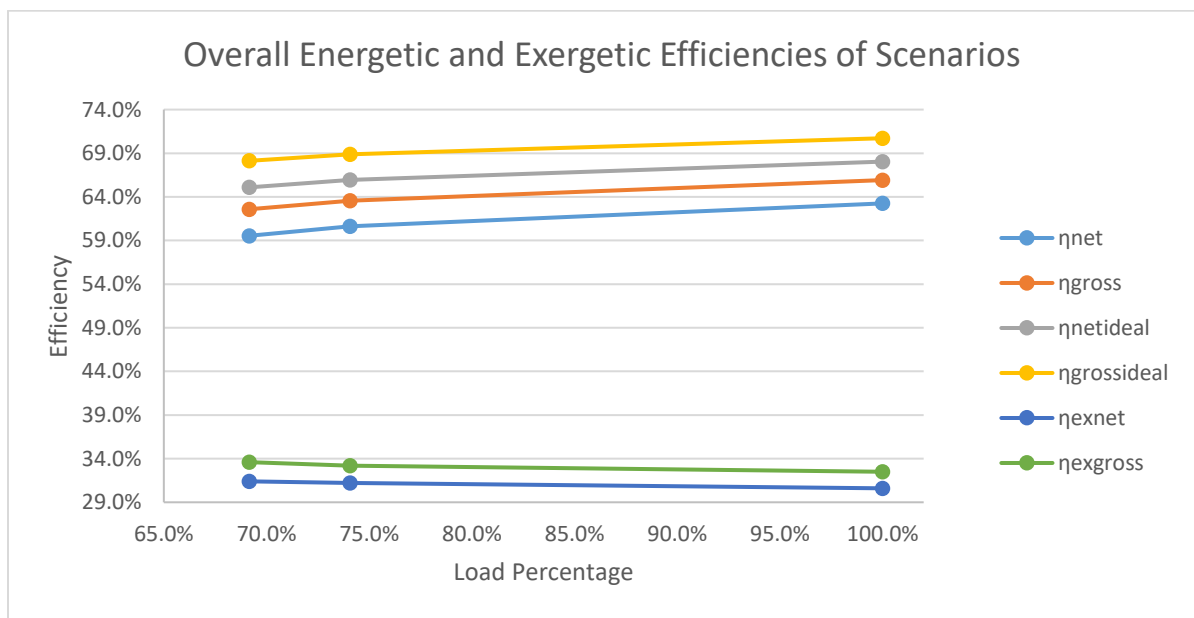


Figure 46: Overall Energetic and Exergetic Efficiencies for the Raw EFB simulation

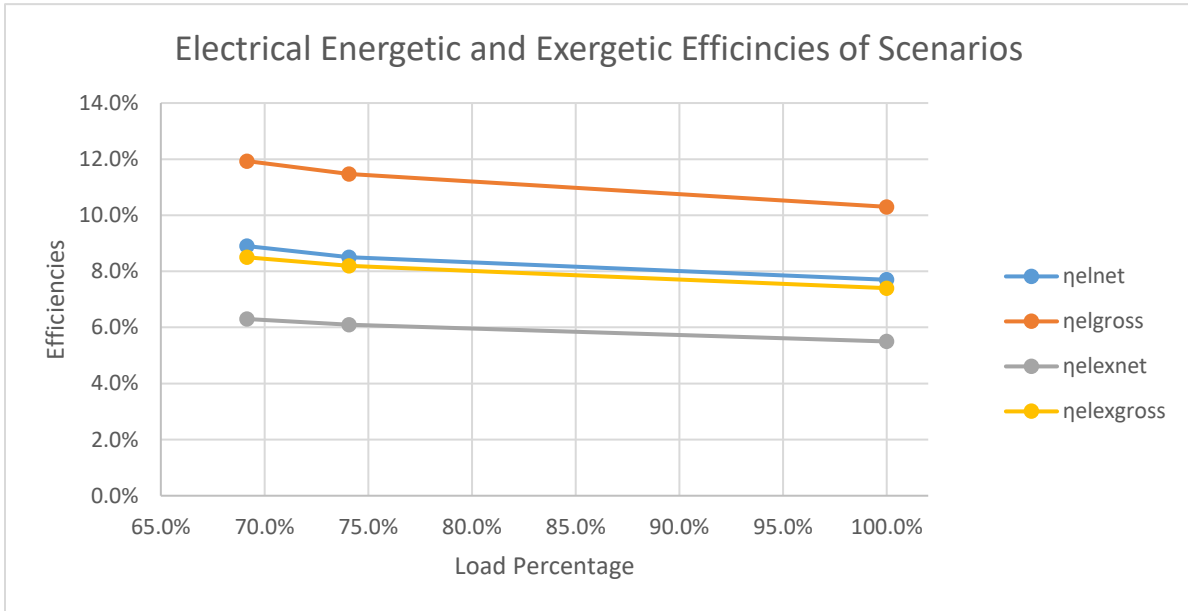


Figure 47: Electrical Energetic and Exergetic Efficiencies for the Raw EFB simulation

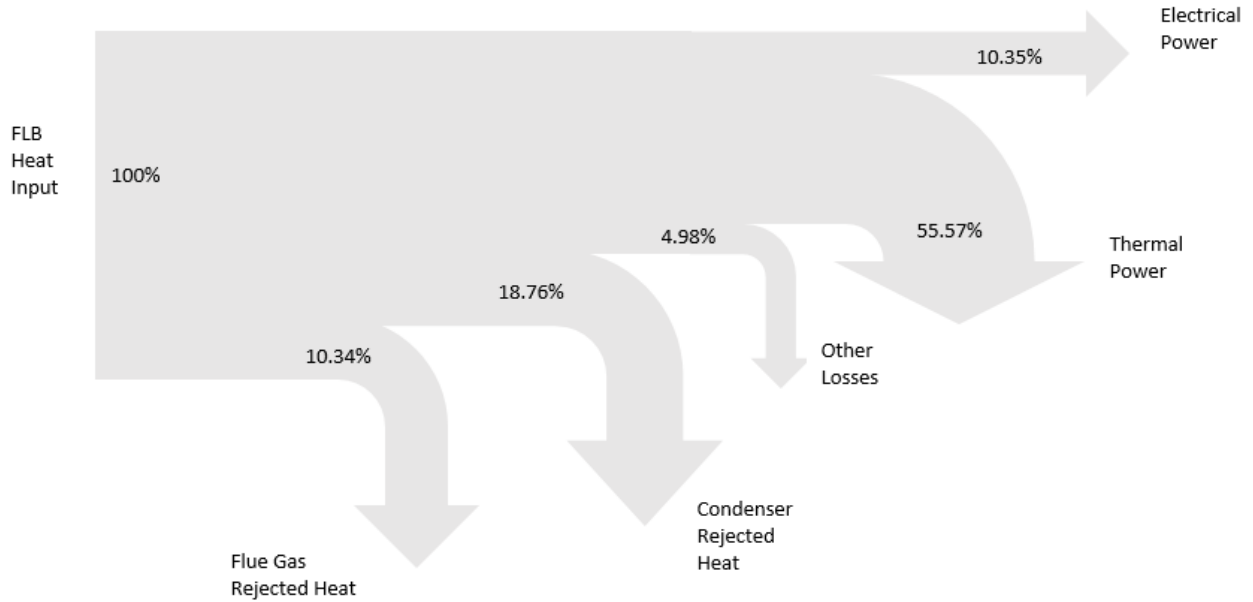


Figure 48: Biomass CHP Power Plant Sankey Diagram for the Raw EFB simulation

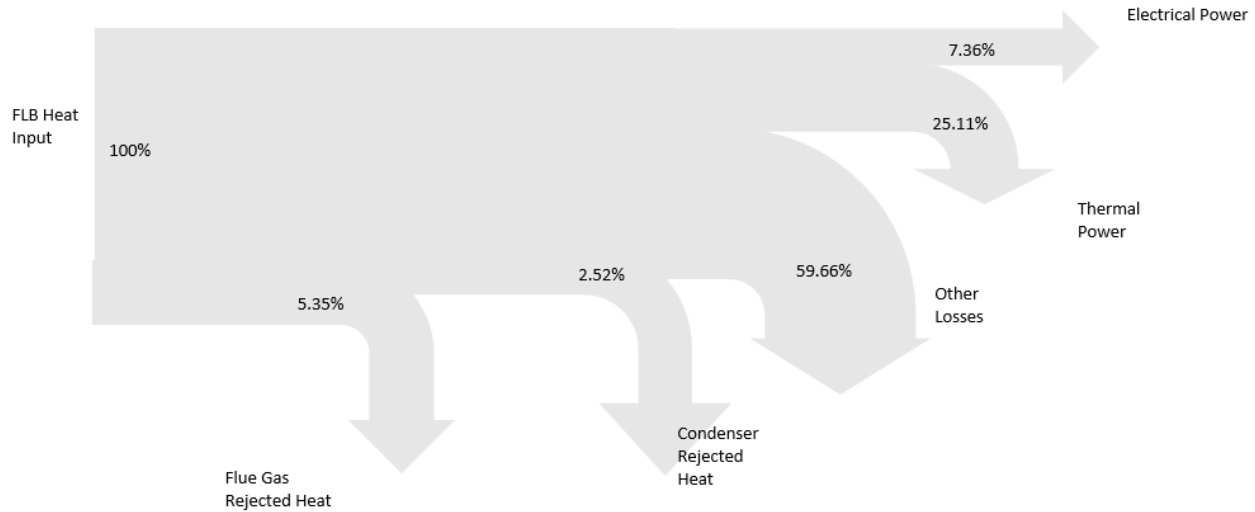


Figure 49: Biomass CHP Power Plant Grassmann Diagram for the Raw EFB simulation

As it can be seen by the above tables and figures, EFBs are a worse fuel than raw spruce although the amount of moisture content is the same to these two fuels. The efficiencies of the EFBs are lower by a small margin because the two fuels are similar in chemical composition and LHV. Although, because of the worse LHV of the EFBs, the nominal thermal input power of the FLB is 20 MW higher than that of the raw spruce, in all scenarios.

Regarding the trends of each efficiency in the different scenarios, total or electrical, energetic or exergetic, they are the same as with those of the raw spruce. The total energetic efficiencies rise as the load rises, while the exergetic efficiencies dwindle due to the deterioration of the quality of the energy. The electrical efficiencies, as with the raw spruce, receive a higher value when the thermal power requested by the Aluminum plant is lower, due to having a steam turbine operating at a constant power value.

As for the Sankey and Grassmann diagrams, they follow the same trend as well, only the flue gas heat loss is higher in percentage than that of the raw spruce, because of the higher flue gas temperature. In addition, the exergy destruction in the boiler is more than half of the exergy input as well, meaning that EFBs have very low combustion properties, something that can be seen by the chemical exergy of them. Calculating the chemical exergy of their EFBs, it results in a value of 7561 kJ/kg, while their LHV is 5380 kJ/kg.

One more thing to note is the significantly higher amount of fuel consumption for the EFB cycle simulation. Due to having such a bad fuel, with high moisture content and difficult combustion process, results in a 50 kg/s rise of consumption. Of course the purpose of this thesis is not to present any economic analysis, but it can be easily arised that such a plant would need a huge supply of EFBs in order to operate. Even though the raw spruce combustion takes place with an air fraction of 0.7 and the EFB with 0.3, the flue gas mass flow is higher, which presents how much more fuel is needed for the operation of the CHP plant.

3.3.3 Results of the Torrefied Spruce Simulation

In this part of the results, the efficiencies and the other thermodynamic parameters of a pretreated biomass fuel will be presented. Since the first biomass fuel was the raw spruce, it was only natural to chose pretreated spruce. The fuel presented here is wet torrefied at 222 °C, meaning it is a hydrochar created by the spruce wood. The ultimate analysis and the dry ash free LHV of the fuel are presented above. This kind of fuel has better characteristics, thus it is expected to provide better yield of its chemical energy, resulting in higher efficiencies.

Table 21: Cycle Thermodynamic Properties for the Torrefied Spruce simulation

Operation	Nominal	S1	S2	Unit
Boiler Thermal Output	734.2	660.4	634.3	MW
Gross Power Output	83.6	83.3	83.2	MW
Net Power Output	62.0	62.0	62.0	MW
Thermal Power Output	448.8	378.3	353.2	MW
Water Mass Flow	236.2	212.5	204.0	kg/s
Flue Gas Mass Flow	389.8	350.6	336.8	kg/s
Fuel Mass Flow	32.5	29.2	28.1	kg/s
Power to Heat Ratio α	18.6%	22.0%	23.6%	

Table 22: Total Energetic and Exergetic Efficiency Values for the Torrefied Spruce simulation

Operation	Nominal	S1	S2
Total Power	100.0%	74.1%	69.2%
η_{net}	69.6%	66.7%	65.5%
η_{gross}	72.5%	69.9%	68.8%
$\eta_{netideal}$	74.8%	72.5%	71.6%
$\eta_{grossideal}$	77.8%	75.8%	74.9%
η_{exnet}	41.7%	43.2%	43.5%
$\eta_{exgross}$	44.4%	46.1%	46.5%

Table 23: Electrical Energetic and Exergetic Efficiency Values for the Torrefied Spruce simulation

Operation	Nominal	S1	S2
Total Power	100.0%	74.1%	69.2%
η_{elnet}	8.4%	9.4%	9.8%
$\eta_{elgross}$	11.4%	12.6%	13.1%
η_{exnet}	7.6%	8.4%	8.8%
$\eta_{exgross}$	10.3%	11.3%	11.8%

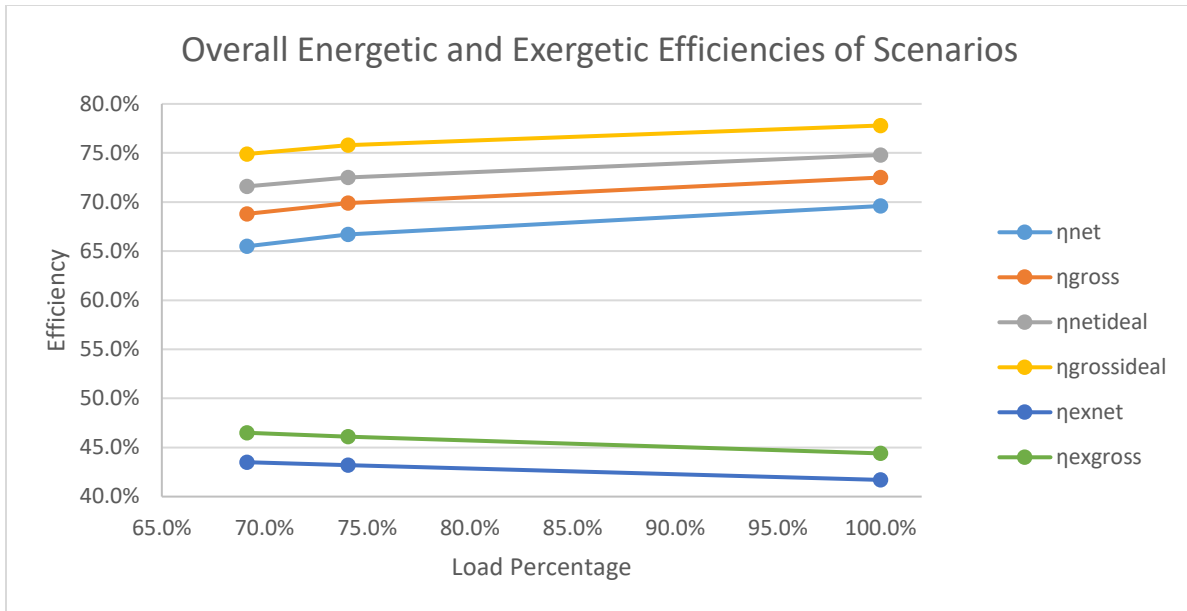


Figure 50: Overall Energetic and Exergetic Efficiencies for the Torrefied Spruce simulation

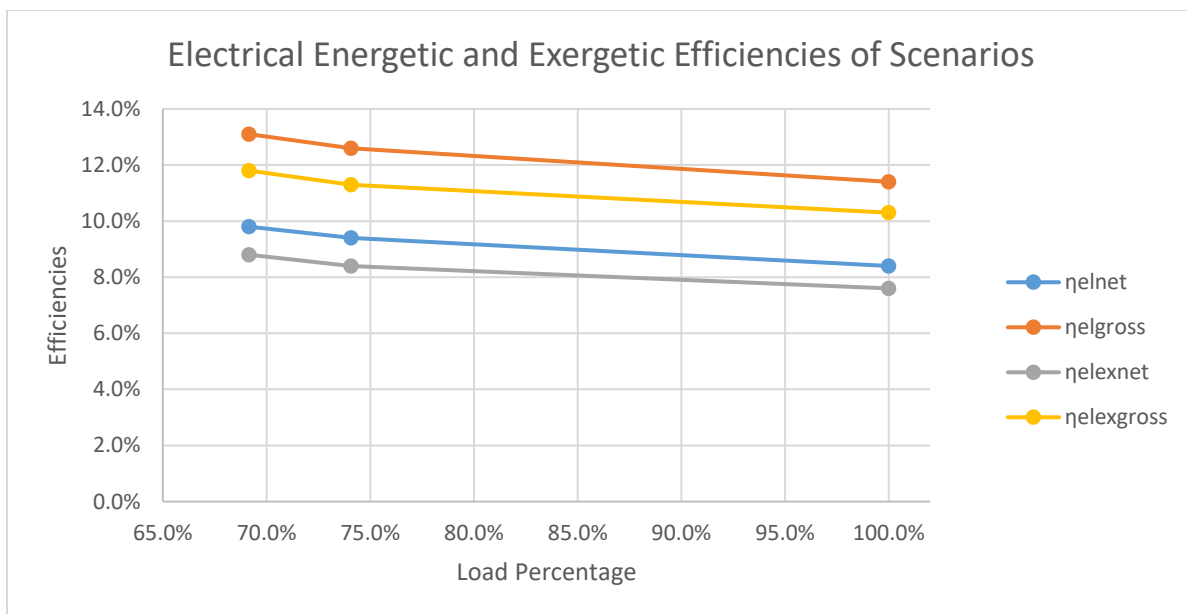


Figure 51: Electrical Energetic and Exergetic Efficiencies for the Torrefied Spruce simulation

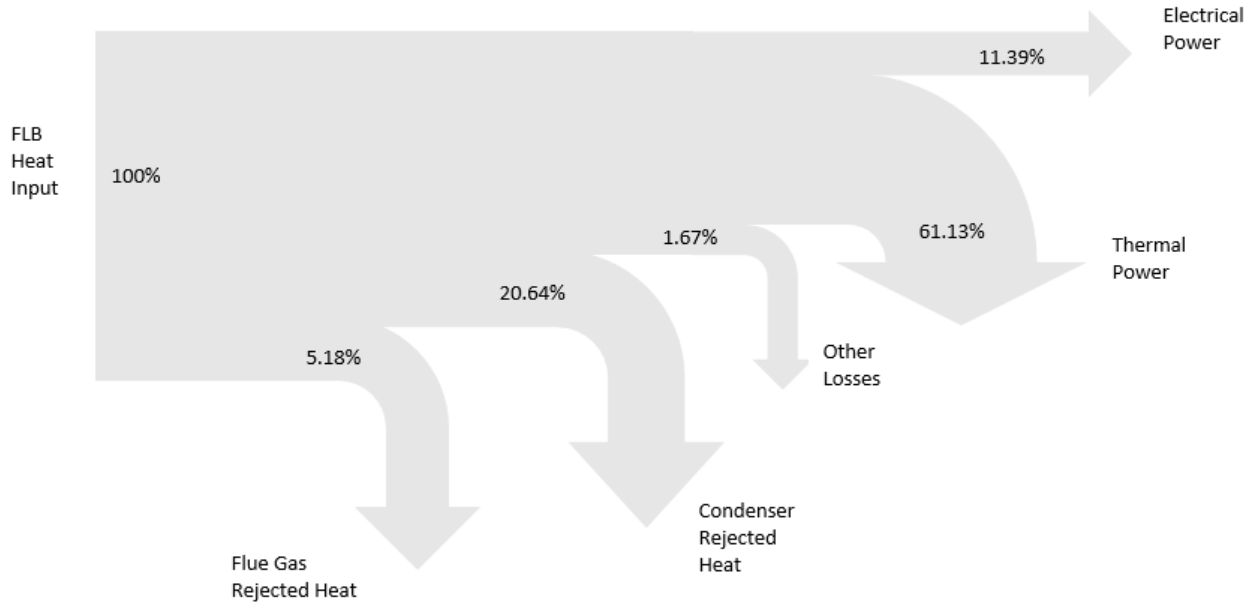


Figure 52: Biomass CHP Power Plant Sankey Diagram for the Torrefied Spruce simulation

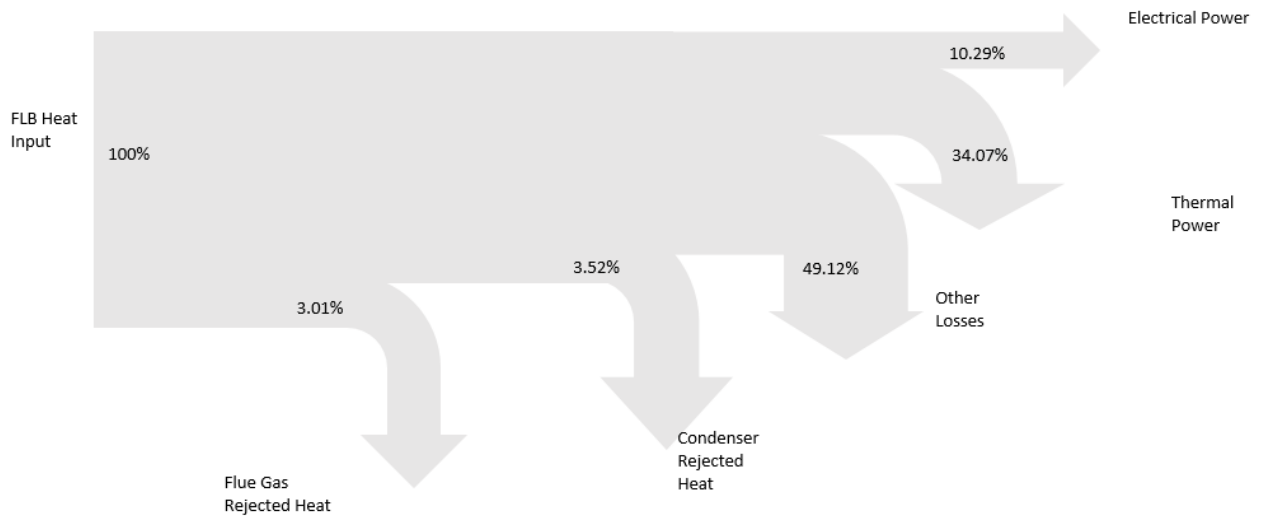


Figure 53: Biomass CHP Power Plant Grassmann Diagram for the Torrefied Spruce simulation

As it was expected, the Torrefied Spruce provides a significantly improved cycle and cycle parameters. The nominal power of the FLB is 60 MW lower than the one operating with the EFBs and 50 MW than that of the raw spruce. As with the previous two fuels, the trend of the efficiencies is the same, namely total energetic efficiencies rising as the load increases, while the electrical and exergetic efficiencies dwindling as the load percentage becomes higher.

The value of the efficiencies is significantly higher than those of the non pretreated fuels, which is a result of the higher energy yield from the torrefaction. The fuel has a massively higher LHV and a chemical composition which provides proper utilization of the fuel's chemical energy and exergy. So the total net efficiency of the cycle is close to 70% and if the configuration had the heat exchangers, instead of the control mixers the efficiency could get as high as approximately 75%.

Taking into account the configuration of the heat part of the model, this efficiency consists a really high one. As far as the exergetic efficiencies are concerned, they break the barrier of the 40% efficiency, which means that as opposed to the other two fuels, torrefied spruce can offer a large portion of its chemical exergy.

One of the most significant improvements provided by this fuel, is the fuel consumption. The fuel consumption has dropped a staggering 69% compared to the raw spruce and a massive 78% compared to the raw EFB. This can be observed at the Sankey diagram as well, where the percentage of the useful power (thermal and electrical) is significantly higher than the previous ones and the percentages of the flue gas and the other losses are lower.

Lastly, what can be observed by the Grassmann diagram, is the massive drop in the percentage of the Other Losses, meaning that the combustion process is much better in the FLB. So the quality of the energy provided to the cycle remains at a high level, meaning that the utilization of the total chemical energy of the fuel is better. All in all, the wet torrefaction provides us with a tremendously better fuel.

3.3.4 Results of the Torrefied EFB Simulation

The results shown below, occur from the simulation of torrefied EFB, at 300°C. As shown above, in the input section, the LHV of the fuel and the carbon content are significantly higher.

Table 24: Cycle Thermodynamic Properties for the Torrefied EFB simulation

Operation	Nominal	S1	S2	Unit
Boiler Thermal Output	732.9	659.3	633.0	MW
Gross Power Output	83.6	83.3	83.2	MW
Net Power Output	62.0	62.0	62.0	MW
Thermal Power Output	448.8	378.3	353.2	MW
Water Mass Flow	236.2	212.5	204.0	kg/s
Flue Gas Mass Flow	373.4	335.9	322.6	kg/s
Fuel Mass Flow	37.7	33.9	32.5	kg/s
Power to Heat Ratio α	18.6%	22.0%	23.6%	

Table 25: Total Energetic and Exergetic Efficiency Values for the Torrefied EFB simulation

Operation	Nominal	S1	S2
Total Power	100.0%	74.1%	69.2%
η_{net}	69.7%	66.8%	65.6%
η_{gross}	72.6%	70.0%	69.0%
$\eta_{netideal}$	75.0%	72.7%	71.7%
$\eta_{grossideal}$	77.9%	75.9%	75.1%
η_{exnet}	42.5%	43.3%	43.6%
$\eta_{exgross}$	45.1%	46.2%	46.6%

Table 26: Electrical Energetic and Exergetic Efficiency Values for the Torrefied EFB simulation

Operation	Nominal	S1	S2
Total Power	100.0%	74.1%	69.2%
η_{elnet}	8.5%	9.4%	9.8%
$\eta_{elgross}$	11.4%	12.6%	13.1%
$\eta_{alexnet}$	7.6%	8.4%	8.8%
$\eta_{alexgross}$	10.2%	11.3%	11.8%

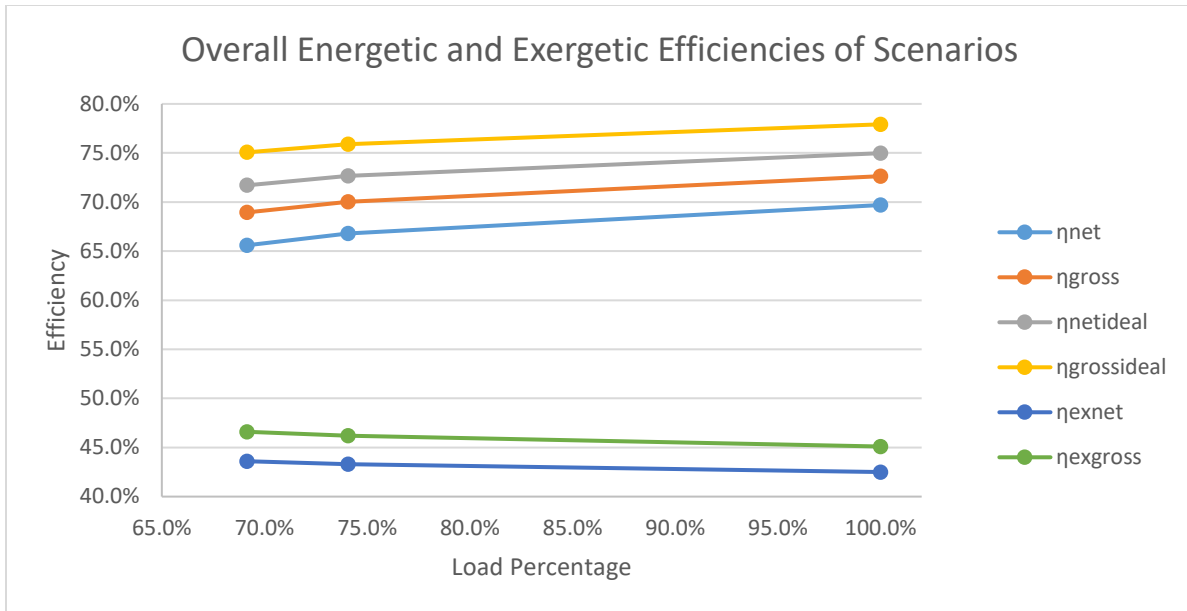


Figure 54: Overall Energetic and Exergetic Efficiencies for the Torrefied EFB simulation

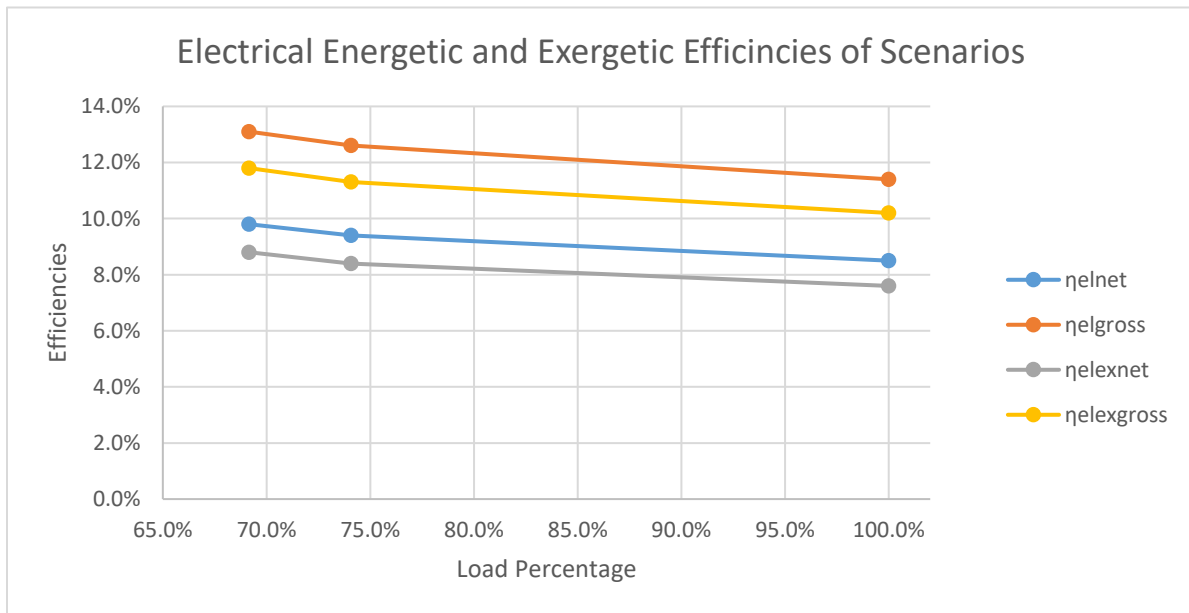


Figure 55: Electrical Energetic and Exergetic Efficiencies for the Torrefied EFB simulation

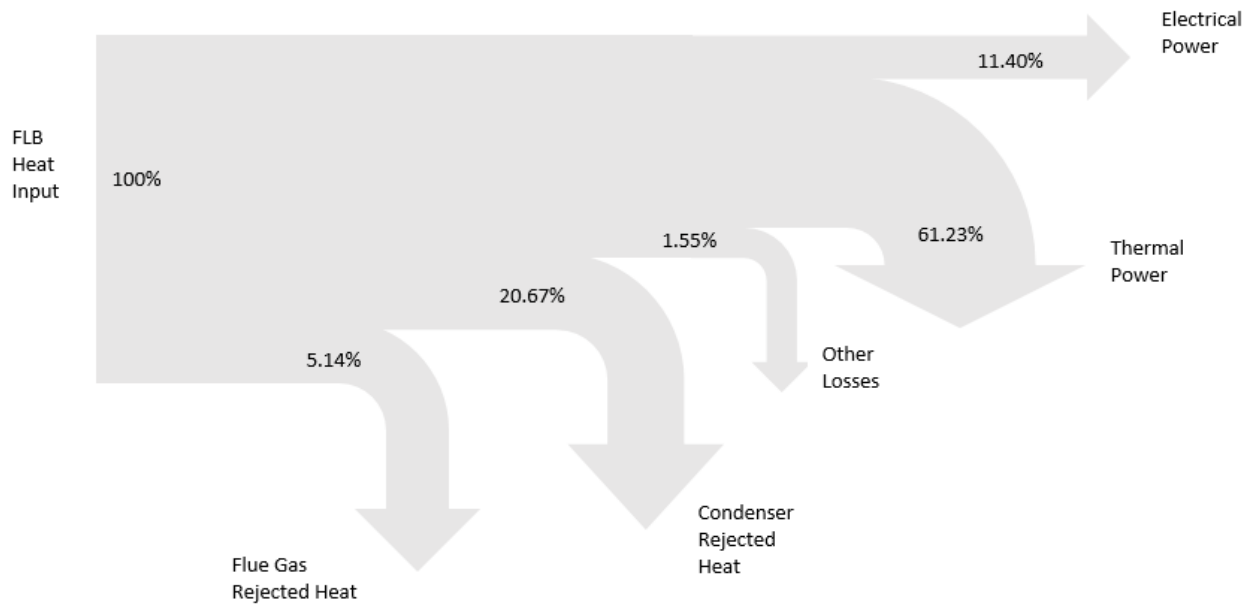


Figure 56: Biomass CHP Power Plant Sankey Diagram for the Torrefied EFB simulation

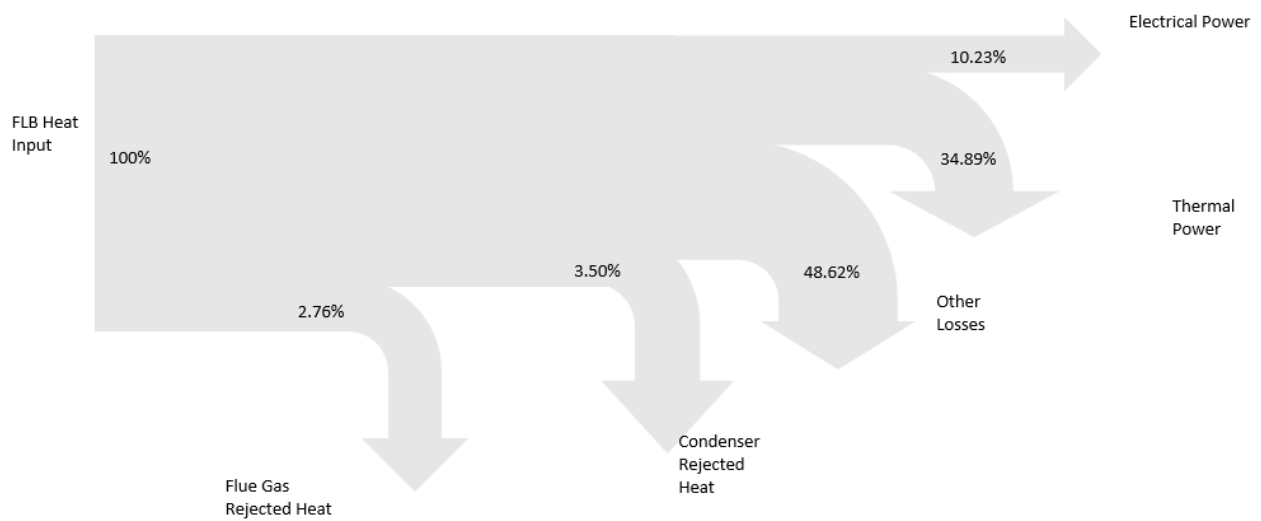


Figure 57: Biomass CHP Power Plant Grassmann Diagram for the Torrefied EFB simulation

As one can observe, the torrefied EFB has almost the same thermodynamic parameters as the torrefied spruce. It would be safe to say that these two fuels are almost identical and obviously have significantly better behaviour than their non pretreated counterparts.

4.Improved CHP Plant

After the modification of the combined cycle which generates electricity, offered to the grid, and heat, offered to the Aluminum plant, the goal was to create a power plant with a higher electrical power output, so as to increase the energetic and exergetic efficiency of the plant.

As the modification took place, it was decided that the steam turbine works at full capacity at all times, contrary to the 10 MW operation of the original combined cycle. This decision came up due to the fact that the gas turbines are now non existent, so a part of the offered electrical power had to be compensated. In this improved model, the major modification is the implementation of a high pressure turbine stage, which will provide a net output of 140 MW, so the total net power output is gonna be 200 MW. This was decided in order to have approximately the same electrical and heat power output as the original plant. Besides the turbine stage, all of the pumps are replaced with improved ones, having isentropic efficiencies of 0.85 instead of 0.75, the condenser operating pressure is now 0.12 bar and in order to have the same thermodynamic characteristics for the steam offered to the Aluminum plant, a reheat is required, occuring at 68 bar. Lastly, in these configurations there are two heat exchangers after the first economizer, in which heat is offered by the flue gases so as to provide cooling and drying.

As for the operation of the plant, there are great alterations. This power plant will operate at significantly higher feedwater pressure and steam temperatures. The steam will operate at near supercritical conditions, while there will be case studies in which the steam is in a supercritical condition. The power plant will operate at a minimum of 160 bar and a maximum of 230 bar, with a minimum of 540 °C and 600 °C. The reheat temperature is kept constant at all times at 480 °C so that the the steam entering the heat part of the model is one that satisfies the needs of the Aluminum plant.

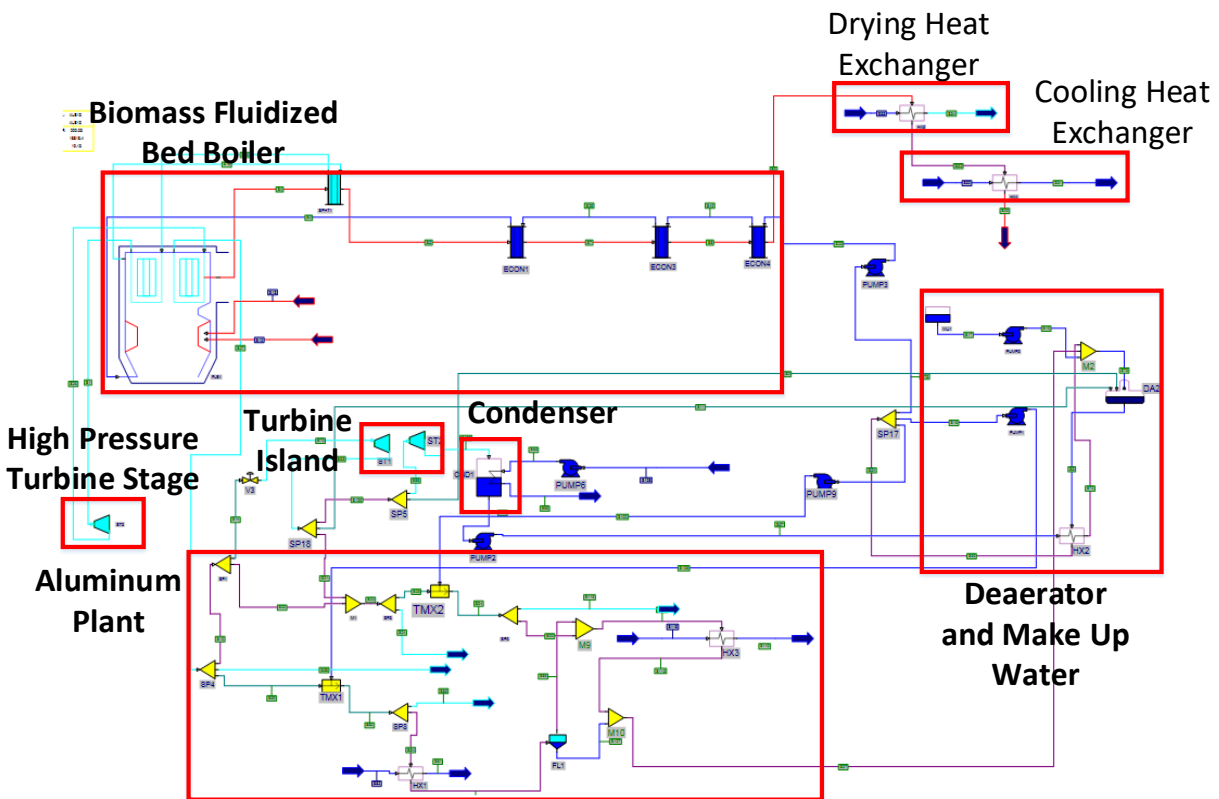


Figure 58: Improved CHP plant model for the non-pretreated fuels

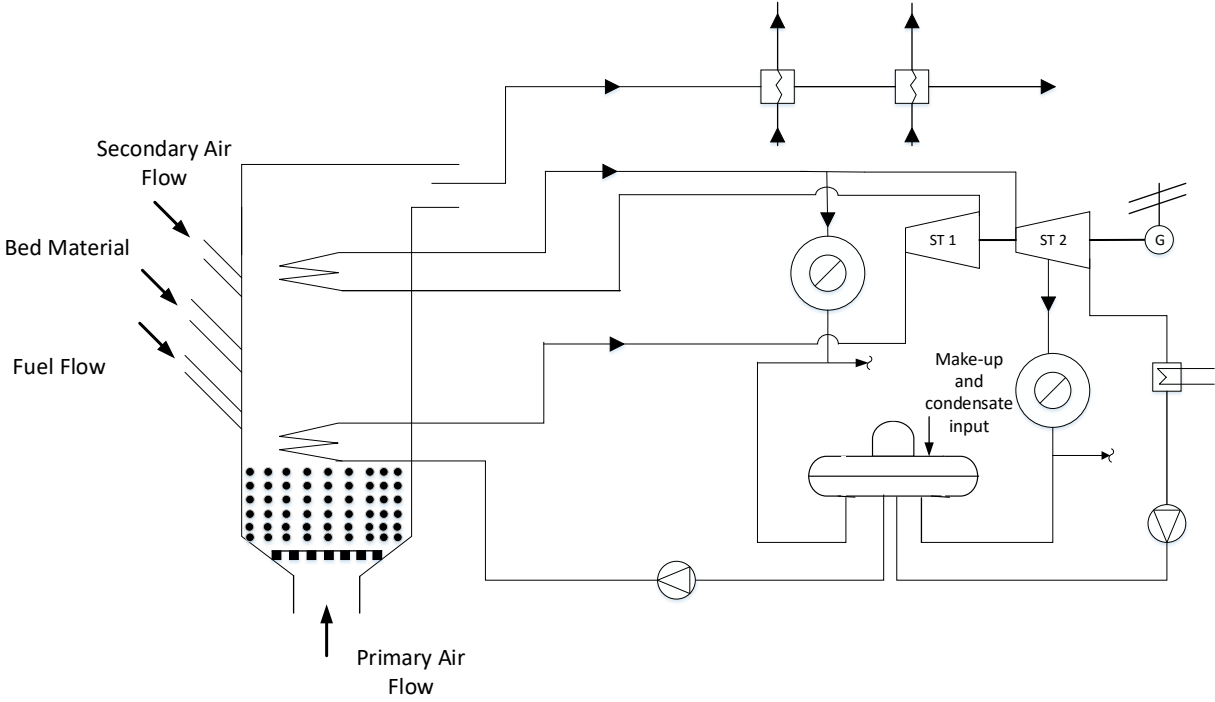


Figure 59: Schematic of the Improved CHP plant model for the non-pretreated fuels

As it can be seen by the model presented above, the model has the aforementioned modifications, with the high pressure turbine stage and the reheating. As one can observe, this model has two heat exchangers instead of one, as described above. The first heat exchanger serves the purpose of drying the raw fuels of EFBs and Spruce wood.

Since these fuels have low LHV and high moisture content, in order to achieve high efficiencies, a drying process must be implemented in the configuration. So the temperature of the flue gases exiting the FLB component is defined accordingly, so the flue gases offer the heat required for the drying of the fuel and the inlet temperature of the flue gases to the second heat exchanger is one that gives a sufficient COP for the cooling absorption or adsorption device. The heat required for the drying of the fuels is calculated by the following equations. It was specified that the final moisture content of the fuels be 12%, since most of the drying processes' final product has approximately that level of moisture, for high moisture content fuels.

Drying Heat Calculation:

$$N = \frac{w - \varepsilon}{1 - \varepsilon} \quad (24)$$

$$q = 1.05 [N \{ r + \bar{c}_{p_d} (\theta_2 - 20) \} + (w - N) (\theta_2 - 20) \bar{c}_{p_w} + (1 - w) (\theta_2 - 20) c_k] \quad [\text{kJ/kg}] \quad (25)$$

$$Q = \dot{m}_B \cdot q \quad [\text{kJ/s}] \quad (26)$$

w: the moisture content of the fuel pre-drying

ε : the desired moisture content after the drying

\bar{c}_{pD} : the mean specific heat of steam in kJ/kg K

\bar{c}_{pw} : the mean specific heat of water in kJ/kg K

c_k : the mean specific heat of the fuel in kJ/kg K

r : the latent heat of evaporation

The drying heat was modelled using a heat exchanger in which the flue gases offer their heat in a stream of water. Several simulation were performed in order to define the fuel flow, and consequently the required heat for this fuel flow. Namely, a first simulation was conducted, the heat offered to the water stream was calculated, then the fuel corresponding to that heat was calculated as well and implemented to the next simulation. This was done until the heat offered to the stream corresponded to the fuel flow of the plant.

4.1 Results of the Improved Biomass CHP Plant – Dried Fuels

The simulation and the results shown in this segment will be solely for the non-pretreated fuels, namely the EFBs and the Spruce wood, whose only pretreatment is the drying. The total number of the simulations for each of the fuels is 17. This number corresponds to all the possible combinations of 4 pressure values and 4 temperature values, plus one simulation of supercritical conditions.

These pressure values and temperatures are 160 bar, 180 bar, 200 bar, 220 bar with 540 °C, 560 °C, 580 °C, 600 °C and a single simulation of 230 bar and 600 °C of live steam. As stated above, the temperature of the reheat is kept constant at 480 °C and 68 bar. The tables shown below will provide information about the fuel chemical composition after the drying, the boiler heat output, the net electrical output, the heat offered to the Aluminum plant, the heat offered to the fuel for the drying, as well as the energetic and exergetic efficiencies of the plant.

Case Study 1: Dry Spruce Wood

Table 27: Dry Spruce Chemical Composition

Dry Spruce	
Moisture Content	12.00%
Ash Content	0.34%
Carbon	48.89%
Hydrogen	4.76%
Nitrogen	0.32%
Sulphur	0.06%
Oxygen	33.63%
Net Calorific Value (LHV) [kJ/kg]	17400

As it can be seen by the LHV and the chemical composition, the drying of the fuel results in a staggering rise of the LHV, meaning that less fuel is required for the satisfaction of the plant's needs. The carbon content of the fuel is now more than double than it previously was, meaning that the quality of the combustion is improved, while there is a rise on the sulphur content as well, but this content is quite low, enabling us to utilize the flue gases' heat even more and go below the barrier of the acid dew point. For that reason, it is specified that the flue gases' temperature at the exit of the plant is 85 °C. Since this power plant is a great improvement from the reference model, where the gas turbines are just replaced by the FLB. Plants with such high steam characteristics are able to utilize most of the flue gases' heat, since biomass fuels in general have low sulphur content.

Table 28: Dry Spruce Improved Model Simulation Outputs for 160 bar

Live Steam Temperature:	600.0	580.0	560.0	540.0	°C
Reheated Steam Temperature:	480.0	480.0	480.0	480.0	°C
Boiler Thermal Output	1045.6	1050.2	1054.9	1059.2	MW
Gross Power Output	222.8	222.8	222.9	222.9	MW
Net Power Output	200.0	200.0	200.0	200.0	MW
Thermal Power to fuel	80.4	80.8	81.1	81.4	MW
Thermal Output	468.0	468.3	468.6	468.4	MW
Water Mass Flow	289.9	291.9	294.0	296.2	kg/s
Flue Gas Mass Flow	651.6	654.4	657.4	660.1	kg/s
Fuel Mass Flow	60.1	60.4	60.6	60.9	kg/s

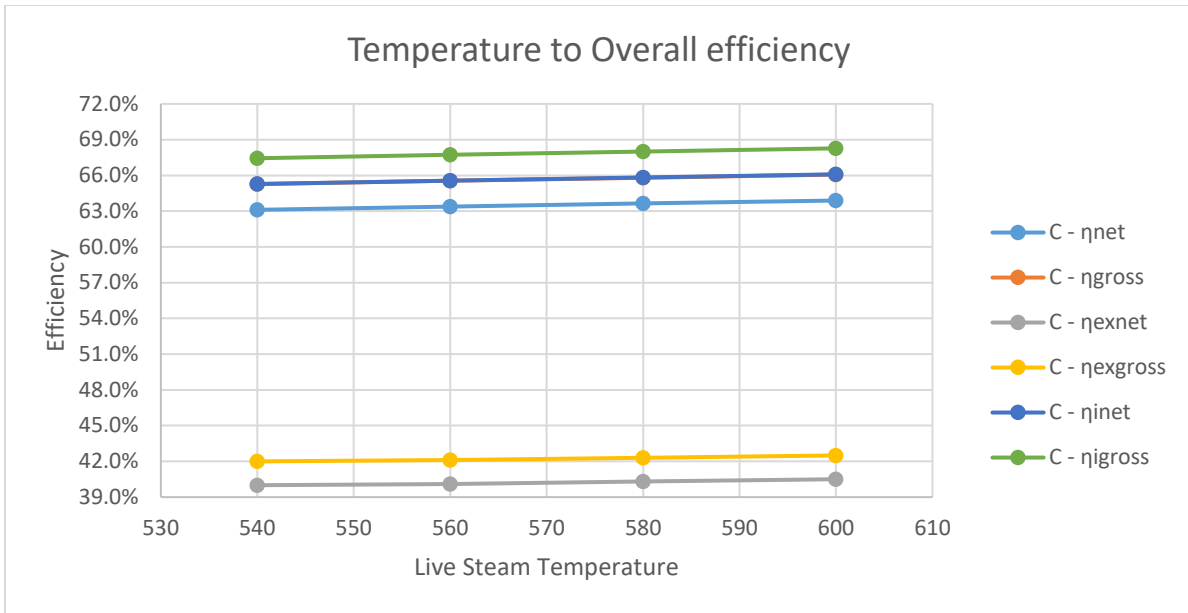


Figure 60: Overall Energetic and Exergetic Efficiencies for the Dry Spruce Simulation of the Improved Model (160 bar)

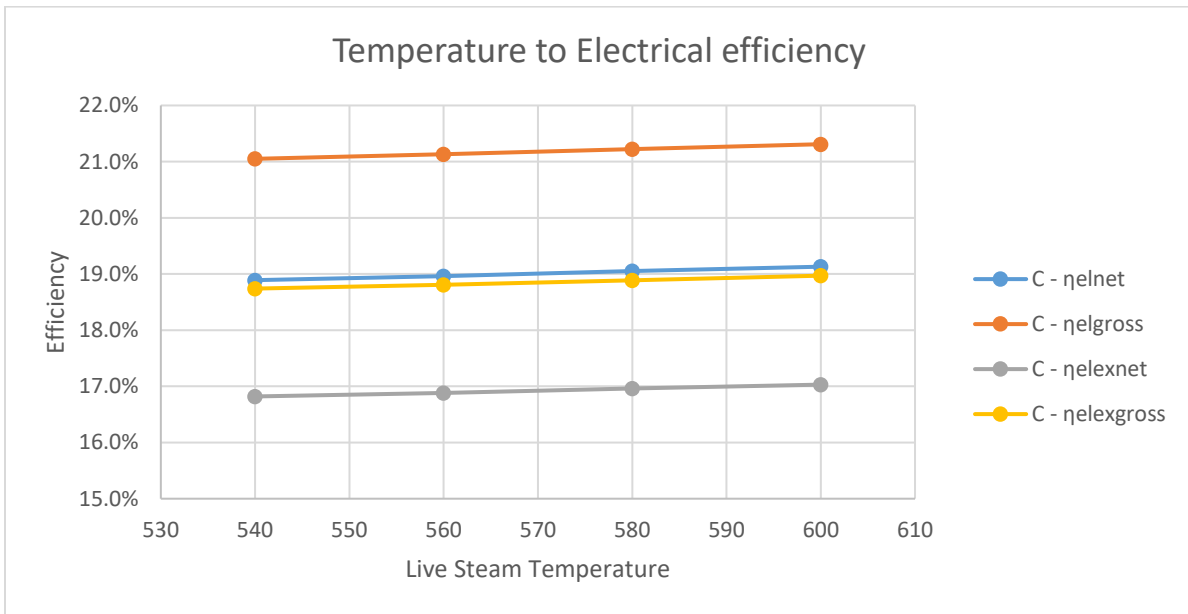


Figure 61: Electrical Energetic and Exergetic Efficiencies for the Dry Spruce Simulation of the Improved Model (160 bar)

Table 29: Dry Spruce Improved Model Simulation Outputs for 180 bar

Live Steam Temperature:	600.0	580.0	560.0	540.0	°C
Reheated Steam Temperature:	480.0	480.0	480.0	480.0	°C
Boiler Thermal Output	1032.3	1036.7	1042.1	1047.7	MW
Gross Power Output	223.4	223.4	223.5	223.6	MW
Net Power Output	200.1	200.0	200.0	200.1	MW
Thermal Power to fuel	79.2	79.7	80.1	80.5	MW
Thermal Output	468.0	467.7	468.0	468.4	MW
Water Mass Flow	283.6	285.9	288.2	290.7	kg/s
Flue Gas Mass Flow	643.3	646.0	649.4	652.9	kg/s
Fuel Mass Flow	59.3	59.6	59.9	60.2	kg/s

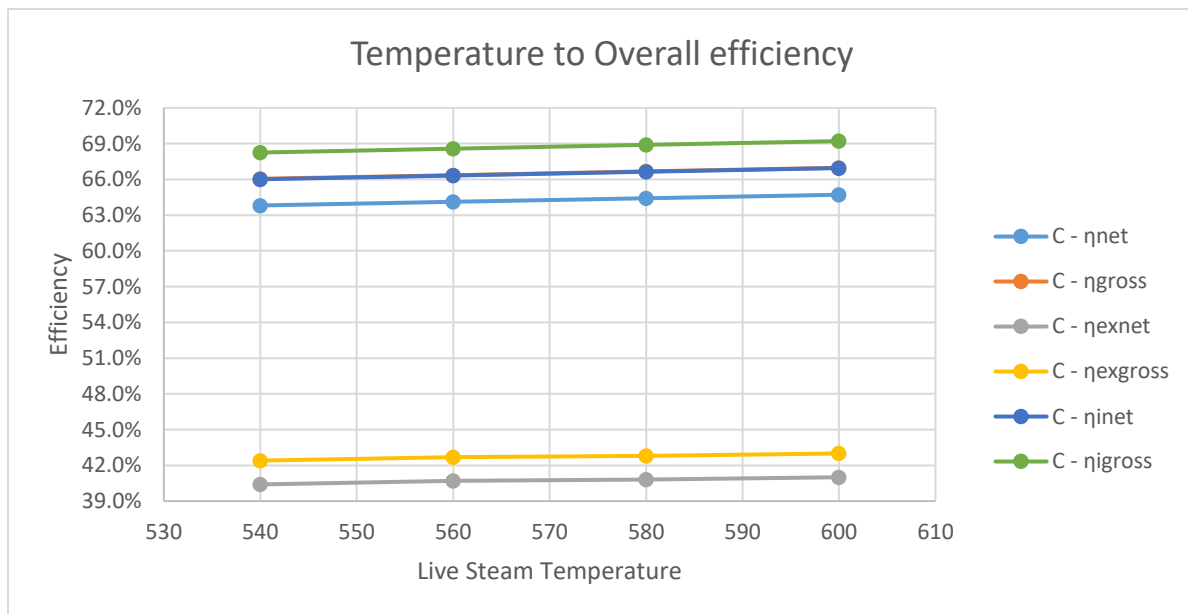


Figure 62: Overall Energetic and Exergetic Efficiencies for the Dry Spruce Simulation of the Improved Model (180 bar)

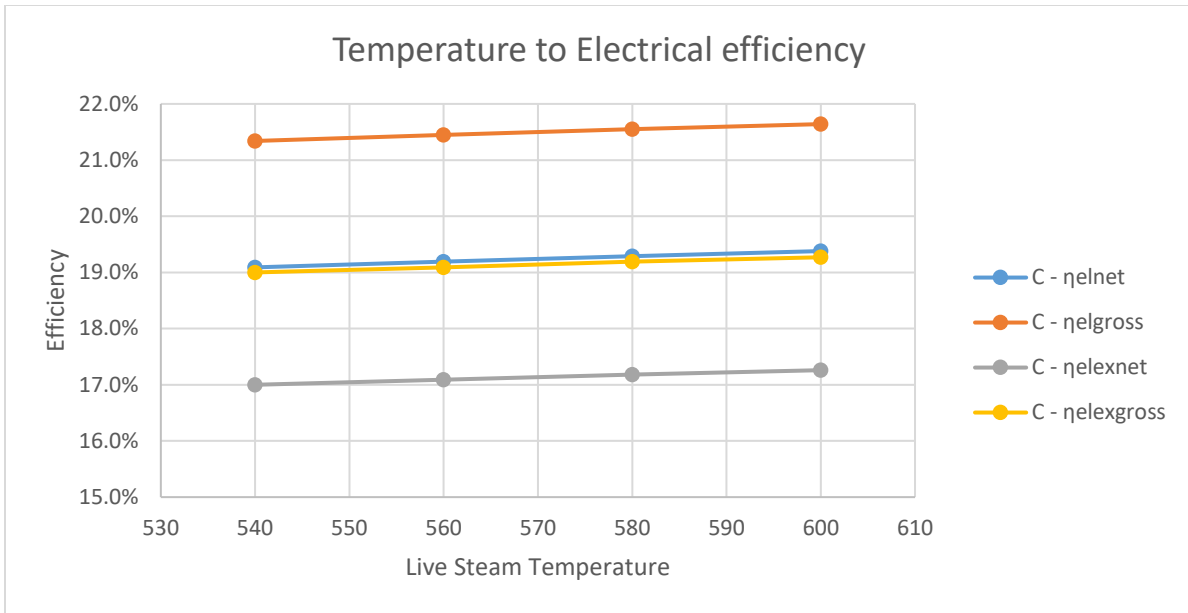


Figure 63: Electrical Energetic and Exergetic Efficiencies for the Dry Spruce Simulation of the Improved Model (180 bar)

Table 30: Dry Spruce Improved Model Simulation Outputs for 200 bar

Live Steam Temperature:	600.0	580.0	560.0	540.0	°C
Reheated Steam Temperature:	480.0	480.0	480.0	480.0	°C
Boiler Thermal Output	1021.3	1026.8	1032.4	1038.1	MW
Gross Power Output	223.9	224.0	224.1	224.2	MW
Net Power Output	200.0	200.0	200.0	200.0	MW
Thermal Power to fuel	78.6	79.0	79.4	79.7	MW
Thermal Power Output	467.3	467.5	467.7	467.9	MW
Water Mass Flow	278.6	281.1	283.7	286.4	kg/s
Flue Gas Mass Flow	636.4	639.9	643.4	646.9	kg/s
Fuel Mass Flow	58.7	59.0	59.3	59.7	kg/s

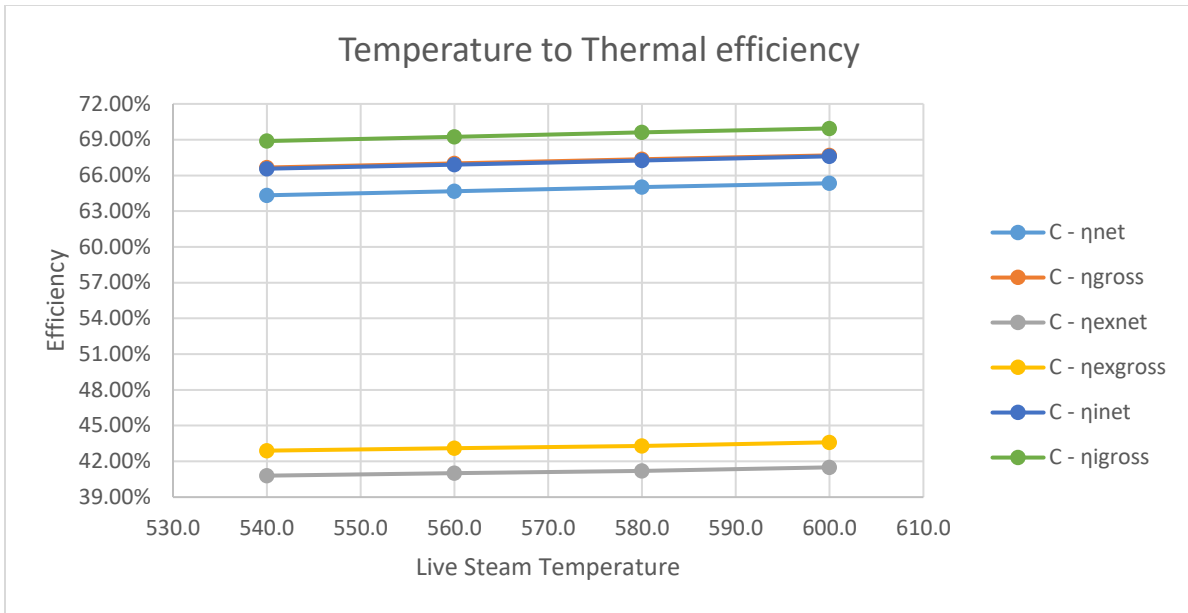


Figure 64: Overall Energetic and Exergetic Efficiencies for the Dry Spruce Simulation of the Improved Model (200 bar)

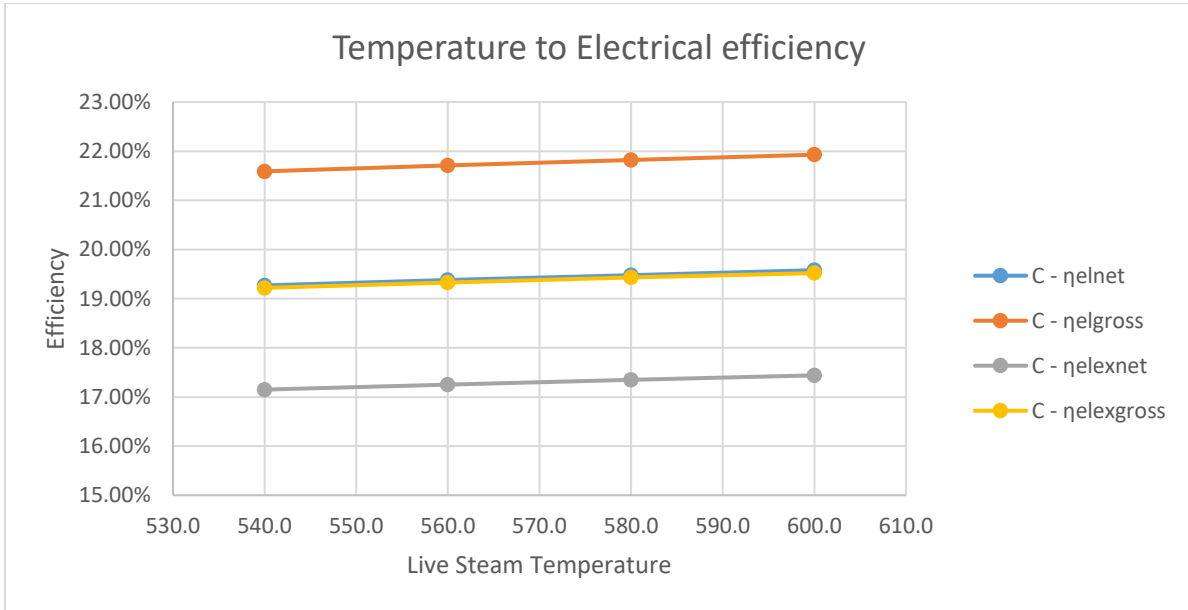


Figure 65: Electrical Energetic and Exergetic Efficiencies for the Dry Spruce Simulation of the Improved Model (200 bar)

Table 31: Dry Spruce Improved Model Simulation Outputs for 220 bar

Live Steam Temperature:	600.0	580.0	560.0	540.0	°C
Reheated Steam Temperature:	480.0	480.0	480.0	480.0	°C
Boiler Thermal Output	1021.3	1026.8	1032.4	1038.1	MW
Gross Power Output	223.9	224.0	224.1	224.2	MW
Net Power Output	200.0	200.0	200.0	200.0	MW
Thermal Power to fuel	78.6	79.0	79.4	79.7	MW
Thermal Power Output	467.3	467.5	467.7	467.9	MW
Water Mass Flow	278.6	281.1	283.7	286.4	kg/s
Flue Gas Mass Flow	636.4	639.9	643.4	646.9	kg/s
Fuel Mass Flow	58.7	59.0	59.3	59.7	kg/s

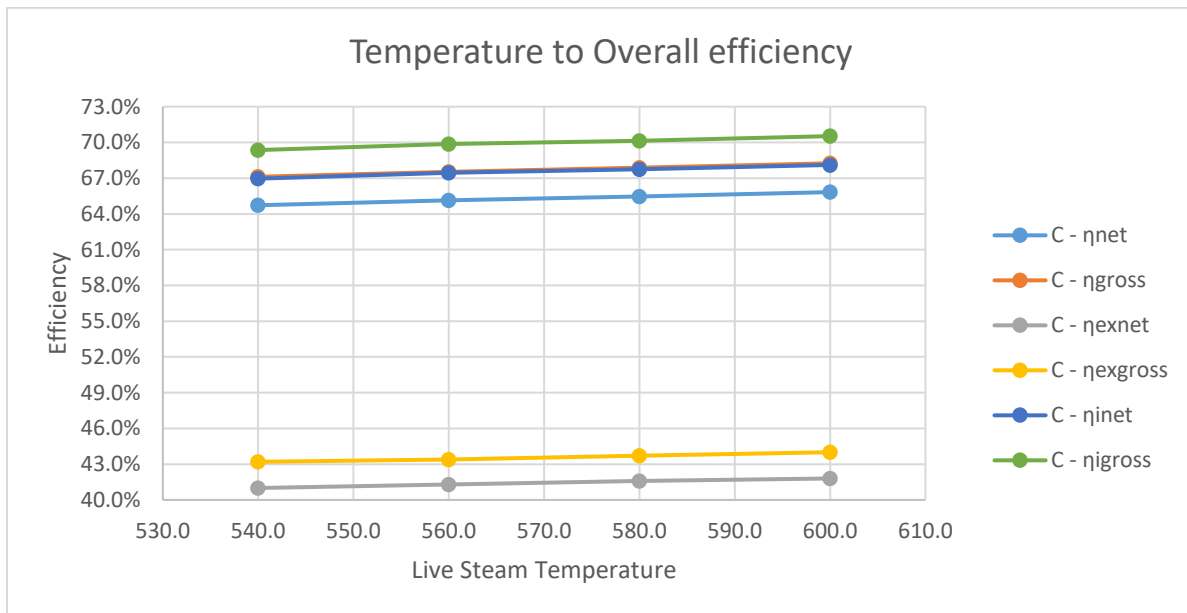


Figure 66: Overall Energetic and Exergetic Efficiencies for the Dry Spruce Simulation of the Improved Model (220 bar)

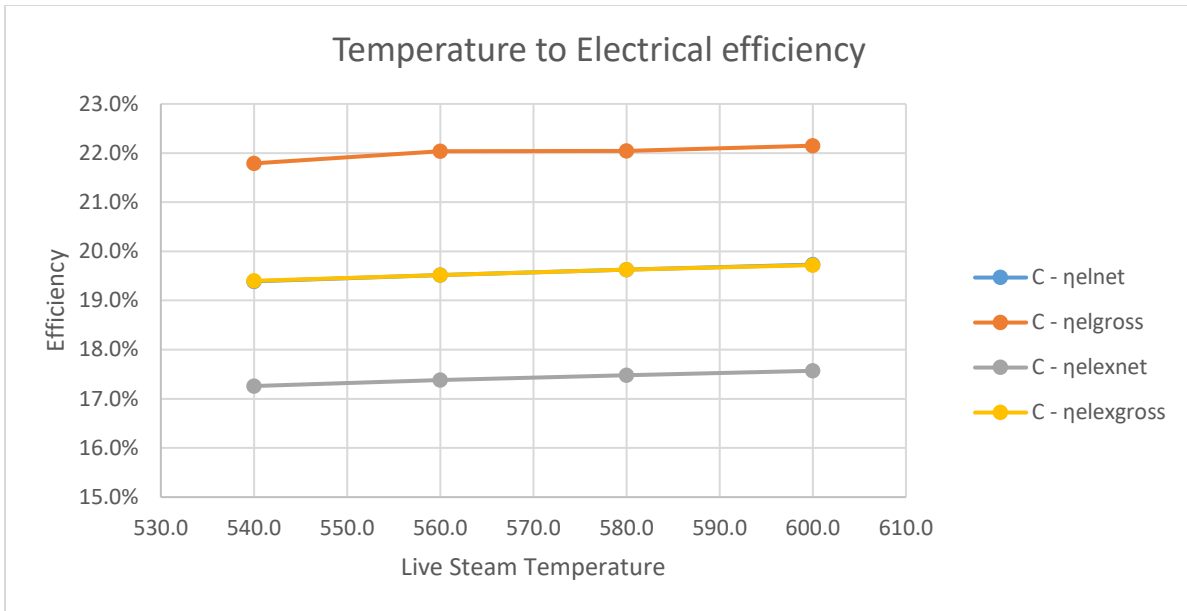


Figure 67: Electrical Energetic and Exergetic Efficiencies for the Dry Spruce Simulation of the Improved Model (220 bar)

Table 32: Dry Spruce Improved Model Simulation Outputs for 230 bar (Supercritical)

Live Steam Temperature:	600	°C
Reheated Steam Temperature:	480.0	°C
Boiler Thermal Output	1007.6	MW
Gross Power Output	224.9	MW
Net Power Output	200.0	MW
Thermal Power to fuel	77.7	MW
Thermal Output	466.6	MW
Water Mass Flow	273.1	kg/s
Flue Gas Mass Flow	627.9	kg/s
Fuel Mass Flow	57.9	kg/s
$\eta_{el(net)}$	19.9%	
$\eta_{el(gross)}$	22.3%	
$\eta(net)$	66.2%	
$\eta(gross)$	68.6%	
$\eta_i(net)$	68.5%	
$\eta_i(gross)$	70.9%	
$\eta_{ex(net)}$	42.0%	
$\eta_{ex(gross)}$	44.2%	
$\eta_{exlex(net)}$	17.7%	
$\eta_{exlex(gross)}$	19.9%	

After the presented tables and charts, one can observe that, as expected, all of the efficiencies, electrical and overall, rise as the live steam temperature rises. Although there is improvement in the efficiency values, this improvement is not particularly high. For example, in all of the simulated operating pressures, the net electrical efficiency rises about 0.1 % for each 20 °C rise of the live steam temperature. This means that the steam's temperature doesn't play a big part in the improvement of efficiencies, after a certain value. As the charts show, the correlation of the temperature increase and the efficiency increase is linear. One more thing to note, is that now the total heat power output of the FLB, stands at 1000 MW.

As for the fuel consumption, the drop for each 20 °C rise in the temperature is 0.3 kg/s. Assuming that the power plant will operate 8500 hours per year at full capacity, this means that for each rise in 20 °C, the power plant will save 9180 tn of fuel. The overall efficiency has the same trend as well, since it rises a 0.3 % for each 20 °C, although its value is again low, standing at 64 %. Again this occurs, due to the fact that the configuration of the heat part of the plant is really complex and with specific needs. As in the reference model, the "ideal" efficiencies are greater, which means that one immediate improvement to the heat part, is the use of heat exchangers, instead of attemperators, in case of a temperature control having a great margin. The exergetic efficiencies are at a good level for a CHP plant, this being a result of the drying process and the increase of the electrical output of the plant. The chemical exergy of the dried Spruce is 19543 kJ/kg.

Following the charts and tables showing the results of the temperature increase for each feedwater pressure level, are the charts and tables showing the increase in efficiency, having a standard temperature level of 600 °C. This is done in order to compare the improvements, the rise in pressure levels and the rise in temperature levels, offer.

Table 33: Dry Spruce Improved Model Simulation Outputs for 600 °C

Operating Pressure:	230.0	220.0	200.0	180.0	160.0	bar
Live Steam Temperature:	600.0	600.0	600.0	600.0	600.0	°C
Reheated Steam Temperature:	480.0	480.0	480.0	480.0	480.0	°C
Boiler Thermal Output	1007.6	1013.6	1021.3	1032.3	1045.6	MW
Gross Power Output	224.9	224.6	223.9	223.4	222.8	MW
Net Power Output	200.0	200.0	200.0	200.1	200.0	MW
Thermal Power to fuel	77.7	78.0	78.6	79.2	80.4	MW
Thermal Power Output	466.6	467.3	467.3	468.0	468.0	MW
Water Mass Flow	273.1	274.7	278.6	283.6	289.9	kg/s
Flue Gas Mass Flow	627.9	631.7	636.4	643.3	651.6	kg/s
Fuel Mass Flow	57.9	58.3	58.7	59.3	60.1	kg/s

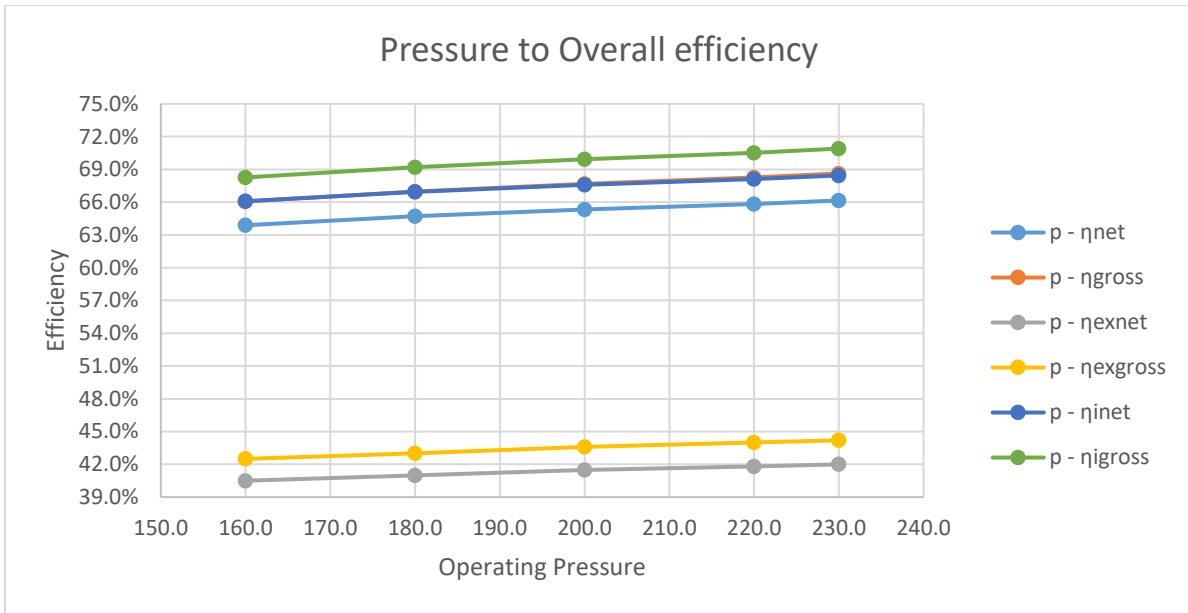


Figure 68: Overall Energetic and Exergetic Efficiencies for the Dry Spruce Simulation of the Improved Model (600 °C)

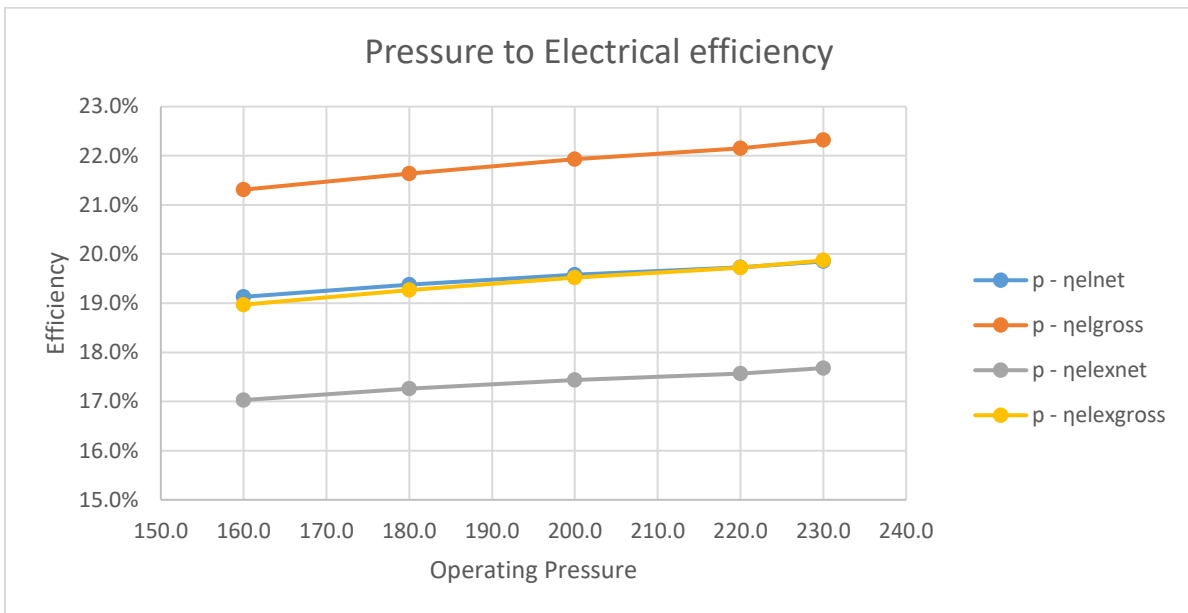


Figure 69: Electrical Energetic and Exergetic Efficiencies for the Dry Spruce Simulation of the Improved Model (600 °C)

Observing the charts and the table, it is obvious that the rise in efficiency is greater for each 20 bar of increase. That means that the rise in operating pressure is more significant in terms of efficiency improvement. Again the rise of the efficiencies seems to be linear to the rise of pressure. Although there is a significant rise in efficiencies, the dry Spruce configuration cannot exceed the barrier of 70%, in terms of overall efficiency of the plant.

As far as the fuel consumption is concerned, the decrease in fuel consumption is quite satisfying, since, from the initial pressure of 160 bar until the supercritical pressure of 230 bar, there is a fuel consumption drop of 2.2 kg/s, amounting to 67320 tn per year. As for the total heat output of the FLB, there is a decrease of circa 10 MW, for each 20 bar of increase, meaning that less power is demanded by the FLB, since more power is provided by the feedwater pump, in order to such a great pressure ratio.

The overall and electrical exergetic efficiencies, follow the same trend as the energetic efficiencies. The electrical exergetic efficiencies have a slightly lower value than the energetic electrical efficiencies, meaning that the chemical exergy of the fuel is utilized properly for the electricity production. Although this power plant has a greater electrical power output, most of its heat output is consumed as heat, meaning that the degradation of heat is still leading the exergetic overall efficiencies to a level of 40 %, almost 30 % lower than the energetic efficiencies.

Last but not least, is the contribution of the supercritical simulation of the dry Spruce Simulation. As one can see, going from 220 bar to 230 has an increase of 0.2 % for the net electrical efficiency and the same increase in the overall efficiency. This means that for an increase of 10 bars from a subcritical pressure, the increase in electrical efficiency is doubled, even if it is a meek 0.2 %. This means that supercritical conditions offer a good rise in electrical efficiencies, which is why more and more biomass and fossil fuel plants, are operating in such conditions.

Case Study 2: Dry Empty Fruit Bunch

Table 34: Dry Spruce Chemical Composition

Dry EFB	
Moisture Content	12.00%
Ash Content	1.60%
Carbon	48.18%
Hydrogen	4.69%
Nitrogen	0.32%
Sulphur	0.06%
Oxygen	33.15%
Net Calorific Value (LHV) [kJ/kg]	14101

As it can be seen by the LHV and the chemical composition, the drying of the fuel results again in a great rise of the LHV. The carbon content of the fuel is now more than double than it previously was, meaning that the combustion process is improved, while there is a rise on the sulphur content as well, same as in the dry spruce, but again this content is low enough to enable us to utilize the flue gas' heat even more and go below the barrier of the acid dew point. For that reason, it is specified that the flue gas' temperature at the exit of the plant is 85 °C, since the same model configuration was used here.

Table 35: Dry EFB Improved Model Simulation Outputs for 160 bar

Live Steam Temperature:	600.0	580.0	560.0	540.0	°C
Reheated Steam Temperature:	480.0	480.0	480.0	480.0	°C
Boiler Thermal Output	1080.2	1084.5	1089.0	1094.2	MW
Gross Power Output	222.8	222.8	222.9	222.9	MW
Net Power Output	200.0	200.0	200.0	200.0	MW
Thermal Power to fuel	11.5	115.8	116.4	116.9	MW
Thermal Output	466.6	466.8	466.6	467.1	MW
Water Mass Flow	289.9	291.9	294.0	296.2	kg/s
Flue Gas Mass Flow	613.9	616.1	618.9	621.9	kg/s
Fuel Mass Flow	76.6	76.9	77.2	77.6	kg/s

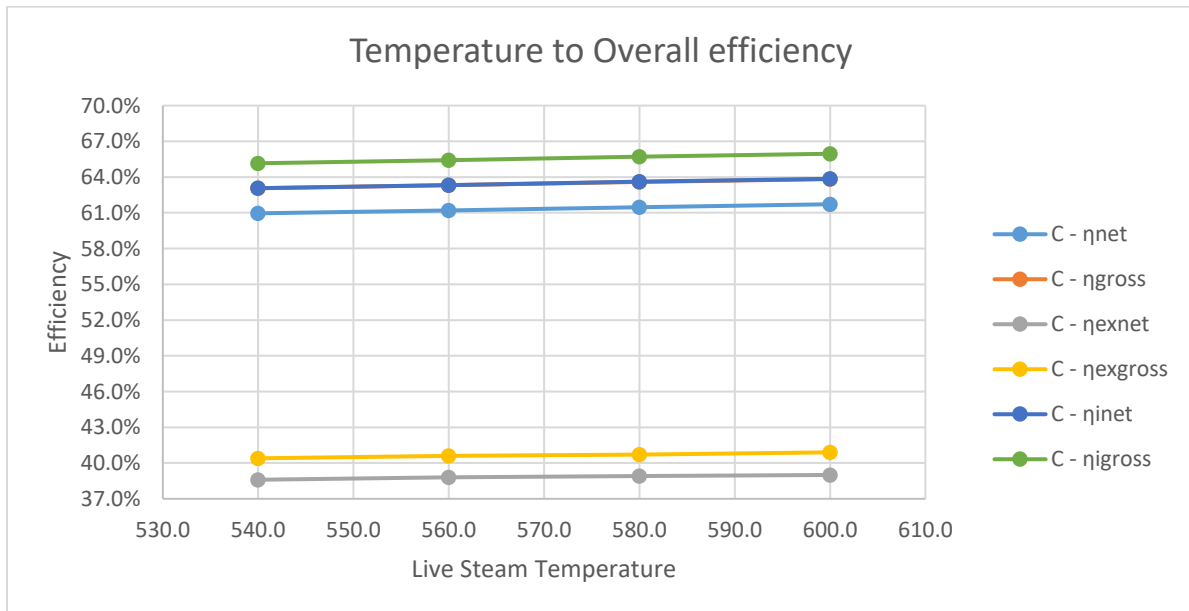


Figure 70: Overall Energetic and Exergetic Efficiencies for the Dry EFB Simulation of the Improved Model (160 bar)

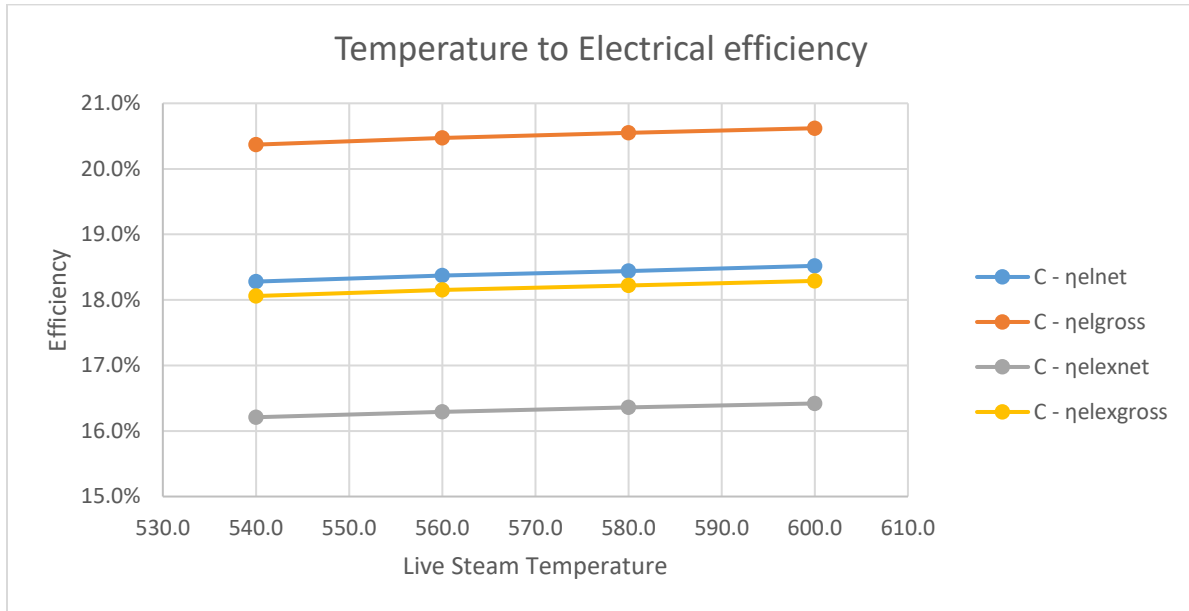


Figure 71: Electrical Energetic and Exergetic Efficiencies for the Dry EFB Simulation of the Improved Model (160 bar)

Table 36: Dry EFB Improved Model Simulation Outputs for 180 bar

Live Steam Temperature:	600	580	560	540	°C
Reheated Steam Temperature:	480.0	480.0	480.0	480.0	°C
Boiler Thermal Output	1050.6	1055.2	1060.7	1066.2	MW
Gross Power Output	223.4	223.4	223.5	223.6	MW
Net Power Output	200.0	200.0	200.1	200.1	MW
Thermal Power to fuel	99.6	99.9	100.5	101.0	MW
Thermal Output	466.2	466.0	466.3	466.5	MW
Water Mass Flow	283.6	285.9	288.3	290.7	kg/s
Flue Gas Mass Flow	597.1	599.6	602.8	605.9	kg/s
Fuel Mass Flow	74.5	74.8	75.2	75.6	kg/s

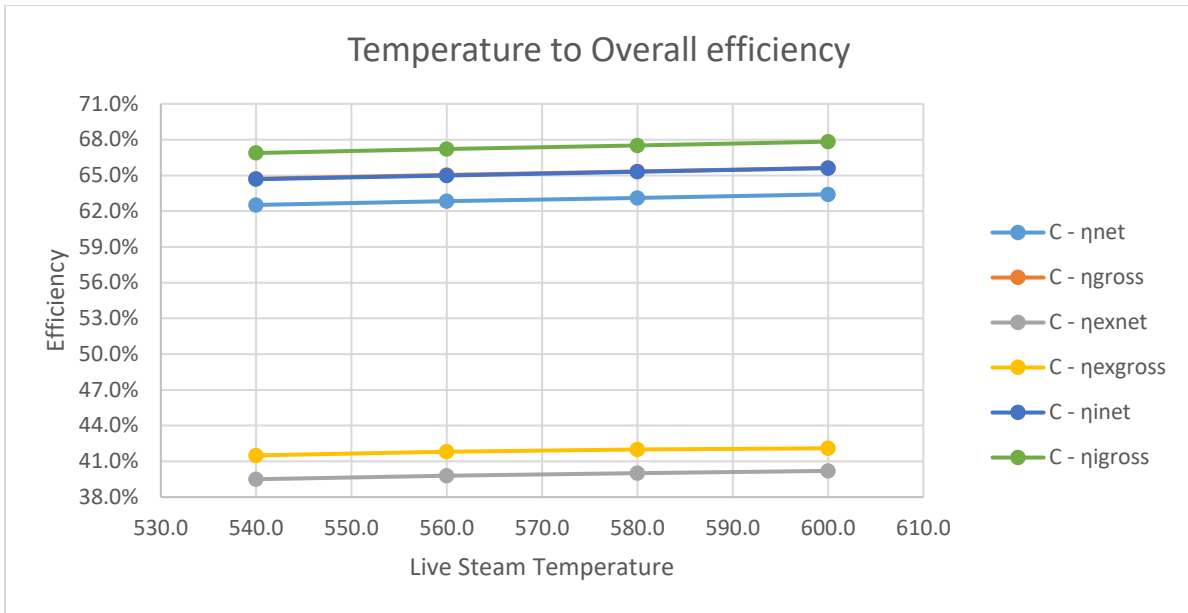


Figure 72: Overall Energetic and Exergetic Efficiencies for the Dry EFB Simulation of the Improved Model (180 bar)

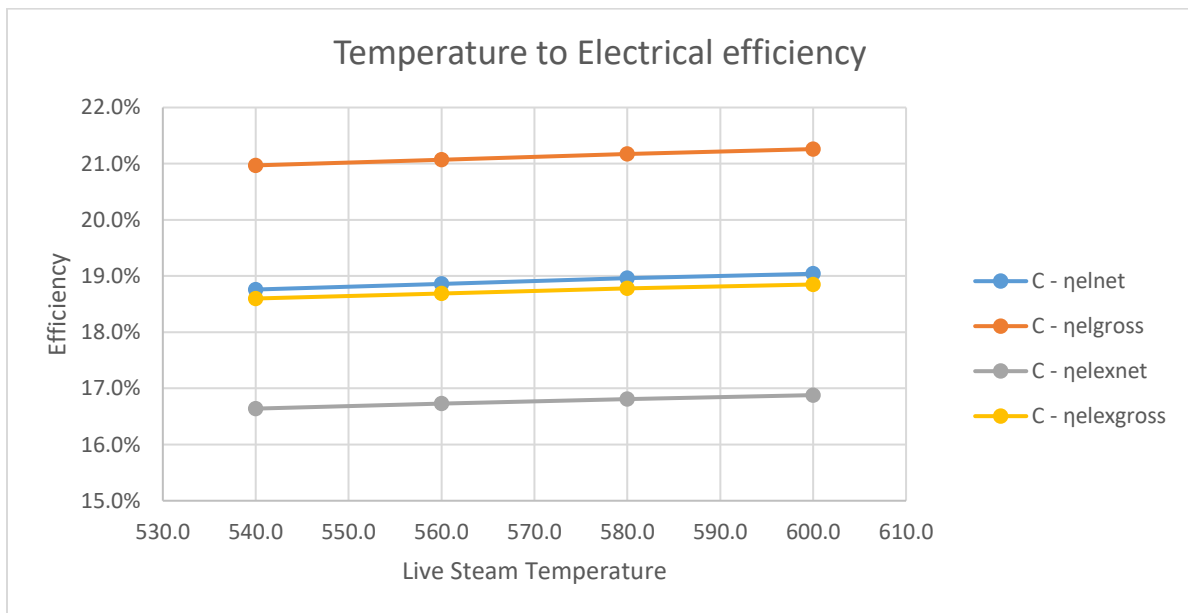


Figure 73: Electrical Energetic and Exergetic Efficiencies for the Dry EFB Simulation of the Improved Model (180 bar)

Table 37: Dry EFB Improved Model Simulation Outputs for 200 bar

Live Steam Temperature:	600	580	560	540	°C
Reheated Steam Temperature:	480.0	480.0	480.0	480.0	°C
Boiler Thermal Output	1039.2	1044.5	1050.5	1056.8	MW
Gross Power Output	224.0	224.0	224.1	224.2	MW
Net Power Output	200.0	200.0	200.0	200.1	MW
Thermal Power to fuel	98.5	98.9	99.4	100.0	MW
Thermal Power Output	465.3	465.6	465.9	466.3	MW
Water Mass Flow	278.7	281.1	283.7	286.4	kg/s
Flue Gas Mass Flow	590.6	593.6	597.0	600.6	kg/s
Fuel Mass Flow	73.7	74.1	74.5	74.9	kg/s

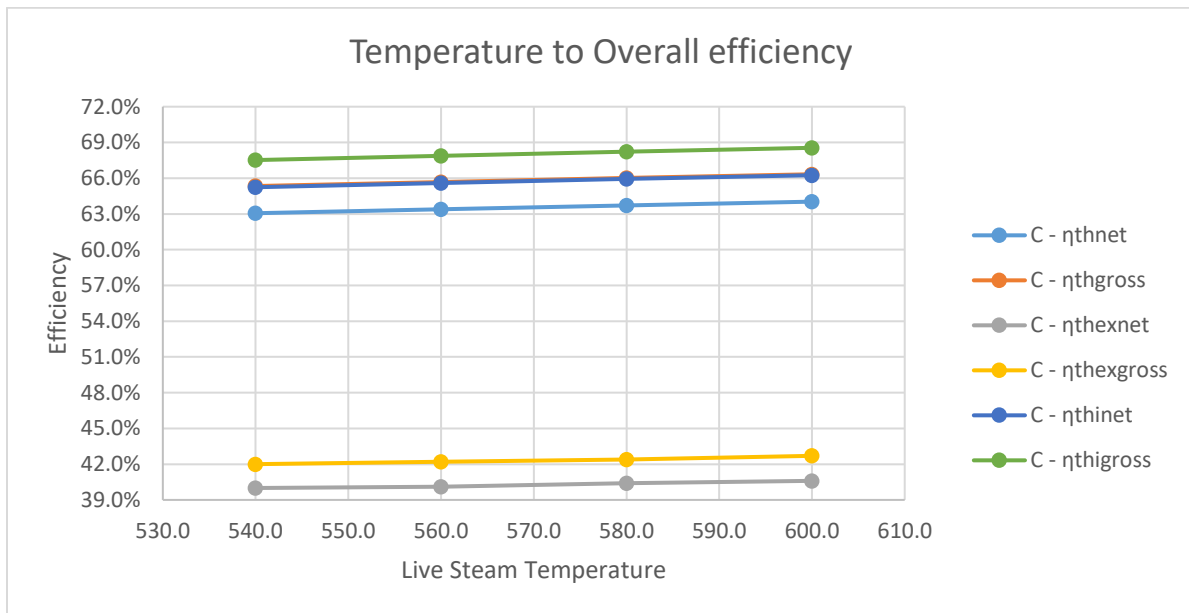


Figure 74: Overall Energetic and Exergetic Efficiencies for the Dry EFB Simulation of the Improved Model (200 bar)

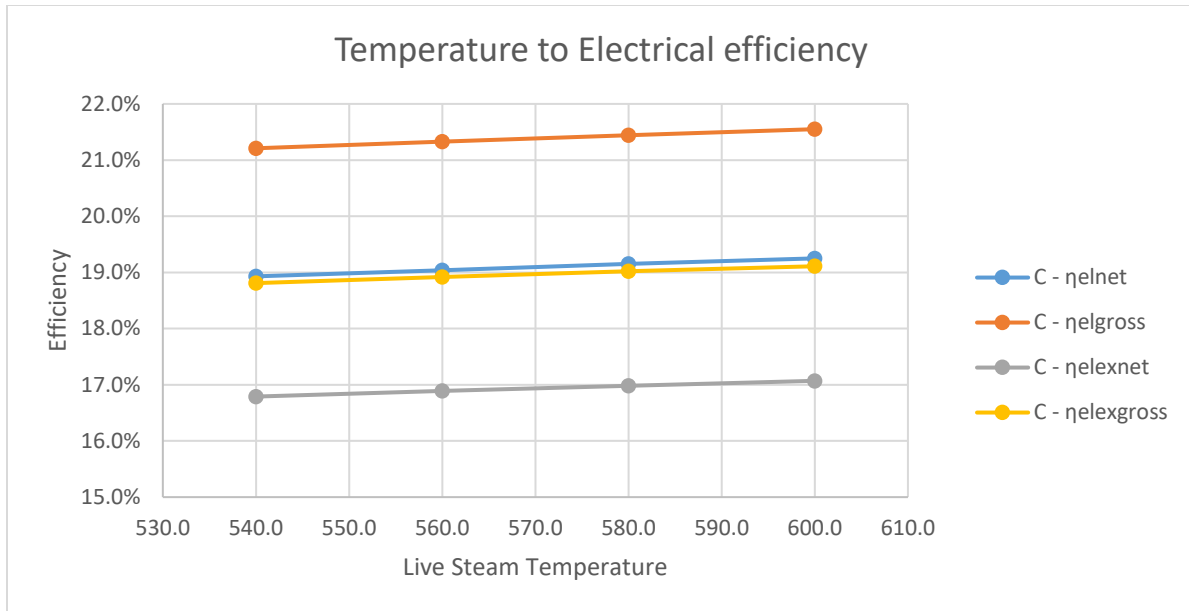


Figure 75: Electrical Energetic and Exergetic Efficiencies for the Dry EFB Simulation of the Improved Model (200 bar)

Table 38: Dry EFB Improved Model Simulation Outputs for 220 bar

Live Steam Temperature:	600	580	560	540	°C
Reheated Steam Temperature:	480.0	480.0	480.0	480.0	°C
Boiler Thermal Output	1031.5	288219.4	1043.4	1049.6	MW
Gross Power Output	224.6	224.7	224.7	224.8	MW
Net Power Output	200.1	200.1	200.1	200.0	MW
Thermal Power to fuel	97.9	98.5	98.8	99.4	MW
Thermal Power Output	465.3	465.6	465.7	465.6	MW
Water Mass Flow	274.7	277.4	280.2	283.2	kg/s
Flue Gas Mass Flow	586.2	589.7	593.0	596.5	kg/s
Fuel Mass Flow	73.2	73.6	74.0	74.4	kg/s

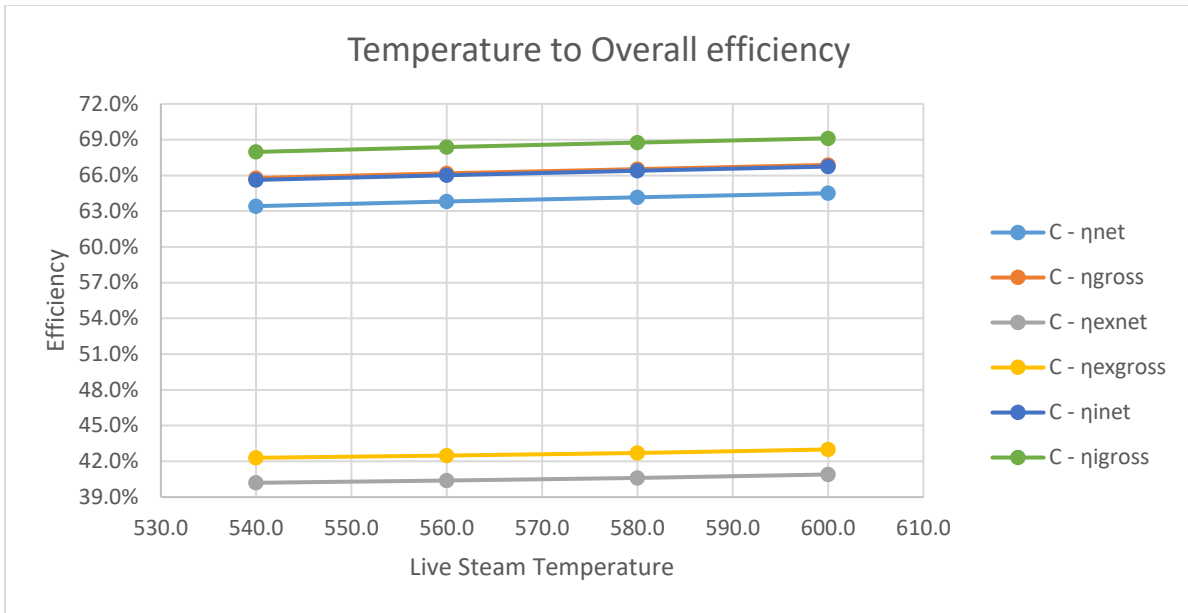


Figure 76: Overall Energetic and Exergetic Efficiencies for the Dry EFB Simulation of the Improved Model (220 bar)

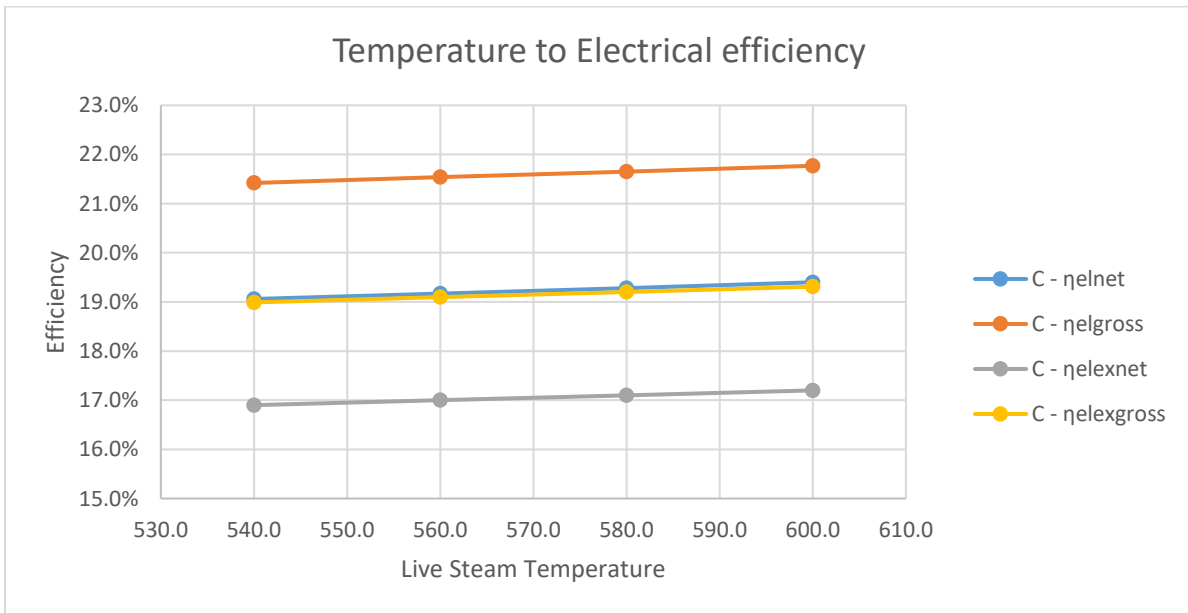


Figure 77: Electrical Energetic and Exergetic Efficiencies for the Dry EFB Simulation of the Improved Model (220 bar)

Table 39: Dry EFB Improved Model Simulation Outputs for 230 bar (Supercritical)

Live Steam Temperature:	600.0	°C
Reheated Steam Temperature:	480.0	°C
Boiler Thermal Output	1025.4	MW
Gross Power Output	224.9	MW
Net Power Output	200.0	MW
Thermal Power to fuel	96.9	MW
Thermal Power Output	465.4	MW
Water Mass Flow	256.4	kg/s
Flue Gas Mass Flow	582.8	kg/s
Fuel Mass Flow	72.7	kg/s
$\eta_{el}(\text{net})$	19.5%	
$\eta_{el}(\text{gross})$	21.9%	
$\eta(\text{net})$	64.9%	
$\eta(\text{gross})$	67.3%	
$\eta_i(\text{net})$	67.2%	
$\eta_i(\text{gross})$	69.6%	
$\eta_{ex}(\text{net})$	41.1%	
$\eta_{ex}(\text{gross})$	43.2%	
$\eta_{lex}(\text{net})$	17.3%	
$\eta_{lex}(\text{gross})$	19.5%	

After the presented tables and charts, one can observe that, as expected again, all of the efficiencies, electrical and overall, rise as the live steam temperature rises. In all of the simulated operating pressures, the net electrical efficiency rises about 0.1 % for each 20 °C rise of the live steam temperature, as with the dry Spruce. Although the EFB efficiency values are lower than that of the dry Spruce, since EFBs are a fuel of lower quality.

As for the fuel consumption, the drop for each 20 °C rise in the temperature is 0.4 kg/s. For an operation of 8500 hours per year at full capacity, this means that for each rise in 20 °C, the power plant will save 12240 tn of fuel. The overall efficiency has the same trend as well, since it rises a 0.3 % for each 20 °C, although its value is again low, standing near 62%. Again this occurs, due to the fact that the configuration of the heat part of the plant is really complex and with specific needs. As in the reference model, the “ideal” efficiencies are greater. The exergetic efficiencies are at a good level for a CHP plant, this being a result of the drying process and the increase of the electrical output of the plant. The chemical exergy of the dried EFBs is 15900 kJ/kg.

Following the charts and tables showing the results of the temperature increase for each feedwater pressure level, are the charts and tables showing the increase in efficiency, having a standard temperature level of 600 °C.

Table 40: Dry EFB Improved Model Simulation Outputs for 600 °C

Operating Pressure:	230	220	200	180	160	bar
Live Steam Temperature:	600.0	600.0	600.0	600.0	600.0	°C
Reheated Steam Temperature:	480.0	480.0	480.0	480.0	480.0	°C
Boiler Thermal Output	1025.4	1031.5	1039.2	1050.6	1080.2	MW
Gross Power Output	224.9	224.6	224.0	223.4	222.8	MW
Net Power Output	200.0	200.1	200.0	200.0	200.0	MW
Thermal Power to fuel	96.9	97.9	98.5	99.6	115.5	MW
Thermal Power Output	465.4	465.3	465.3	466.2	466.6	MW
Water Mass Flow	256.4	274.7	278.7	283.6	289.9	kg/s
Flue Gas Mass Flow	582.8	586.2	590.6	597.1	613.9	kg/s
Fuel Mass Flow	72.7	73.2	73.7	74.5	76.6	kg/s

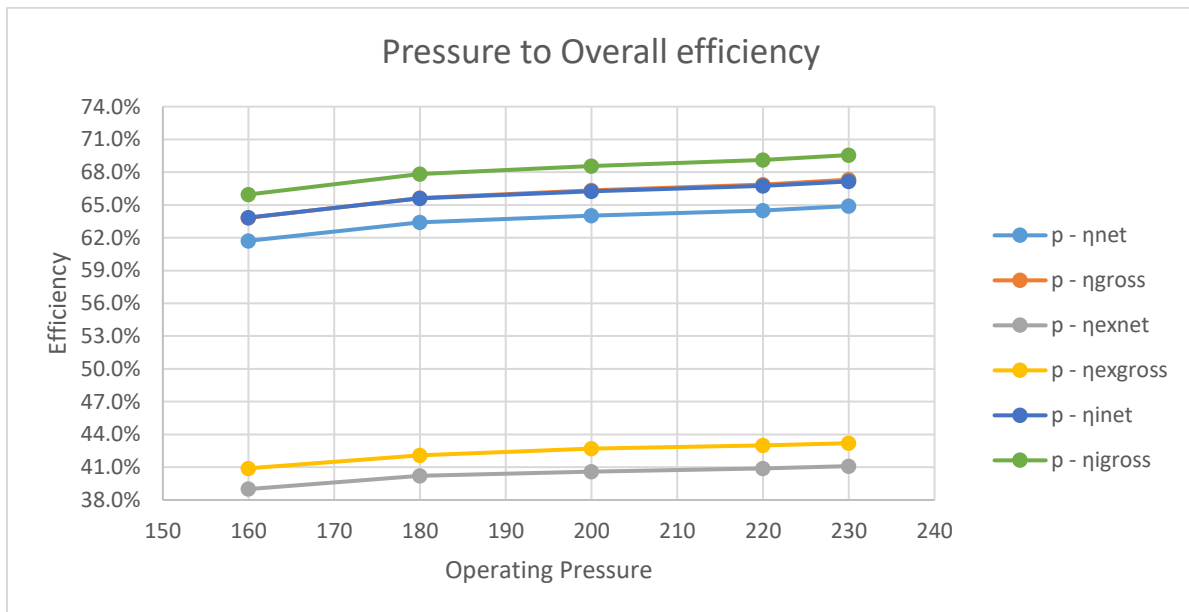


Figure 78: Overall Energetic and Exergetic Efficiencies for the Dry EFB Simulation of the Improved Model (600 °C)

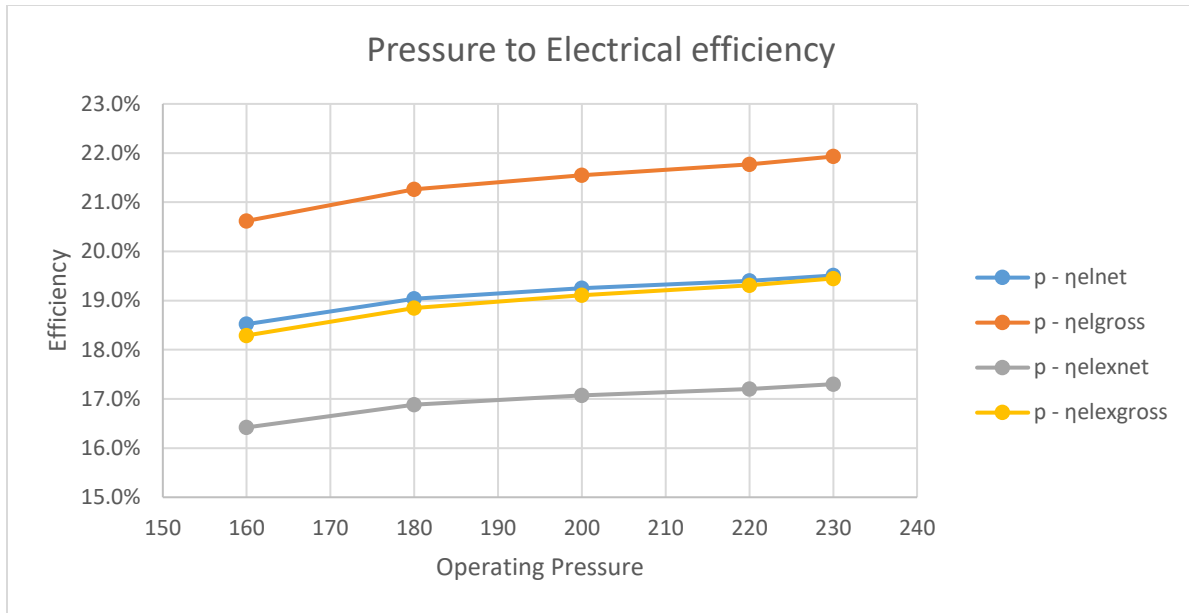


Figure 79: Electrical Energetic and Exergetic Efficiencies for the Dry EFB Simulation of the Improved Model (600 °C)

Observing the charts and the table, it is obvious that the rise in efficiency is greater for each 20 bar of increase for the dry EFBs as well. The increase of the efficiencies, as opposed to the dry Spruce, is not linear, but rather, it has a diminishing rate of increase until the last subcritical operating pressure of 220 bar. As with the dry Spruce, there is a slight increase of the rate when there is an operation of supercritical conditions.

As far as the fuel consumption is concerned, the decrease in fuel consumption is substantial, since there is a really big drop of 3.9 kg/s from the initial pressure of 160 bar until the supercritical pressure of 230 bar, almost double than that of the dry Spruce, amounting to a staggering 119340 tn of fuel saved per year. As for the total heat output of the FLB, the decrease is not constant since, there is a drop of 30 MWs from 160 bar to 180 bar and then the drop amounts to 7-11 MWs for each 20 bar of increase.

The overall and electrical exergetic efficiencies, follow the same trend as the energetic efficiencies. The electrical exergetic efficiencies have a slightly lower value than the energetic electrical efficiencies, meaning that the chemical exergy of the fuel is utilized properly for the electricity production. Although this power plant has a greater electrical power output, most of its heat output is consumed as heat, meaning that the degradation of heat is still leading the exergetic overall efficiencies to a level of 40 %, almost 30 % lower than the energetic efficiencies.

Last but not least, is the contribution of the supercritical simulation of the dry EFB Simulation. As opposed to the dry Spruce simulation, the increase of the operating pressure to supercritical conditions, has no real impact on the operation of the dry EFB plant. This could be attributed to the fact that the 10 bar increase from a nearly supercritical operation at 220 bar for the EFBs, is not enough to show the impact of a supercritical operation for this type of fuel. The impact in the electrical and overall energetic and exergetic efficiencies is the same as before, although with half the increase in operating pressure. So even though the increase seems unimportant, we can deduce that with the same increase of operating pressure, in the supercritical region, the improvement is doubled.

4.2 Results of the Improved Biomass CHP Plant – Pretreated Fuels

The simulation and the results shown in this section will be only for the pretreated fuels, namely the wet torrefied Spruce wood and the torrefied EFBs. The tables shown below will provide information about the boiler heat output, the net electrical output, the heat offered to the Aluminum plant, the heat offered to the fuel for the drying, as well as the energetic and exergetic efficiencies of the plant.

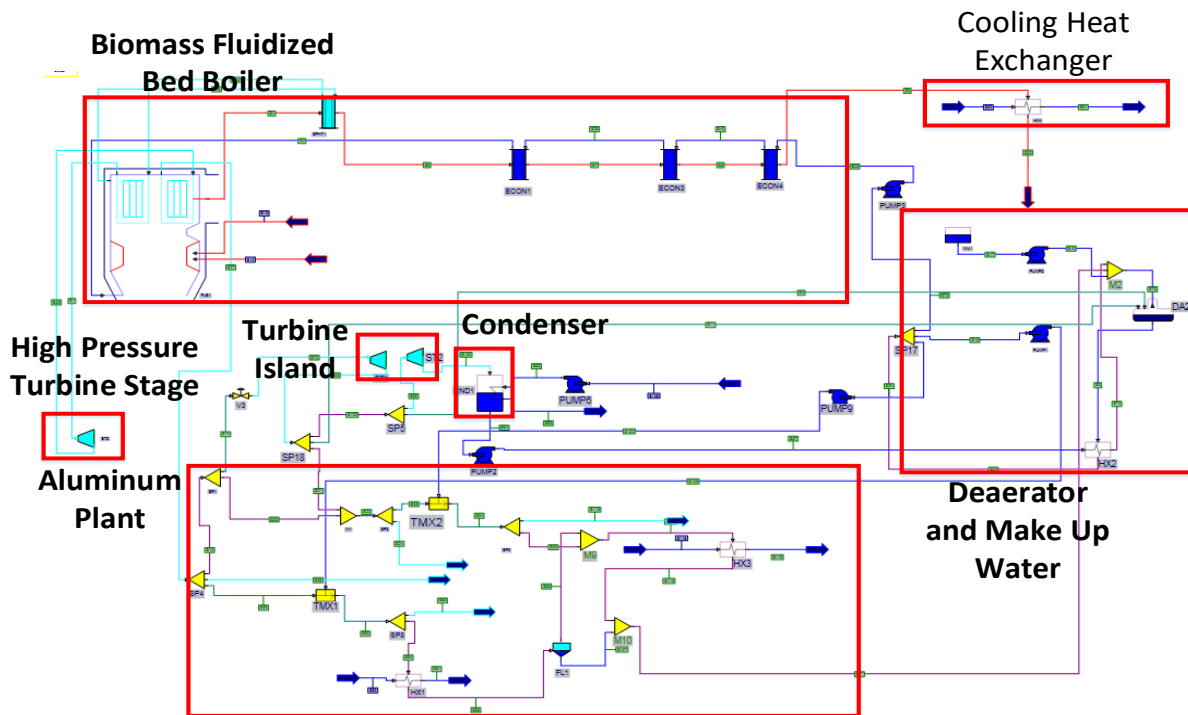


Figure 80: Improved CHP plant model for the pretreated fuels

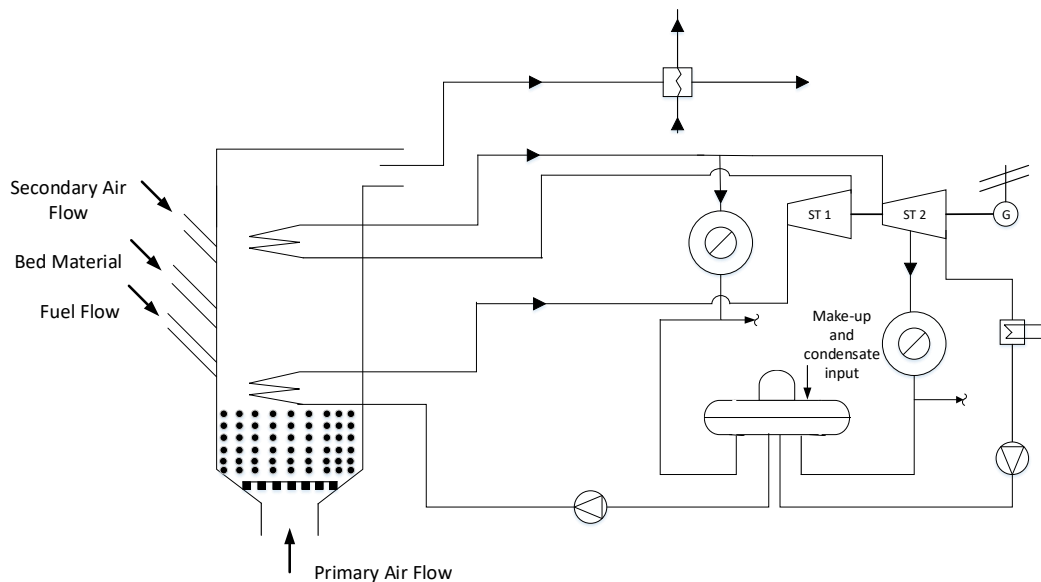


Figure 81: Schematic of the Improved CHP plant model for the pretreated fuel

As it can be seen by the model presented in figures 80 and 81, the model has the aforementioned modifications, with the high pressure turbine stage and the reheating. Instead of two heat exchangers, this model has one, since there is no need for drying. So the heat exchanger serves the purpose of providing heat, in a cooling device.

Since the EFBs and the Spruce wood are fuels with a high content of moisture, it is necessary to show the effect a pretreating process has, regarding the upgrade of the fuel, in terms of LHV, but chemical exergy as well, which is directly connected to the moisture content and the chemical composition as a whole. The inlet temperature of the flue gases to the second heat exchanger is one that gives a sufficient COP for the cooling absorption or adsorption device. The outlet temperature of the flue gases is specified at 90 °C, so that there is a great utilization of the flue gases' heat, since the biomass fuels have a less than significant sulphur content. So the plant can operate with flue gas temperatures lower than the acid dew point.

Case Study 3: Wet Torrefied Spruce Wood

The chemical composition of the wet torrefied Spruce wood is presented above, but it is deemed meaningful that the chemical composition is presented here as well.

Table 41: Torrefied Spruce Chemical Composition

Wet Torrefied Spruce Bark	
Moisture Content	-
Ash Content	-
Carbon	55.70%
Hydrogen	6.10%
Nitrogen	0.10%
Sulphur	0.00%
Oxygen	38.10%
Net Calorific Value (LHV) [kJ/kg]	22600
Gross Calorific Value (HHV) [kJ/kg]	-

Table 42: Wet Torrefied Spruce Improved Model Simulation Outputs for 160 bar

Live Steam Temperature:	600.0	580.0	560.0	540.0	°C
Reheated Steam Temperature:	480.0	480.0	480.0	480.0	°C
Boiler Thermal Output	955.6	960.4	962.9	967.7	MW
Gross Power Output	222.8	222.9	222.9	222.9	MW
Net Power Output	200.0	200.1	200.0	200.0	MW
Thermal Output	468.9	469.6	468.3	468.9	MW
Water Mass Flow	289.9	292.0	294.0	296.2	kg/s
Flue Gas Mass Flow	508.3	510.8	512.2	514.8	kg/s
Fuel Mass Flow	42.3	42.5	42.6	42.8	kg/s

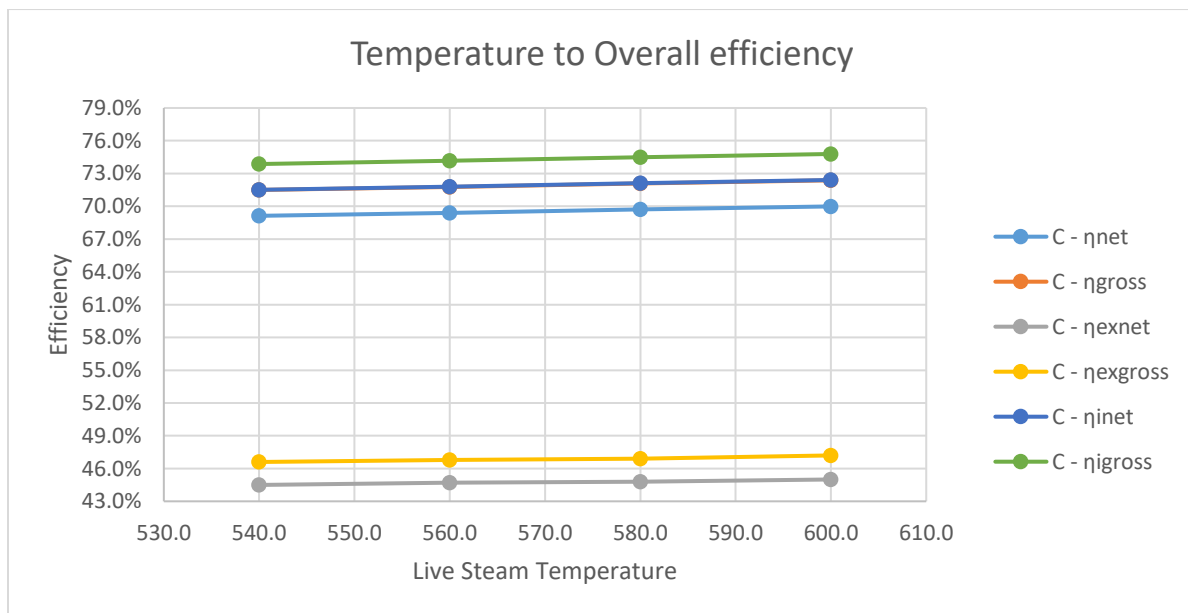


Figure 82: Overall Energetic and Exergetic Efficiencies for the Torrefied Spruce Simulation of the Improved Model (160 bar)

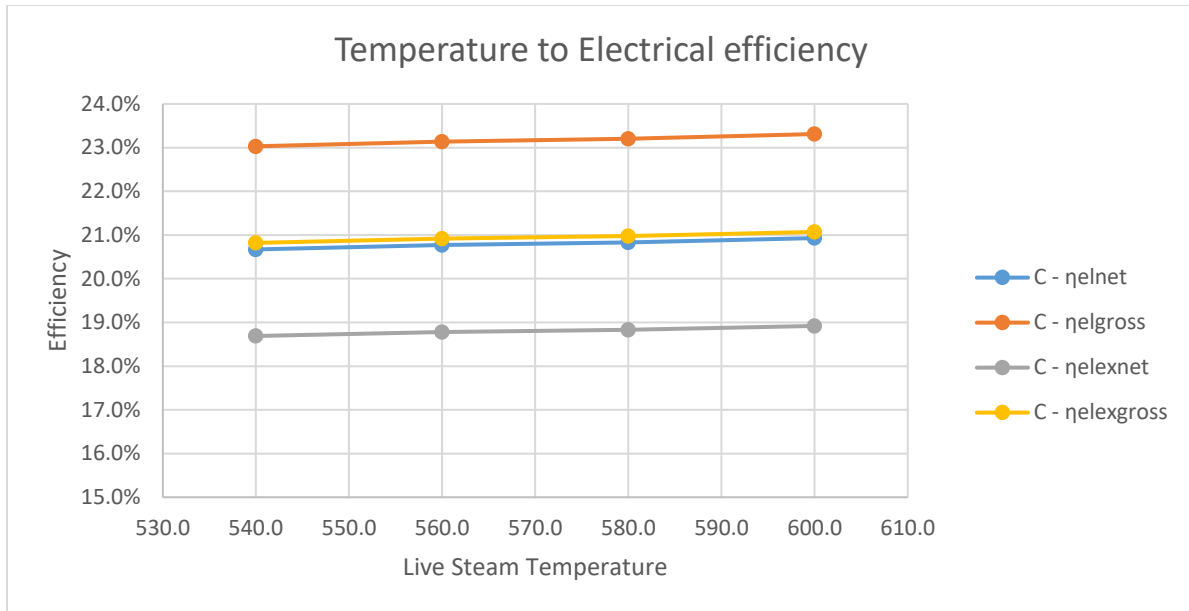


Figure 83: Electrical Energetic and Exergetic Efficiencies for the Torrefied Spruce Simulation of the Improved Model (160 bar)

Table 43: Wet Torrefied Spruce Improved Model Simulation Outputs for 180 bar

Live Steam Temperature:	600.0	580.0	560.0	540.0	°C
Reheated Steam Temperature:	480.0	480.0	480.0	480.0	°C
Boiler Thermal Output	942.2	946.8	952.9	957.0	MW
Gross Power Output	223.4	223.4	223.5	223.5	MW
Net Power Output	200.1	200.0	200.0	200.0	MW
Thermal Output	467.5	467.9	469.3	468.7	MW
Water Mass Flow	283.7	285.9	288.2	290.7	kg/s
Flue Gas Mass Flow	501.2	503.6	506.8	509.0	kg/s
Fuel Mass Flow	41.7	41.9	42.2	42.3	kg/s

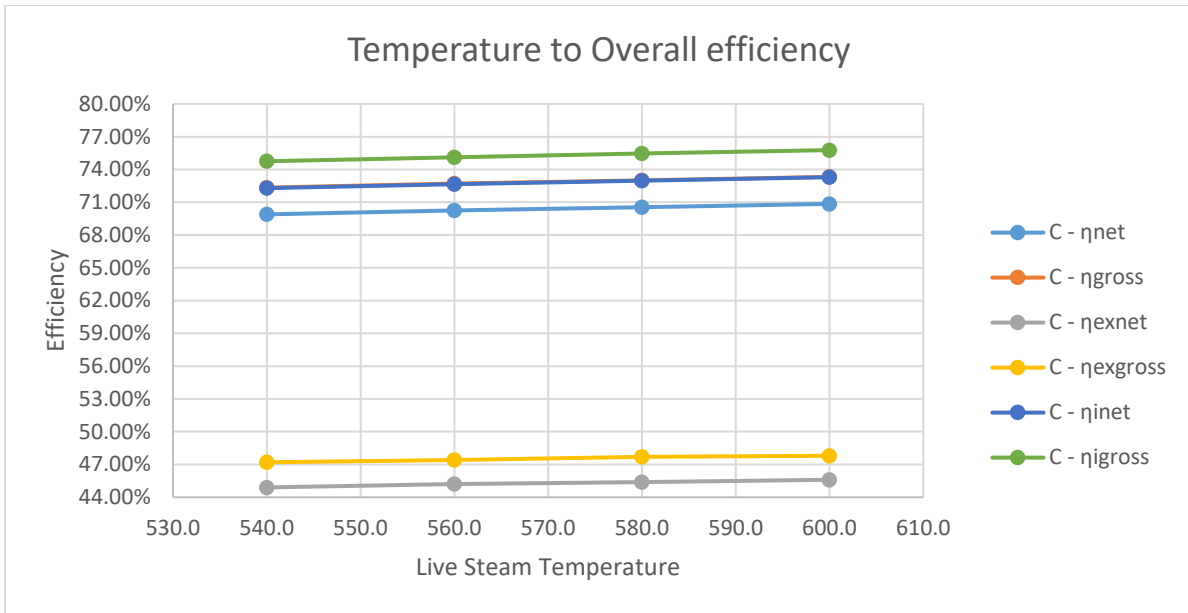


Figure 84: Overall Energetic and Exergetic Efficiencies for the Torrefied Spruce Simulation of the Improved Model (180 bar)

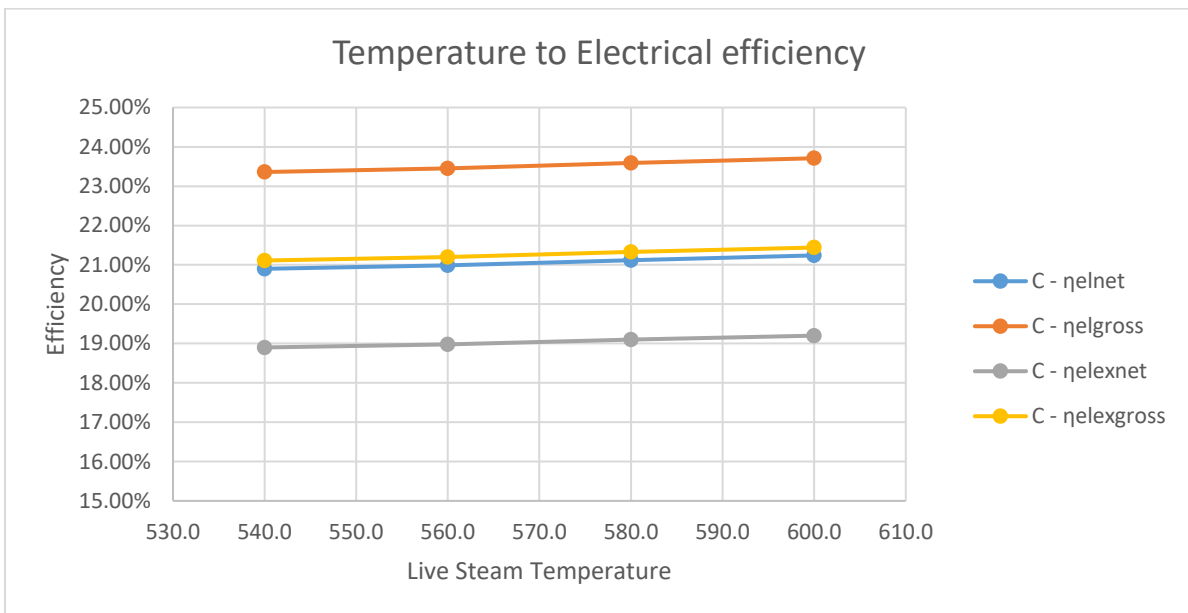


Figure 85: Electrical Energetic and Exergetic Efficiencies for the Torrefied Spruce Simulation of the Improved Model (180 bar)

Table 44: Wet Torrefied Spruce Improved Model Simulation Outputs for 200 bar

Live Steam Temperature:	600.0	580.0	560.0	540.0	°C
Reheated Steam Temperature:	480.0	480.0	480.0	480.0	°C
Boiler Thermal Output	934.0	939.1	944.3	949.9	MW
Gross Power Output	223.9	224.0	224.1	224.2	MW
Net Power Output	200.0	200.0	200.0	200.1	MW
Thermal Power Output	468.8	469.1	469.3	469.5	MW
Water Mass Flow	278.6	281.1	283.7	286.5	kg/s
Flue Gas Mass Flow	496.8	499.5	502.3	505.3	kg/s
Fuel Mass Flow	41.3	41.6	41.8	42.0	kg/s

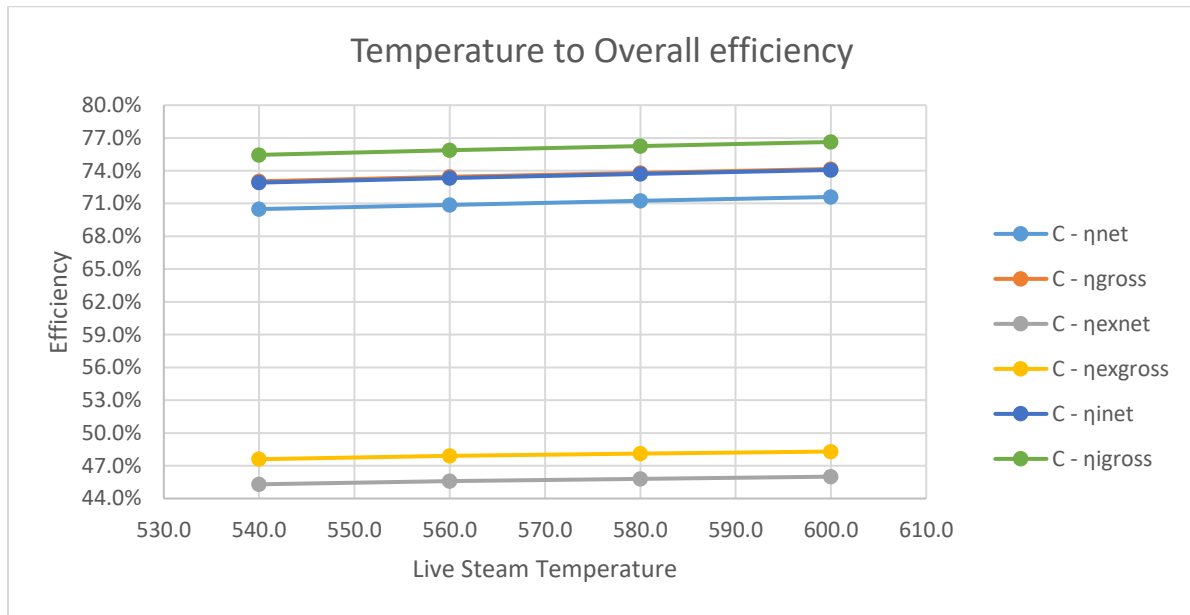


Figure 86: Overall Energetic and Exergetic Efficiencies for the Torrefied Spruce Simulation of the Improved Model (200 bar)

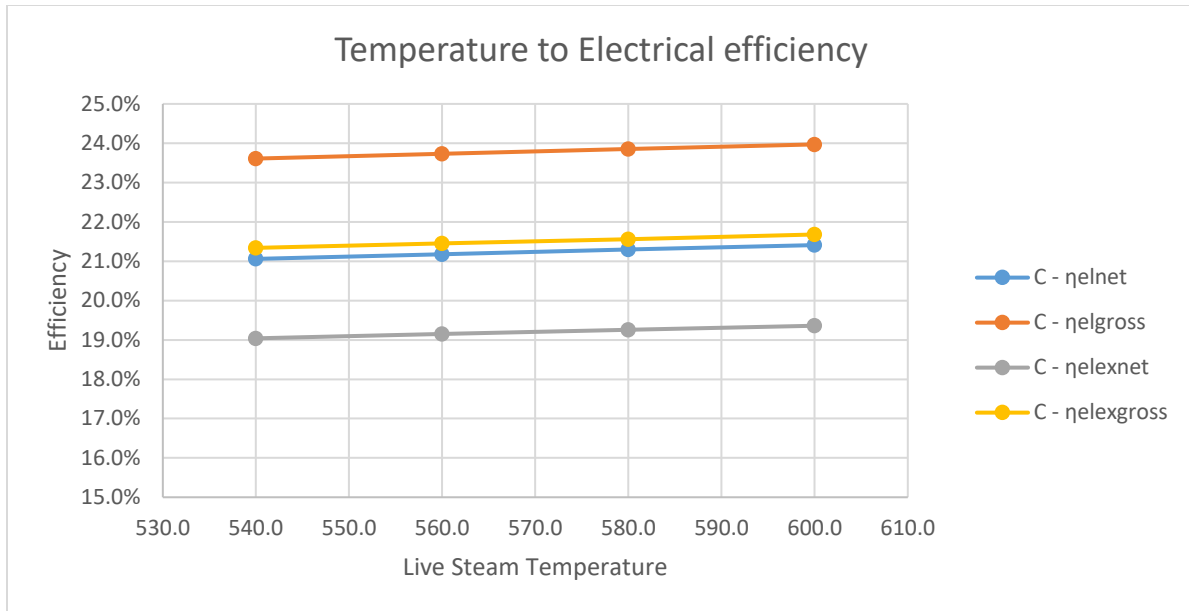


Figure 87: Electrical Energetic and Exergetic Efficiencies for the Torrefied Spruce Simulation of the Improved Model (200 bar)

Table 45: Wet Torrefied Spruce Improved Model Simulation Outputs for 220 bar

Live Steam Temperature:	600.0	580.0	560.0	540.0	°C
Reheated Steam Temperature:	480.0	480.0	480.0	480.0	°C
Boiler Thermal Output	924.5	930.6	939.1	949.9	MW
Gross Power Output	224.6	224.7	224.8	224.8	MW
Net Power Output	200.0	200.1	200.1	200.1	MW
Thermal Power Output	466.4	467.2	470.1	474.9	MW
Water Mass Flow	274.7	277.4	280.3	283.2	kg/s
Flue Gas Mass Flow	491.8	495.0	499.5	505.3	kg/s
Fuel Mass Flow	40.9	41.2	41.6	42.0	kg/s

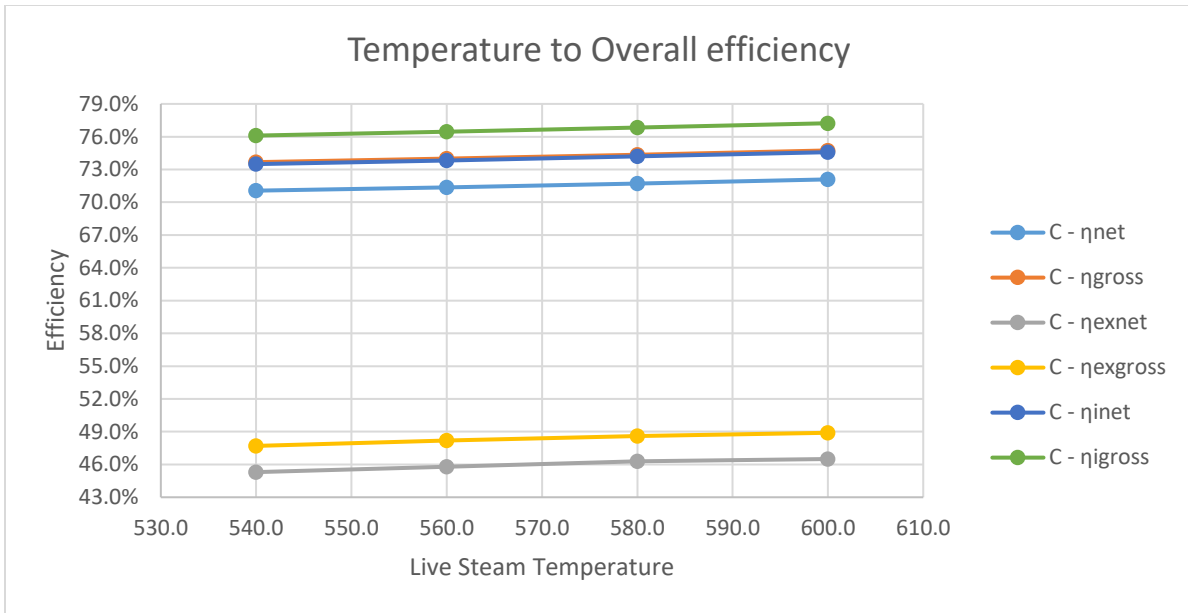


Figure 88: Overall Energetic and Exergetic Efficiencies for the Torrefied Spruce Simulation of the Improved Model (220 bar)

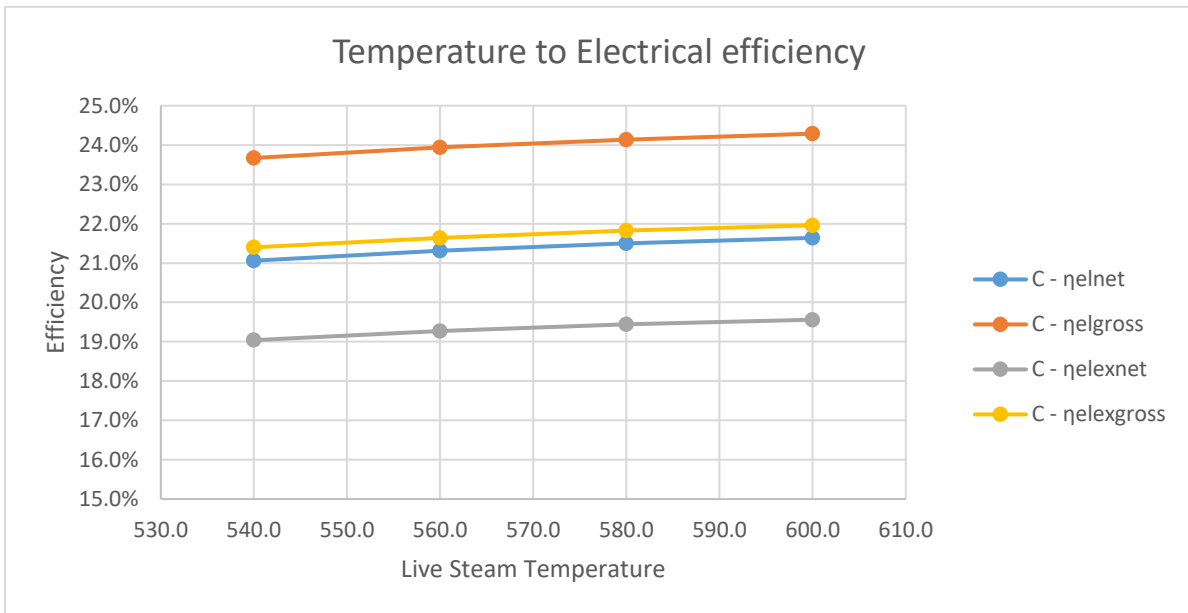


Figure 89: Electrical Energetic and Exergetic Efficiencies for the Torrefied Spruce Simulation of the Improved Model (220 bar)

Table 46: Wet Torrefied Spruce Improved Model Simulation Outputs for 230 bar (Supercritical)

Live Steam Temperature:	600.0	°C
Reheated Steam Temperature:	480.0	°C
Boiler Thermal Output	922.0	MW
Gross Power Output	224.9	MW
Net Power Output	200.0	MW
Thermal Power Output	466.4	MW
Water Mass Flow	273.1	kg/s
Flue Gas Mass Flow	490.4	kg/s
Fuel Mass Flow	40.8	kg/s
$\eta_{el}(\text{net})$	21.7%	
$\eta_{el}(\text{gross})$	24.4%	
$\eta_{th}(\text{net})$	72.5%	
$\eta_{th}(\text{gross})$	75.2%	
$\eta_{thi}(\text{net})$	75.0%	
$\eta_{thi}(\text{gross})$	77.8%	
$\eta_{thex}(\text{net})$	46.6%	
$\eta_{thex}(\text{gross})$	49.1%	
$\eta_{elex}(\text{net})$	19.6%	
$\eta_{elex}(\text{gross})$	22.1%	

The above charts and tables regarding the CHP plant of the torrefied Spruce wood, in each operating pressure, give us the same results as with the dry Spruce, in terms of efficiency increase and how it is influenced by the temperature increase.

Although there is improvement in the efficiency values, this improvement is not particularly high here as well. For example, in all of the simulated operating pressures, the net electrical efficiency rises about 0.1 % for each 20 °C rise of the live steam temperature. Though the increase of each 20 °C is not high, the value of both the electrical and overall efficiencies for the torrefied Spruce wood in the lowest operating pressure and temperature, is higher than the highest achieved efficiencies of the dry Spruce CHP plant.

One more thing to note, is that now the total heat power output of the FLB, stands now well below than 1000 MW. At the 160 bar operation the heat power output of the FLB is the highest, standing at 968 MW, while the decrease in FLB heat power output is lower in the current case study for each 20 °C increase.

As for the fuel consumption, the drop for each 20 °C rise in the temperature is 0.2 - 0.3 kg/s. With the assumption of the 8500 hours operation, the power plant will save 6120 to 9180 tn of fuel per year for each 20 °C. The CHP plant with the pretreated Spruce wood, exceeds the barrier of 70% overall net efficiency, reaching the original overall net efficiency of the combined cycle plant which stands at around 72-73 %. Although the original power plant operates at lower feedwater pressure and temperatures, it is fueled by natural gas which is a fuel, at least twice as good, in terms of LHV, as the torrefied Spruce. This is a huge result for this biomass fuel, because it means, at least in theory, that a big CHP plant can operate on biomass, having a satisfying efficiency.

As in the reference model, the “ideal” efficiencies are greater, which means that one immediate improvement to the heat part, is the use of heat exchangers, instead of attemperators, in case of a temperature control having a great margin. The exergetic efficiencies are at a good level, this being a result of the pretreatment process and the increase of the electrical output of the plant. The chemical exergy of the wet torrefied Spruce is 24998 kJ/kg.

Following the charts and tables showing the results of the temperature increase for each feedwater pressure level, are the charts and tables showing the increase in efficiency, having a standard temperature level of 600 °C. This is done in order to compare the improvements, the rise in pressure levels and the rise in temperature levels, offer.

Table 47: Wet Torrefied Spruce Improved Model Simulation Outputs for 600 °C

Operating Pressure:	230	220	200	180	160	bar
Live Steam Temperature:	600.0	600.0	600.0	600.0	600.0	°C
Reheated Steam Temperature:	480.0	480.0	480.0	480.0	480.0	°C
Boiler Thermal Output	922.0	924.5	934.0	942.2	955.6	MW
Gross Power Output	224.9	224.6	223.9	223.4	222.8	MW
Net Power Output	200.0	200.0	200.0	200.1	200.0	MW
Thermal Power Output	466.4	466.4	468.8	467.5	468.9	MW
Water Mass Flow	273.1	274.7	278.6	283.7	289.9	kg/s
Flue Gas Mass Flow	490.4	491.8	496.8	501.2	508.3	kg/s
Fuel Mass Flow	40.8	40.9	41.3	41.7	42.3	kg/s

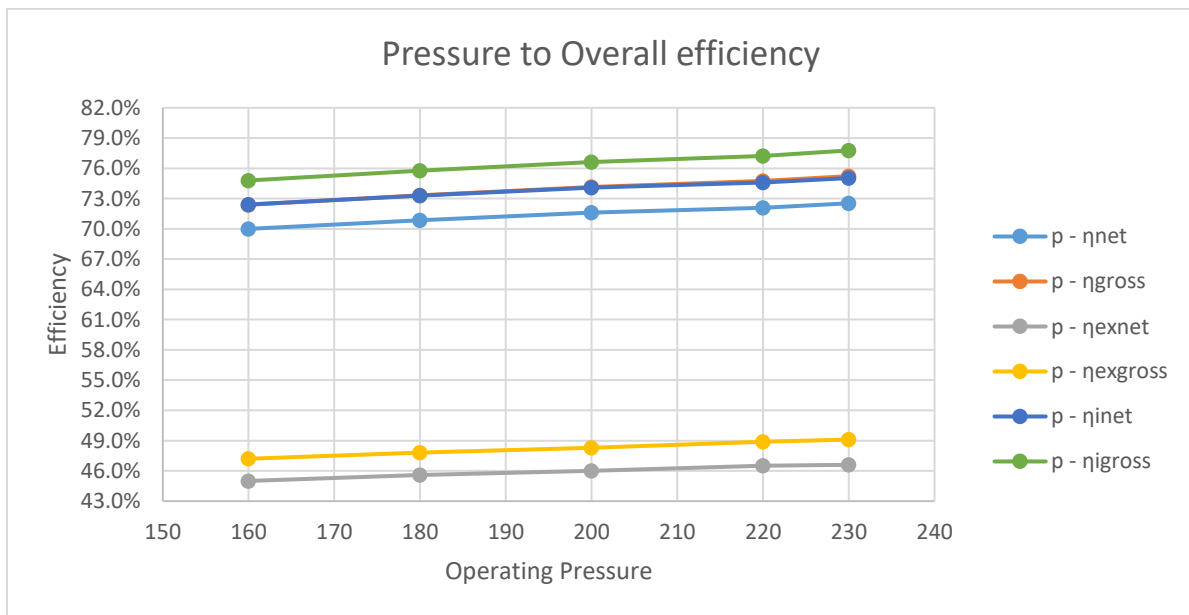


Figure 90: Overall Energetic and Exergetic Efficiencies for the Torrefied Spruce Simulation of the Improved Model (600 °C)

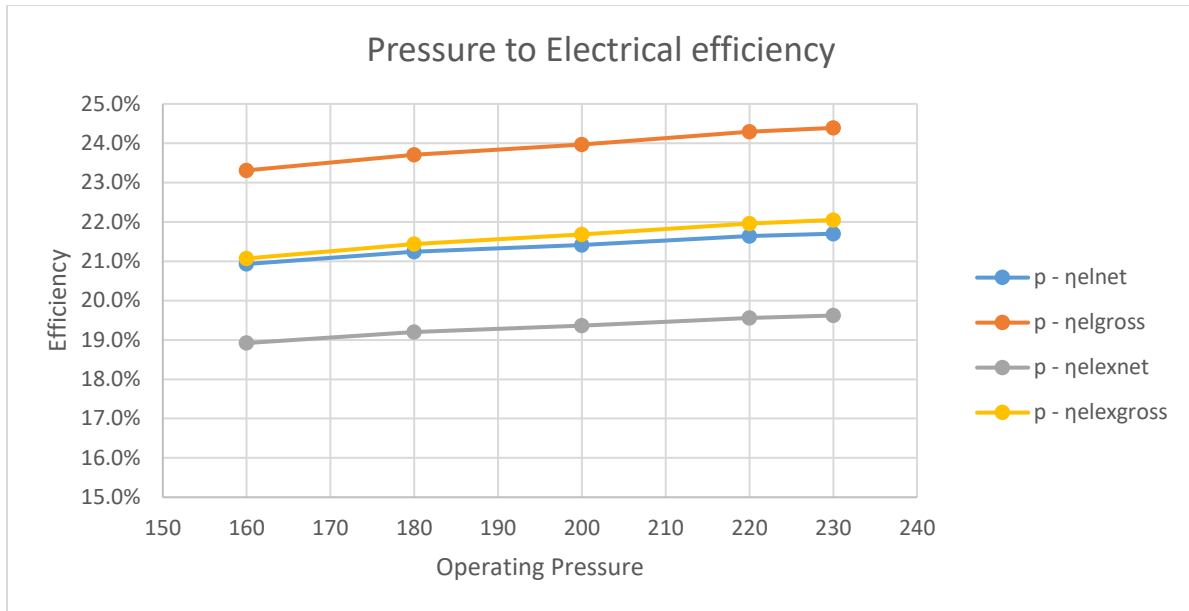


Figure 91: Electrical Energetic and Exergetic Efficiencies for the Torrefied Spruce Simulation of the Improved Model (600 °C)

Observing the charts and the table, it is obvious that the rise in efficiency is greater for each 20 bar of increase for the torrefied Spruce as well. The increase of the efficiencies is almost linear, but one can discern that the rate of increase is really low. The increase from the subcritical to the supercritical region seems again to have a slightly increased rate.

As far as the fuel consumption is concerned, the decrease in fuel consumption is a bit low, since there is a drop of 1.5 kg/s from the initial pressure of 160 bar until the supercritical pressure of 230 bar, amounting to 45900 tn of fuel saved per year. As for the total heat output of the FLB, the decrease is relatively constant, standing at 10 MW per 20 bar of increase. The decrease from 220 to 230 bar though, is really low, almost 2 MWs.

The overall and electrical exergetic efficiencies, follow the same trend as the energetic efficiencies. The value of the electrical efficiency stands now over 21%, a value not reachable by the dried fuels, while the increase is still low, standing at 0.1%. The increase of the overall efficiency stands at 0.4%, exceeding as aforementioned, the barrier of 70%.

Last but not least, is the contribution of the supercritical simulation of the wet torrefied Spruce wood. Although the impact of the supercritical conditions show no real significance for the electrical efficiency, the overall efficiency is increased the same for an increase of just 10 bars, in the supercritical region. That means that for an increase of 20 bars, the increase in overall efficiency would lead to a massive 0.8%.

Case Study 4: Torrefied Empty Fruit Bunches

Table 48: Torrefied EFBs Chemical Composition

Torrefied EFB	
Moisture Content	-
Ash Content	-
Carbon	51.14%
Hydrogen	4.38%
Nitrogen	1.27%
Sulphur	0.02%
Oxygen	43.19%
Net Calorific Value (LHV) [kJ/kg]	19450
Gross Calorific Value (HHV) [kJ/kg]	-

Table 49: Torrefied EFBs Improved Model Simulation Outputs for 160 bar

Live Steam Temperature:	600.0	580.0	560.0	540.0	°C
Reheated Steam Temperature:	480.0	480.0	480.0	480.0	°C
Boiler Thermal Output	953.3	957.8	962.4	965.2	MW
Gross Power Output	222.8	222.8	222.9	222.9	MW
Net Power Output	200.0	200.0	200.0	200.0	MW
Thermal Output	467.5	468.1	468.7	467.4	MW
Water Mass Flow	289.9	291.9	294.0	296.2	kg/s
Flue Gas Mass Flow	492.2	494.5	496.9	498.3	kg/s
Fuel Mass Flow	49.0	49.2	49.5	49.6	kg/s

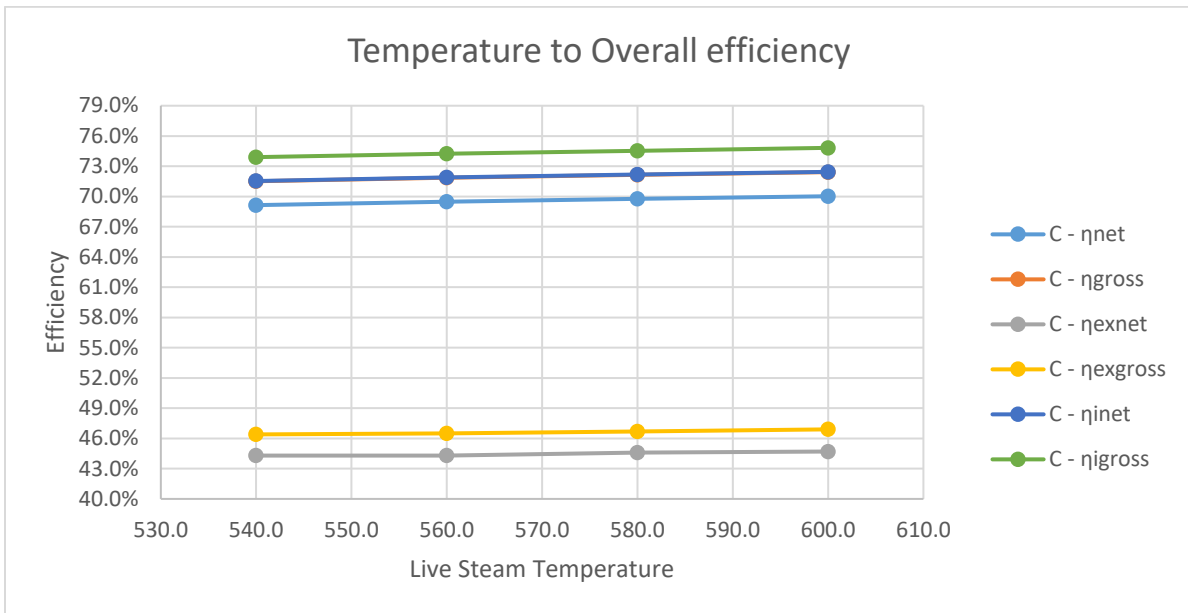


Figure 92: Overall Energetic and Exergetic Efficiencies for the Torrefied EFBs Simulation of the Improved Model (160 bar)

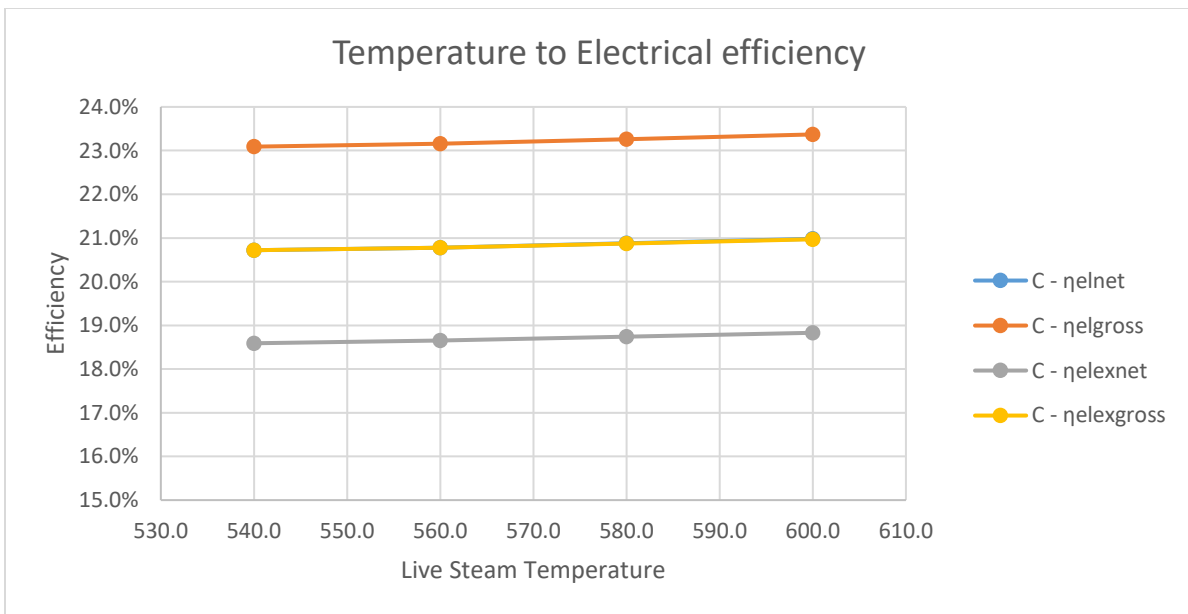


Figure 93: Electrical Energetic and Exergetic Efficiencies for the Torrefied EFBs Simulation of the Improved Model (160 bar)

Table 50: Torrefied EFBs Improved Model Simulation Outputs for 180 bar

Live Steam Temperature:	600.0	580.0	560.0	540.0	°C
Reheated Steam Temperature:	480.0	480.0	480.0	480.0	°C
Boiler Thermal Output	944.7	947.5	950.5	955.4	MW
Gross Power Output	223.4	223.4	223.5	223.5	MW
Net Power Output	200.1	200.1	200.1	200.0	MW
Thermal Output	470.6	469.2	467.8	468.1	MW
Water Mass Flow	283.7	285.9	288.3	290.6	kg/s
Flue Gas Mass Flow	487.8	489.2	490.8	493.2	kg/s
Fuel Mass Flow	48.6	48.7	48.9	49.1	kg/s

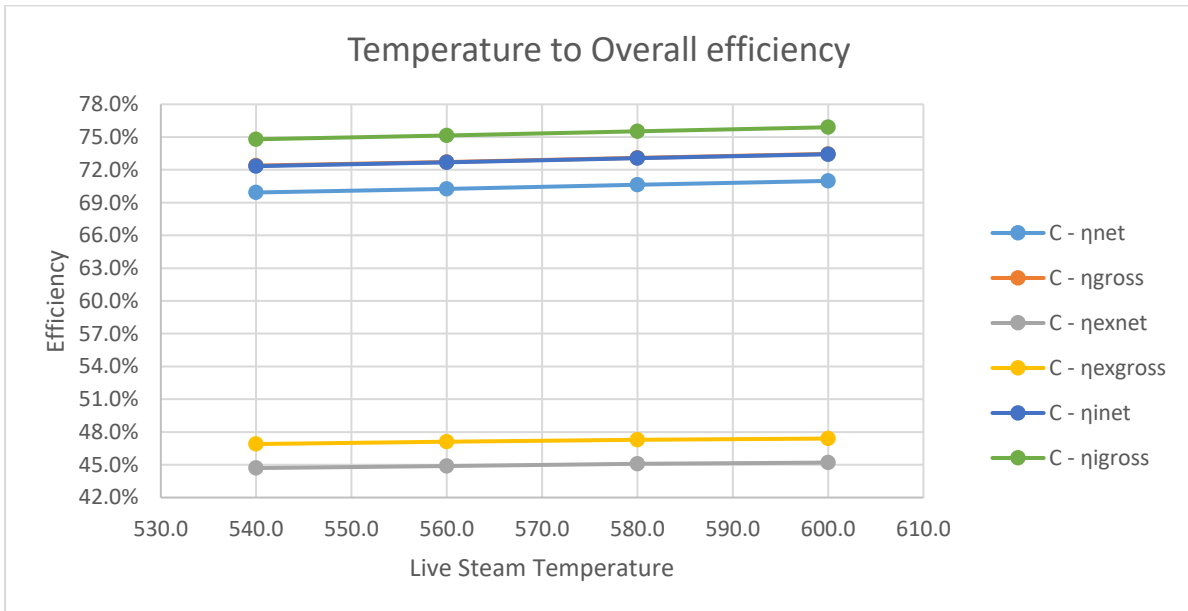


Figure 94: Overall Energetic and Exergetic Efficiencies for the Torrefied EFBs Simulation of the Improved Model (180 bar)

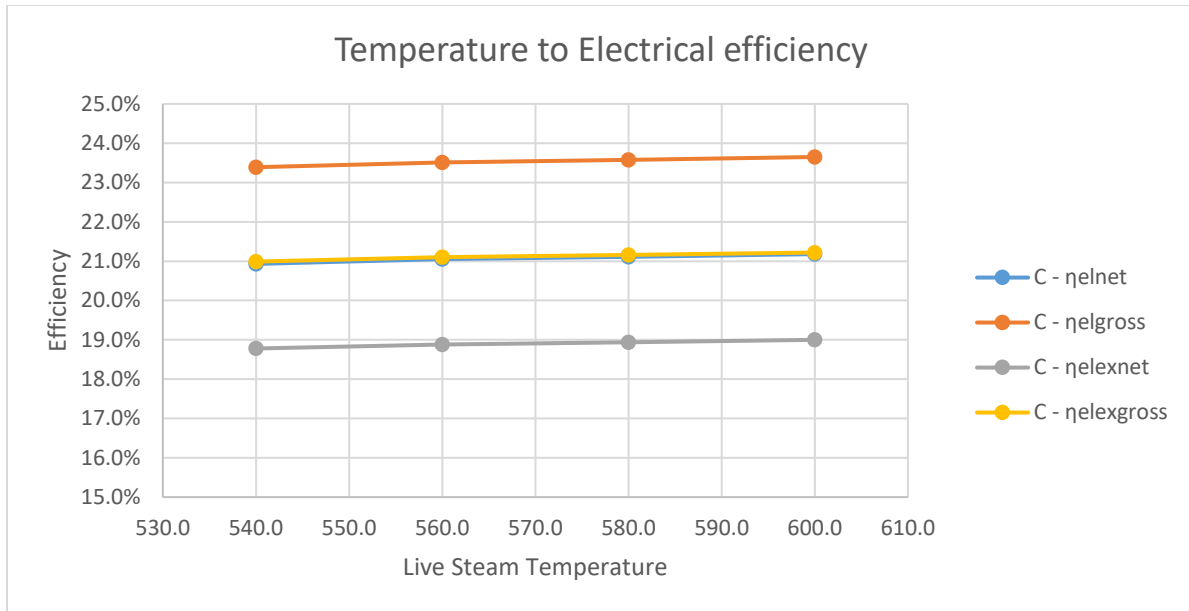


Figure 95: Electrical Energetic and Exergetic Efficiencies for the Torrefied EFBs Simulation of the Improved Model (180 bar)

Table 51: Torrefied EFBs Improved Model Simulation Outputs for 200 bar

Live Steam Temperature:	600.0	580.0	560.0	540.0	°C
Reheated Steam Temperature:	480.0	480.0	480.0	480.0	°C
Boiler Thermal Output	931.6	936.4	261160.8	946.9	MW
Gross Power Output	224.0	224.0	62245.3	224.2	MW
Net Power Output	200.1	200.0	55563.9	200.0	MW
Thermal Power Output	467.1	467.3	129482.6	467.6	MW
Water Mass Flow	278.7	281.1	283.7	286.4	kg/s
Flue Gas Mass Flow	481.0	483.3	485.4	488.9	kg/s
Fuel Mass Flow	47.9	48.1	48.3	48.7	kg/s

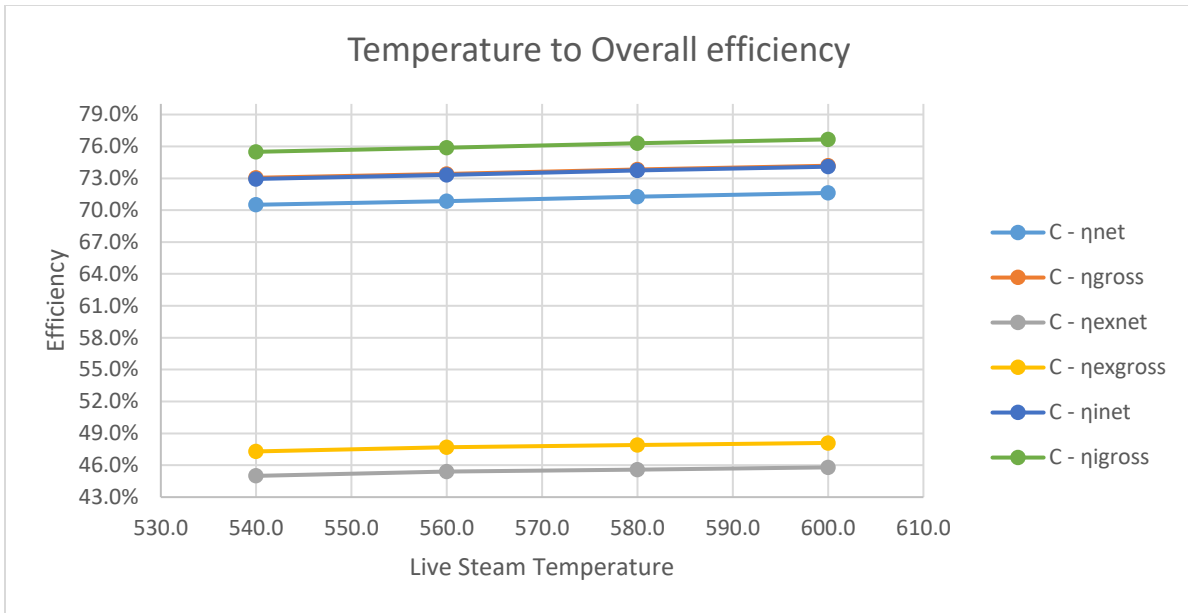


Figure 96: Overall Energetic and Exergetic Efficiencies for the Torrefied EFBs Simulation of the Improved Model (200 bar)

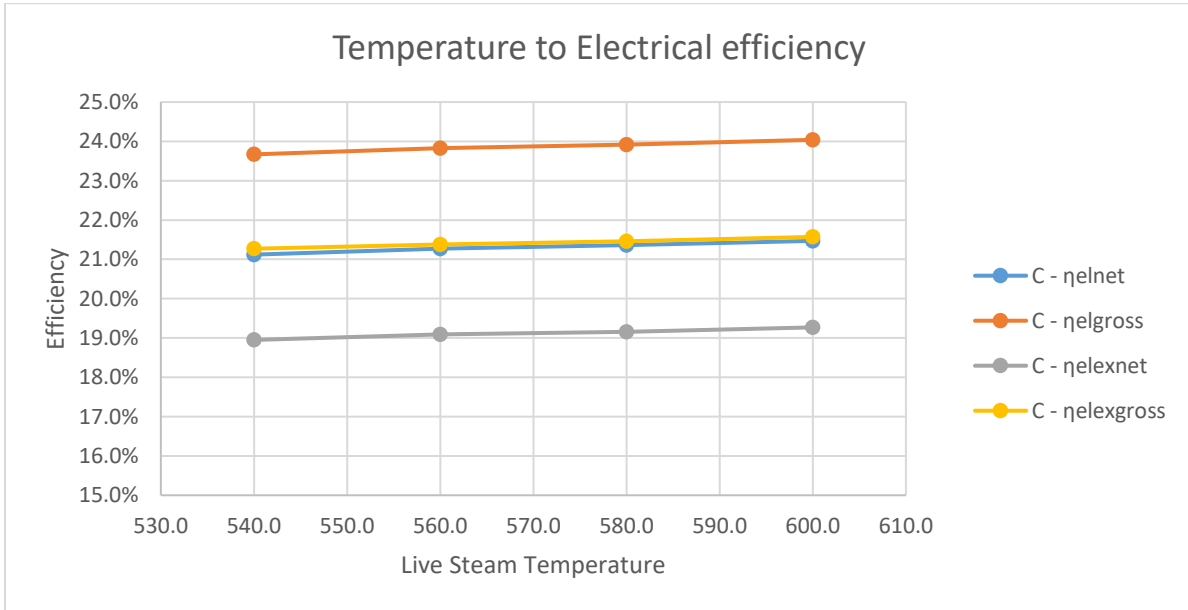


Figure 97: Electrical Energetic and Exergetic Efficiencies for the Torrefied EFBs Simulation of the Improved Model (200 bar)

Table 52: Torrefied EFBs Improved Model Simulation Outputs for 220 bar

Live Steam Temperature:	600.0	580.0	560.0	540.0	Celsius
Reheated Steam Temperature:	480.0	480.0	480.0	480.0	Celsius
Boiler Thermal Output	924.1	929.0	935.1	941.4	MW
Gross Power Output	224.6	224.6	224.7	224.8	MW
Net Power Output	200.0	200.0	200.0	200.0	MW
Thermal Power Output	466.8	466.5	467.2	467.8	MW
Water Mass Flow	274.7	277.4	280.2	283.1	kg/s
Flue Gas Mass Flow	477.1	479.6	482.8	486.0	kg/s
Fuel Mass Flow	47.5	47.8	48.1	48.4	kg/s

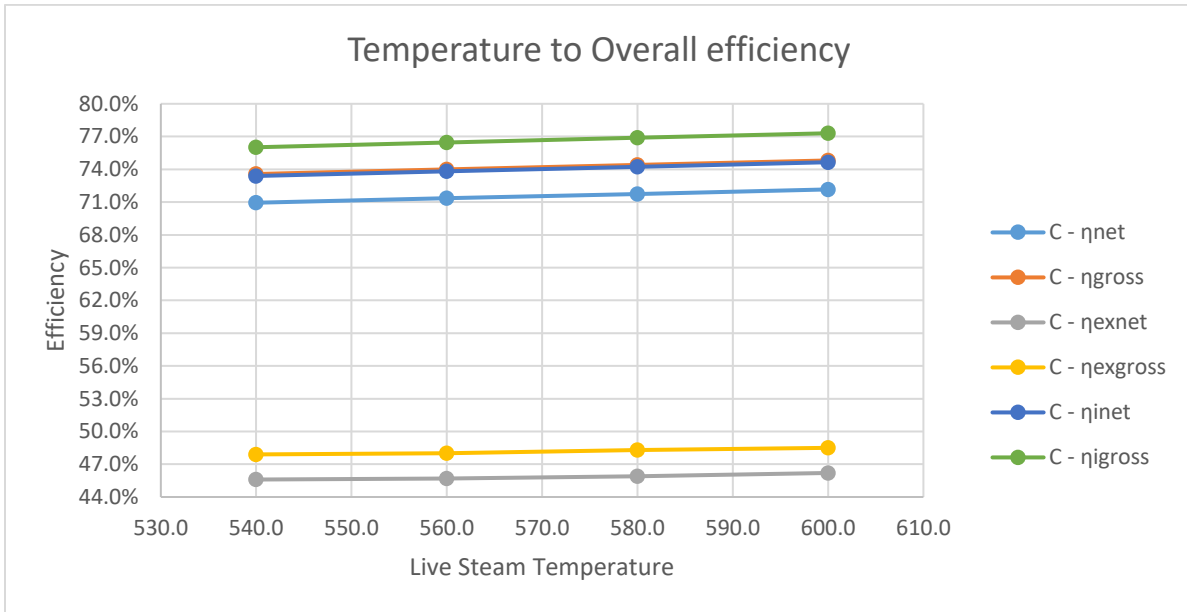


Figure 98: Overall Energetic and Exergetic Efficiencies for the Torrefied EFBs Simulation of the Improved Model (220 bar)

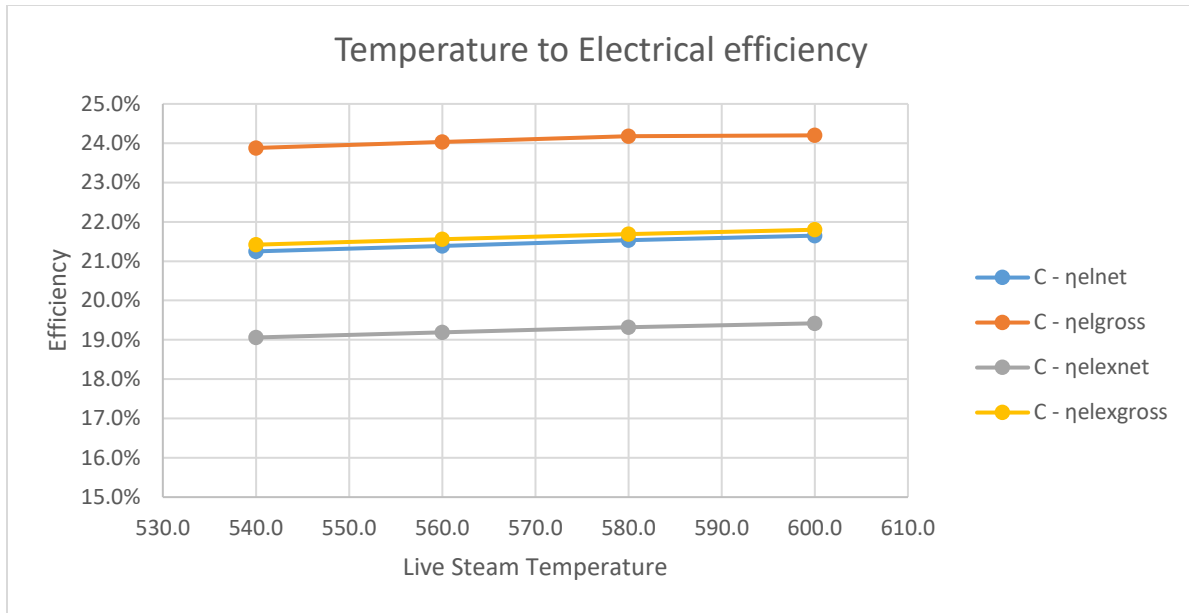


Figure 99: Electrical Energetic and Exergetic Efficiencies for the Torrefied EFBs Simulation of the Improved Model (220 bar)

Table 53: Torrefied EFBs Improved Model Simulation Outputs for 230 bar (Supercritical)

Live Steam Temperature:	600.0	Celsius
Reheated Steam Temperature:	480.0	Celsius
Boiler Thermal Output	917.6	MW
Gross Power Output	224.9	MW
Net Power Output	200.1	MW
Thermal Power Output	465.3	MW
Water Mass Flow	273.1	kg/s
Flue Gas Mass Flow	473.8	kg/s
Fuel Mass Flow	47.2	kg/s
$\eta_{el(net)}$	21.8%	
$\eta_{el(gross)}$	24.5%	
$\eta_{th(net)}$	72.5%	
$\eta_{th(gross)}$	75.2%	
$\eta_{thi(net)}$	75.0%	
$\eta_{thi(gross)}$	77.7%	
$\eta_{thex(net)}$	46.5%	
$\eta_{thex(gross)}$	49.0%	
$\eta_{elex(net)}$	19.6%	
$\eta_{elex(gross)}$	22.0%	

As shown above the improvement is not particularly high here as well. In all of the operating pressures, the net electrical efficiency rises about 0.1 % for each 20 °C rise of the live steam temperature. Though the increase of each 20 °C is not high, the value of both the electrical and overall efficiencies for the torrefied EFBs in the lowest operating pressure and temperature, is higher than the highest achieved efficiencies of the dry EFB CHP plant, with a margin of circa 1.5%.

One more thing to note, is that now the total heat power output of the FLB, stands now well below than 1000 MW again. At the 160 bar operation the heat power output of the FLB is the highest, standing at 965 MW, while the decrease in FLB heat power output is low as well in the current case study for each 20 °C increase.

As for the fuel consumption, the drop for each 20 °C rise in the temperature is 0.3 - 0.4 kg/s. With the assumption of the 8500 hours operation, the power plant will save 9180 to 12240 tn of fuel per year for each 20 °C. The CHP plant with the pretreated EFBs, exceeds the barrier of 70% overall net efficiency as well.

As in the reference model, the “ideal” efficiencies are greater, which means that one immediate improvement to the heat part. The exergetic efficiencies are at a good level, this being a result of the pretreatment process and the increase of the electrical output of the plant. The chemical exergy of the torrefied EFBs is 21679 kJ/kg.

Following the charts and tables showing the results of the temperature increase for each feedwater pressure level, are the charts and tables showing the increase in efficiency, having a standard temperature level of 600 °C.

Table 54: Torrefied EFB Improved Model Simulation Outputs for 600 °C

Operating Pressure:	230	220	200	180	160	bar
Live Steam Temperature:	600.0	600.0	600.0	600.0	600.0	Celsius
Reheated Steam Temperature:	480.0	480.0	480.0	480.0	480.0	Celsius
Boiler Thermal Output	917.6	924.1	931.6	944.7	953.3	MW
Gross Power Output	224.9	224.6	224.0	223.4	222.8	MW
Net Power Output	200.1	200.0	200.1	200.1	200.0	MW
Thermal Power Output	465.3	466.8	467.1	470.6	467.5	MW
Water Mass Flow	273.1	274.7	278.7	283.7	289.9	kg/s
Flue Gas Mass Flow	473.8	477.1	481.0	487.8	492.2	kg/s
Fuel Mass Flow	47.2	47.5	47.9	48.6	49.0	kg/s

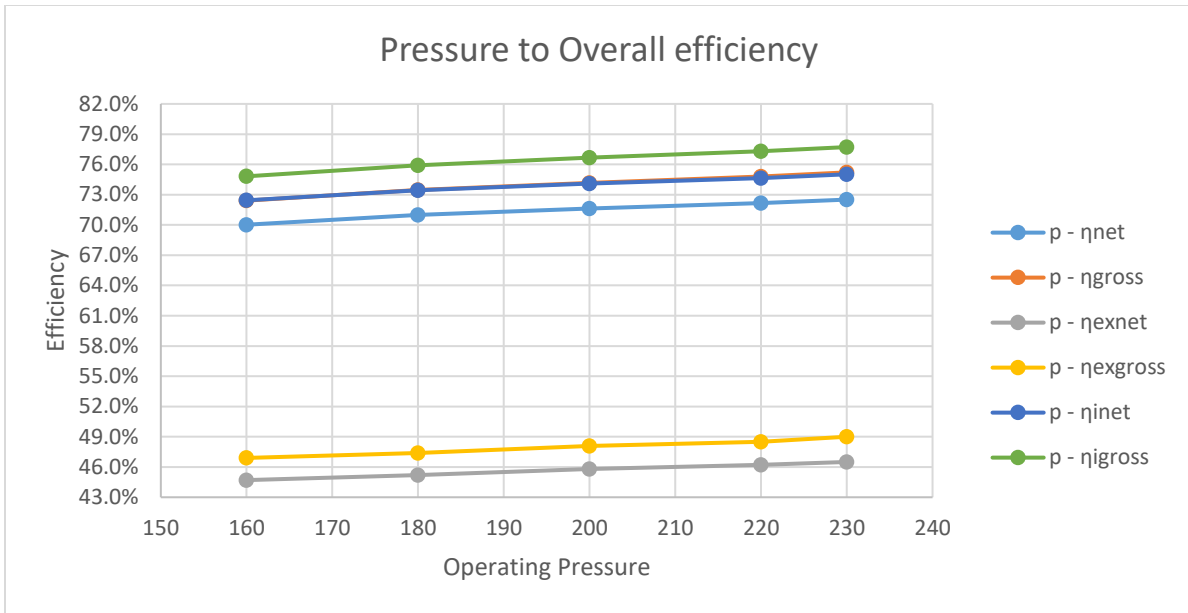


Figure 100: Overall Energetic and Exergetic Efficiencies for the Torrefied EFBs Simulation of the Improved Model (600 °C)

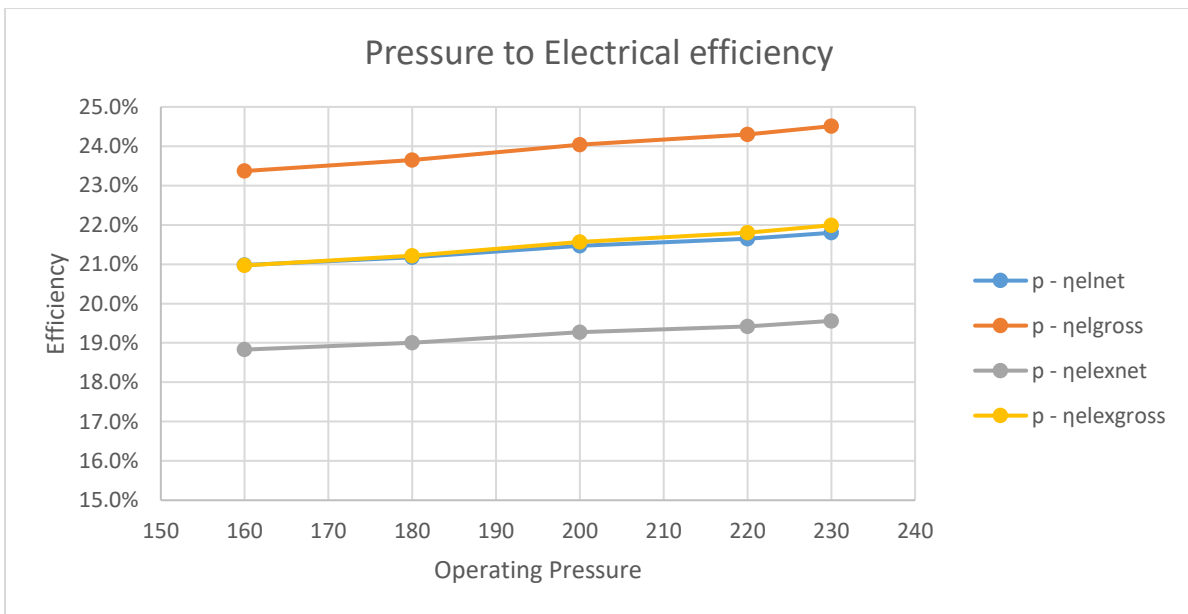


Figure 101: Electrical Energetic and Exergetic Efficiencies for the Torrefied EFBs Simulation of the Improved Model (600 °C)

Observing the charts and the table, it is obvious that the rise in efficiency is greater for each 20 bar of increase for the torrefied EFBs as well. The increase of the overall efficiencies is almost linear, while the increase of the electrical efficiencies is jerky. The increase from the subcritical to the supercritical region seems again to have a slightly increased rate here too.

As far as the fuel consumption is concerned, the decrease in fuel consumption is satisfying, since there is a drop of 2.8 kg/s from the initial pressure of 160 bar until the supercritical pressure of 230 bar, amounting to 85680 tn of fuel saved per year, almost twice of that from the wet torrefied Spruce wood simulation. As for the total heat output of the FLB, the decrease is relatively constant, standing over 10 MW per 20 bar of increase. The decrease from 220 to 230 bar for this fuel is higher than that of the torrefied Spruce, since the drop is 7 MW.

The overall and electrical exergetic efficiencies, follow the same trend as the energetic efficiencies. The value of the electrical efficiency stands near 22% a value not reachable by the dried fuels, while the increase is still low, standing at 0.1%. The increase of the overall efficiency stands at 0.5%, exceeding as aforementioned, the barrier of 70%.

Last but not least, is the contribution of the supercritical simulation of the torrefied EFBs. Although the impact of the supercritical conditions show no real significance for the electrical efficiency, the overall efficiency is increased the same for an increase of just 10 bars, in the supercritical region. That means that for an increase of 20 bars, the increase in overall efficiency would lead to a huge 1%.

4.3 Comparison of the four biomass fuels, Part Load Operation of the best fuel and Cooling Power Output

In this section, the aggregated overall and electrical efficiencies of the best case scenarios, from each fuel, will be shown. Namely, the below charts will provide us a complete picture which will show us the efficiencies and will determine which fuel will be used for the final simulations, of part load operation. The charts are comprised of bars, so the comparison between each fuel is direct, but the values are also presented in order to avoid any confusion. It is necessary to mention that these values are the ones from the supercritical simulations having 230 bar and 600 °C of live steam conditions. The below efficiencies are only shown, because they are the highest from any simulation and they represent all of the other simulations, which follow the same trend.

Comparison of the four biomass fuels:

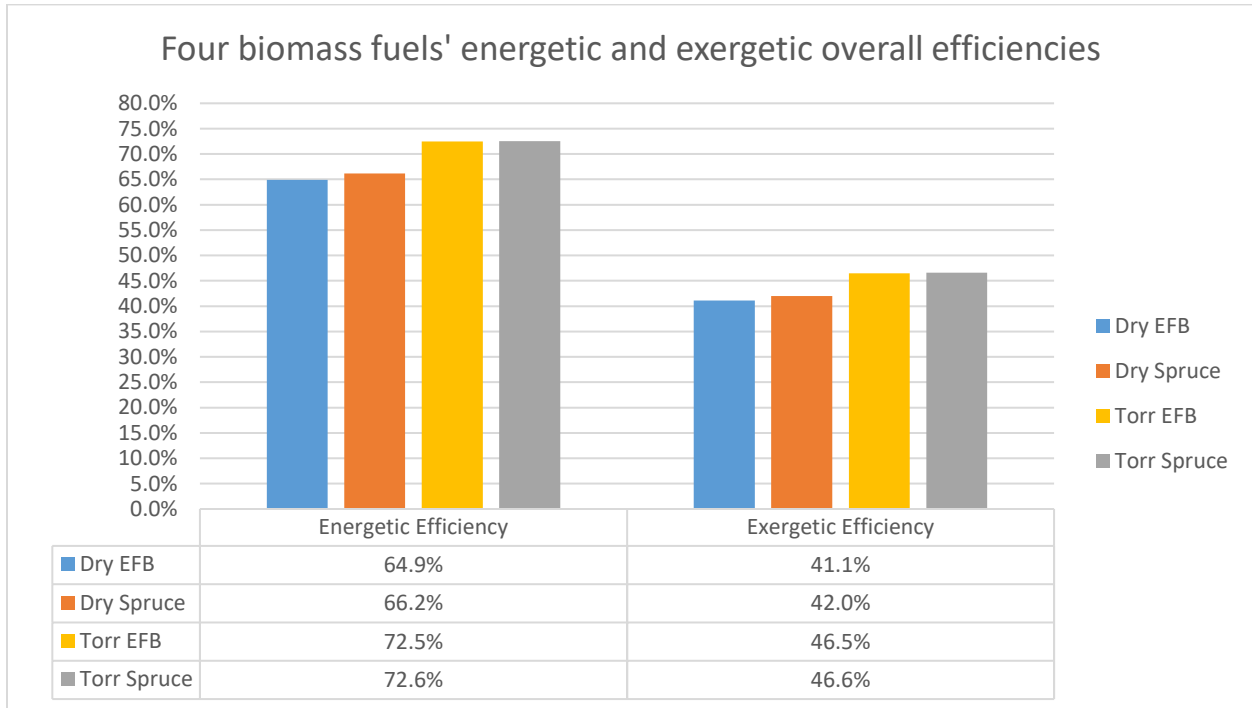


Figure 102: Comparison of the overall energetic and exergetic efficiencies of the four biomass fuels (dried and pretreated)

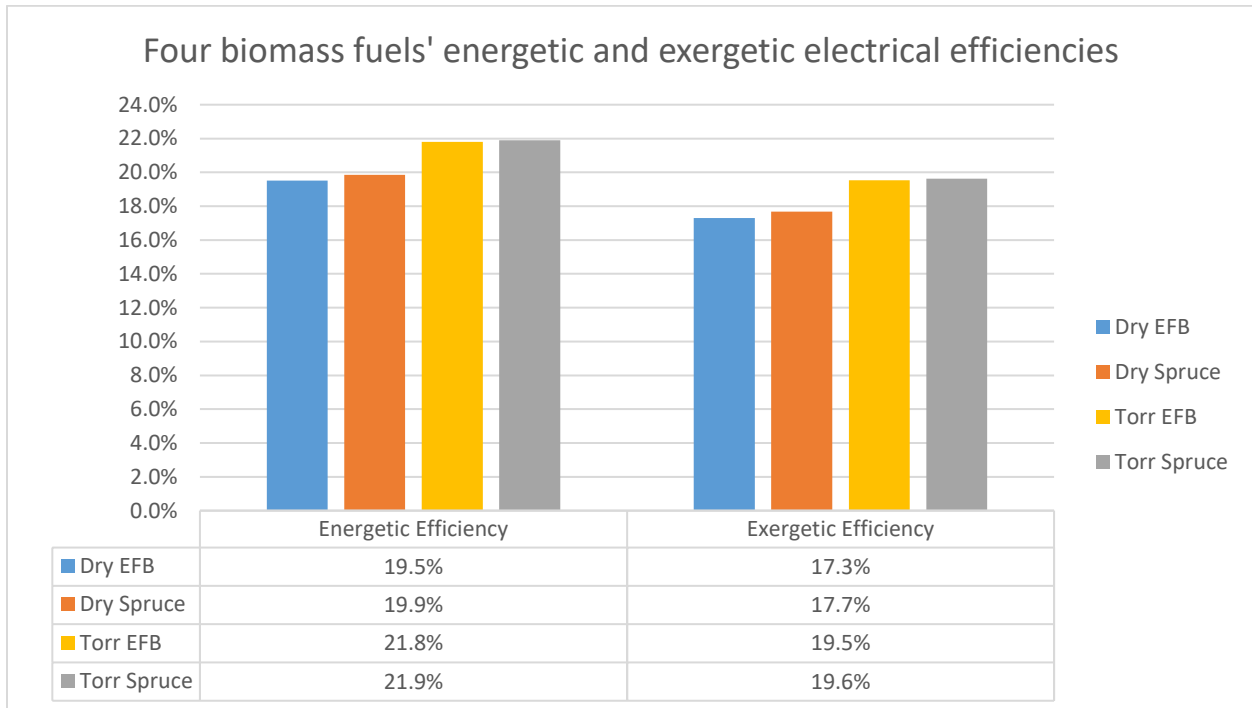


Figure 103: Comparison of the electrical energetic and exergetic efficiencies of the four biomass fuels (dried and pretreated)

In figure 102 and 103, one can clearly see, initially that the torrefied fuels, are by far better than the dried ones, showing us again that pretreatment plays a huge part in the upgrade of a biomass fuel. As mentioned above, torrefaction is a process which concentrates the chemical power of the biomass fuel. So the biomass fuel becomes a nearly fossil fuel with high chemical and thermodynamic capabilities.

As for the best fuel of the four, that is the torrefied Spruce, only by a small margin from the torrefied EFBs. The net electrical and overall efficiencies of the torrefied Spruce stand at 21.9% and 72.6% respectively. These efficiencies are really high, taking into account the configuration of the combined and heat power plant. Following the comparison of these fuels, will be the part load simulations of the torrefied Spruce wood.

Part Load Operation of the best biomass fuel plant:

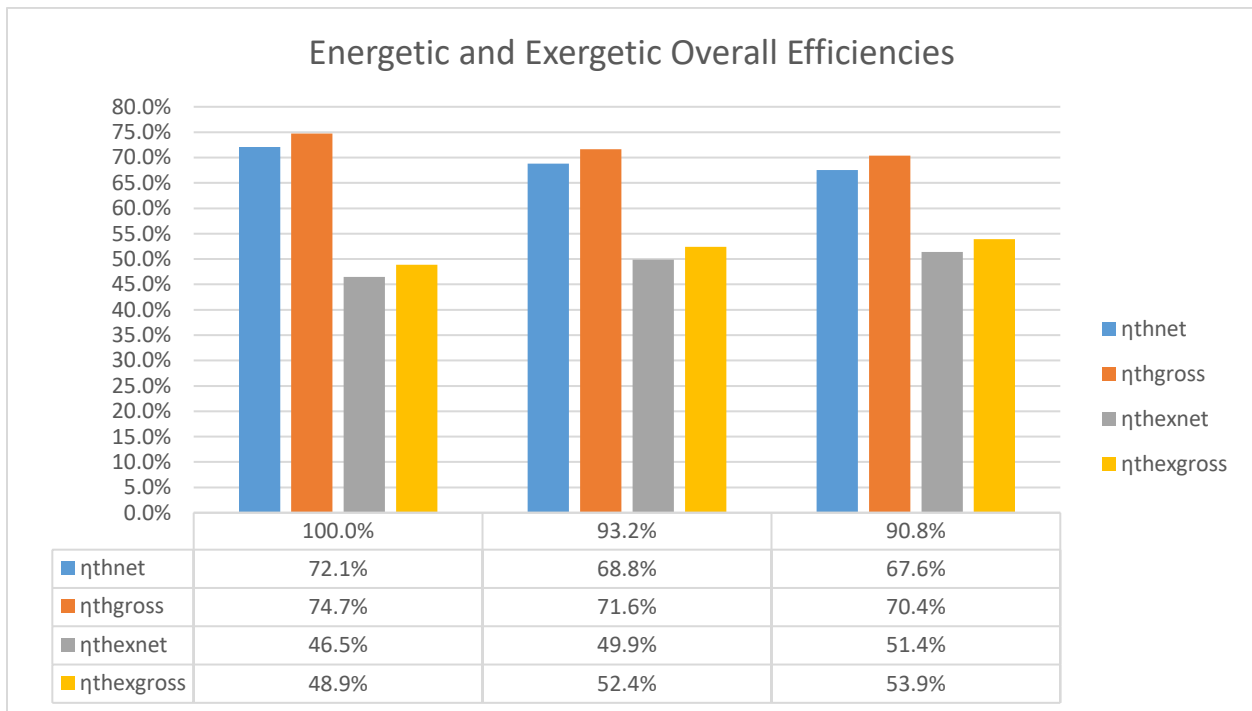


Figure 104: Energetic and Exergetic Overall efficiencies for the full and part load operation of the torrefied Spruce

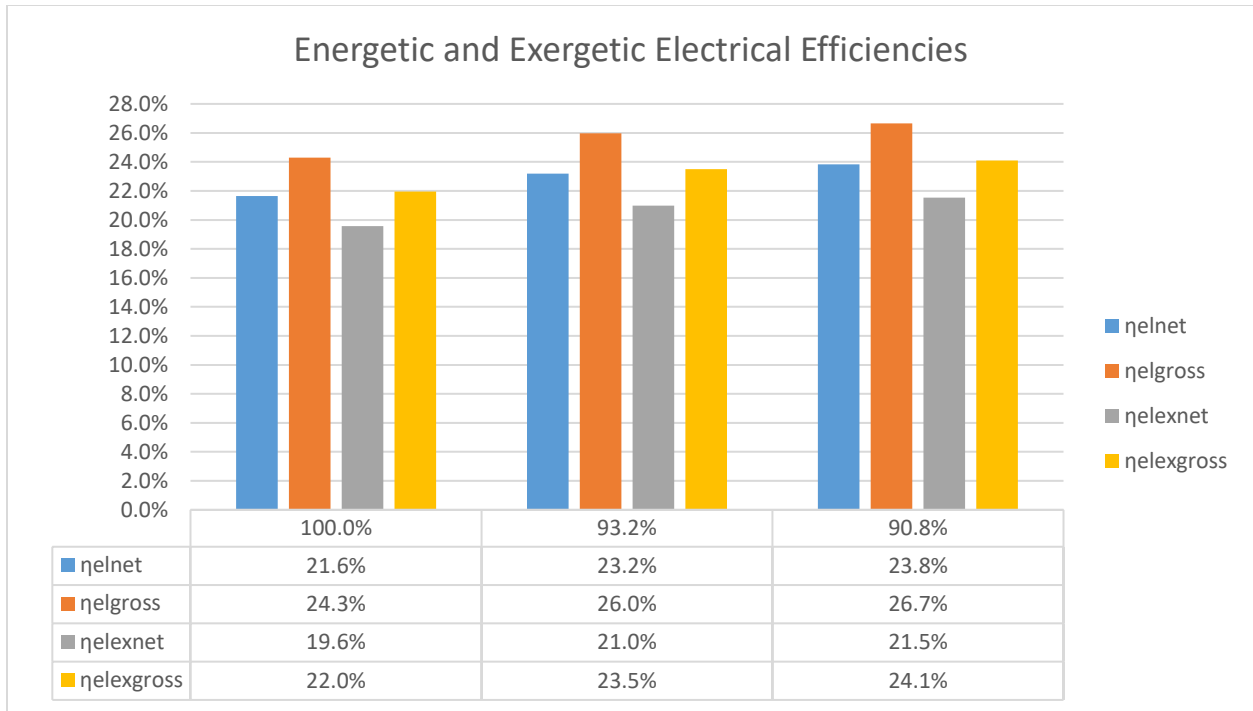


Figure 105: Energetic and Exergetic Electrical efficiencies for the full and part load operation of the torrefied Spruce

As the figures 104 and 105 present, the efficiencies of the improved CHP model, running at 220 bar and 600 °C, are quite satisfying and they follow the same trend as the first reference models presented in chapter 3.3. Since the electrical power output is kept constant throughout the part load operations, the part load refers to part load thermal operation. So it is only logical that the electrical energetic and exergetic efficiencies increase as the load decreases. The highest overall energetic efficiency stands at full load at 72.1% which is only natural since the plant is designed to operate at that capacity.

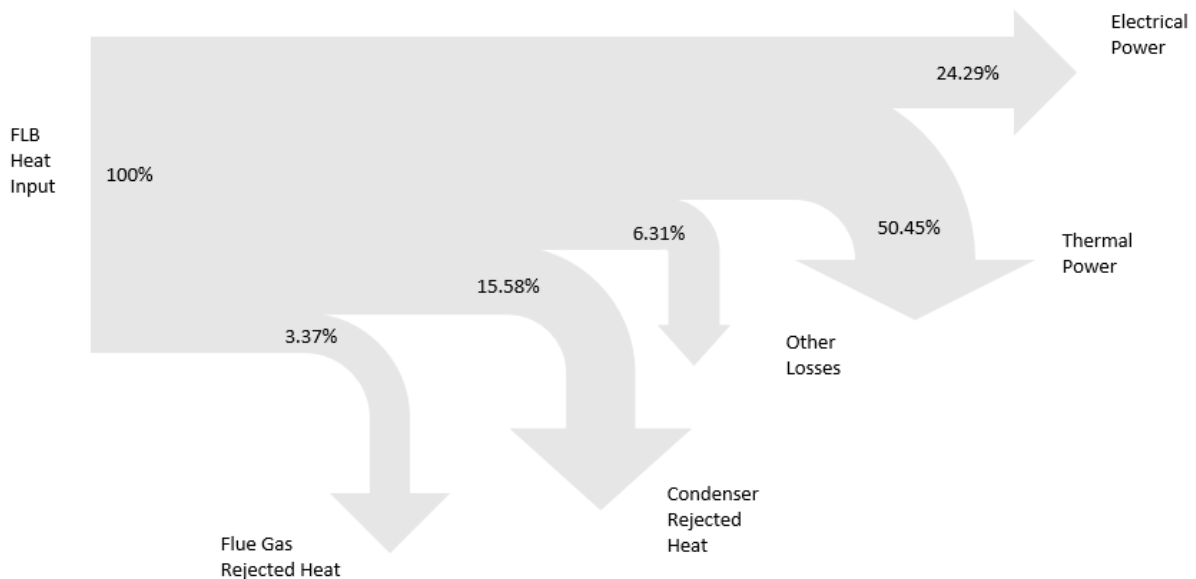


Figure 106: Biomass CHP Power Plant Sankey Diagram for the Torrefied Spruce simulation

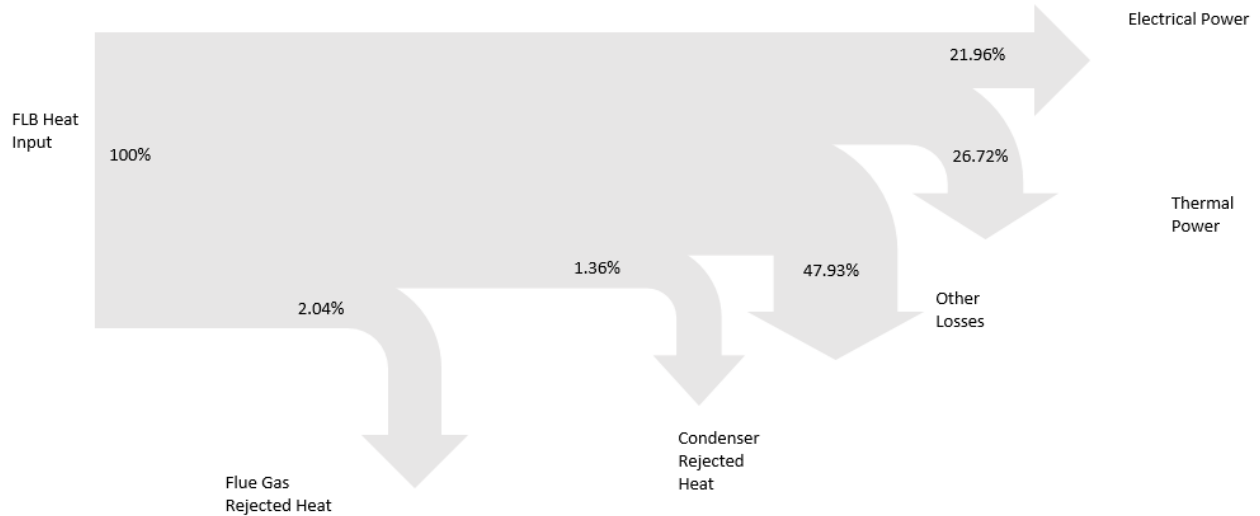


Figure 107: Biomass CHP Power Plant Grassmann Diagram for the Raw EFB simulation

Besides those two part load scenarios, one more was tested, in which the heat load of the high pressure steam was kept constant, meaning that the mass flow of the high pressure process steam (68 bar and 480 °C) and the mass flow needed for the heat transferred through Heat Exchanger 1 (down and left as shown in figure 80) are kept constant.

The current CHP model operates with a minimum of 615 tn/hr of water mass flow, and the high pressure heat load requires 304.51 tn/hr. So for each scenario, a percentage of the high pressure mass flow is added to the overall mass flow. For example, the first scenario starts with an excess of 10%, so the total mass flow will now be: $615 + 0.1 \cdot 304.51 = 645.45$ tn/hr and so on. The purpose of this simulation was to show how do the electrical, thermal and overall efficiencies alter when a part of the heat load is kept constant and the electrical output is increased.

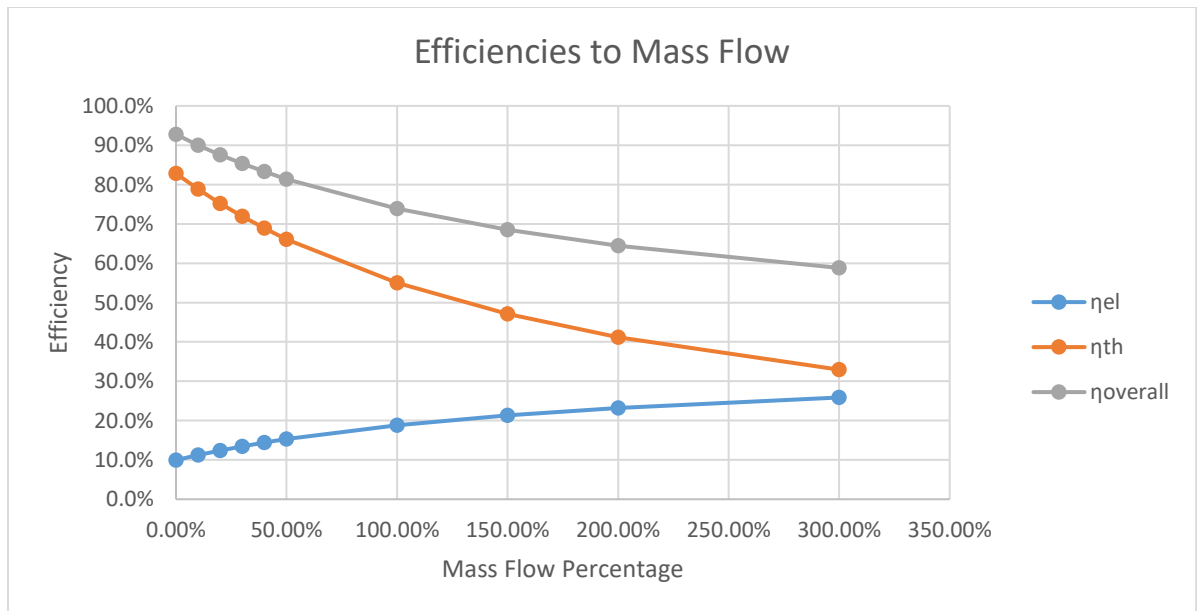


Figure 108: Electrical, Thermal and Overall efficiencies depending to the mass flow

As shown in figure 108 the electrical efficiency increases as the electrical power output increases, while the thermal efficiency decreases since the heat load remains constant. The most interesting thing noted from these simulations is that the increase of the electrical efficiency is lower than the decrease of the thermal efficiency, which leads the overall efficiency to drop at a lower rate than the thermal efficiency. The reason, the electrical efficiency increases with a lower rate than the rate the thermal efficiency drops, is that, due to the Carnot Rule, in order to generate work one must reject heat to the environment, so a large part of the heat offered to the cycle is not used. So, as the mass flow increases indefinitely the overall efficiency will become equal to the electrical efficiency.

Cooling Power Output:

Lastly, as shown in figures 58 and 80, one heat exchanger is used in order to utilize the flue gases' heat for the production of cooling power. The produced cooling power is conducted by two different cooling devices for the four biomass fuels. An Ejector Compression Cycle (ECC) is used for the production of the cooling power from the torrefied fuels, since there is no need for another heat exchanger in the plant, which dries the fuels. So the temperature entering the cooling device is higher. While the torrefied fuels feed an ECC, the dried fuels feed an absorption chiller, since before the cooling heat exchanger, there is one that dries the fuels, so the inlet temperature of the fuels gases is lower in this case study, one with which the absorption chiller can operate with. The COP of these two devices are shown below, followed by the tables presenting the cooling power they offer. In addition, it is noted that the cooling medium has an outlet temperature of 10 °C.

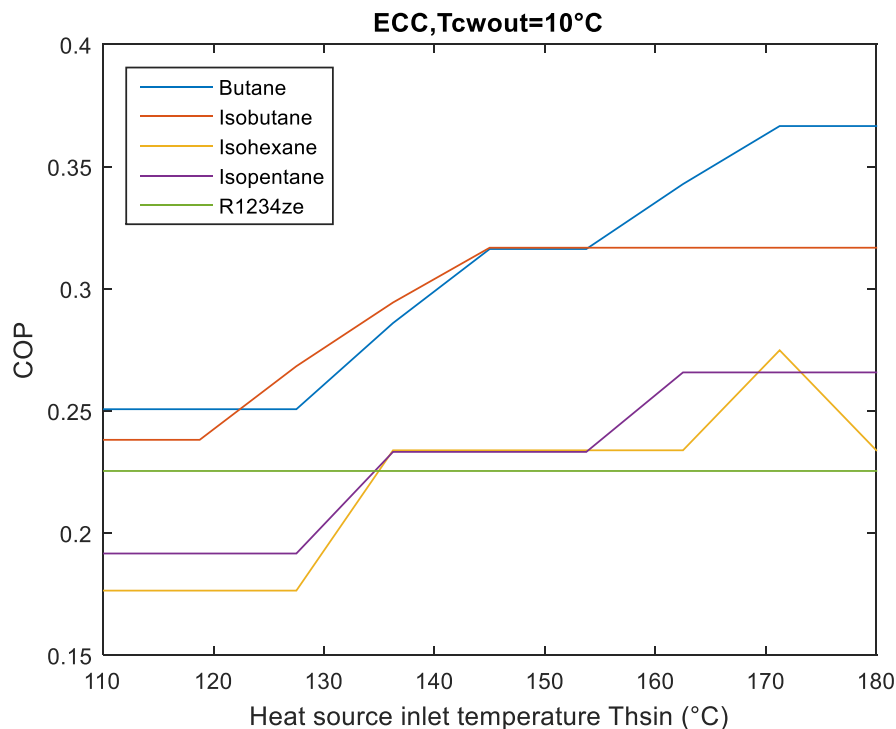


Figure 109: Variation of the COP of the ECC system with the heat source inlet temperature for chilled water outlet temperature of 10 °C[54]

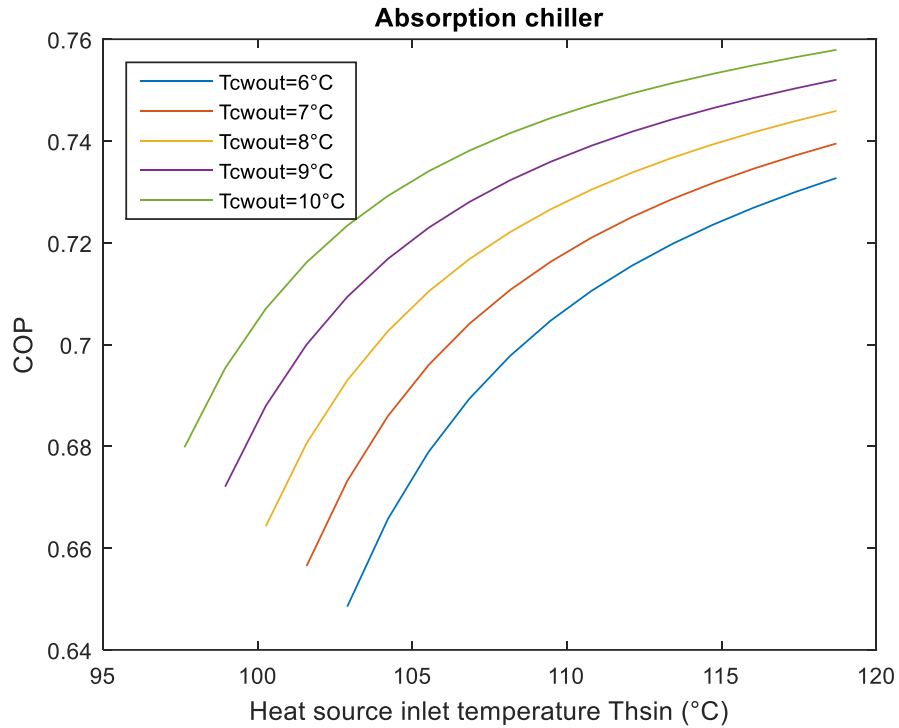


Figure 110: COP variation with the hot water inlet and chilled water outlet temperatures for the absorption chiller[54]

Table 55: Cooling Power Output for the Dry Spruce with COP = 0.763

	160 bar 540 C	180 bar 540 C	200 bar 540 C	220 bar 540 C	230 bar 540 C	
T_{in}	128.4	128.9	128.4	128.6	127.8	C
Q_{in}	29.9	29.9	29.4	29.3	28.1	MW
Q_{out}	22.8	22.8	22.4	22.4	21.4	MW
	160 bar 560 C	180 bar 560 C	200 bar 560 C	220 bar 560 C		
T_{in}	128.9	128.5	128.4	128.5		C
Q_{in}	30.2	29.6	29.2	29.1		MW
Q_{out}	23.0	22.5	22.3	22.2		MW
	160 bar 580 C	180 bar 580 C	200 bar 580 C	220 bar 580 C		
T_{in}	128.6	128.3	128.4	128.2		C
Q_{in}	29.8	29.2	29.0	28.7		MW
Q_{out}	22.7	22.3	22.2	21.9		MW
	160 bar 600 C	180 bar 600 C	200 bar 600 C	220 bar 600 C		
T_{in}	128.4	128.8	128.3	127.8		C
Q_{in}	29.5	29.5	28.8	28.1		MW
Q_{out}	22.5	22.5	22.0	21.4		MW

Table 56: Cooling Power Output for the Dry EFBs with COP = 0.763

	160 bar 540 C	180 bar 540 C	200 bar 540 C	220 bar 540 C	230 bar 540 C	
Tin	128.4	128.9	128.4	128.6	127.8	C
Qin	29.9	29.9	29.4	29.3	28.1	MW
Qout	22.8	22.8	22.4	22.4	21.4	MW
	160 bar 560 C	180 bar 560 C	200 bar 560 C	220 bar 560 C		
Tin	128.9	128.5	128.4	128.5		C
Qin	30.2	29.6	29.2	29.1		MW
Qout	23.0	22.5	22.3	22.2		MW
	160 bar 580 C	180 bar 580 C	200 bar 580 C	220 bar 580 C		
Tin	128.6	128.3	128.4	128.2		C
Qin	29.8	29.2	29.0	28.7		MW
Qout	22.7	22.3	22.2	21.9		MW
	160 bar 600 C	180 bar 600 C	200 bar 600 C	220 bar 600 C		
Tin	128.4	128.8	128.3	127.8		C
Qin	29.5	29.5	28.8	28.1		MW
Qout	22.5	22.5	22.0	21.4		MW

Table 57: Cooling Power Output for the Torrefied Spruce with COP = 0.3168

	160 bar 540 C	180 bar 540 C	200 bar 540 C	220 bar 540 C	230 bar 540 C	
Tin	146.9	147.2	148.9	159.2	149.2	C
Qin	30.5	30.3	31.0	36.4	30.2	MW
Qout	9.7	9.6	9.8	11.5	9.6	MW
	160 bar 560 C	180 bar 560 C	200 bar 560 C	220 bar 560 C		
Tin	146.1	148.4	149.0	150.8		C
Qin	29.9	30.8	30.8	31.6		MW
Qout	9.5	9.8	9.8	10.0		MW
	160 bar 580 C	180 bar 580 C	200 bar 580 C	220 bar 580 C		
Tin	148.6	146.2	148.9	145.9		C
Qin	31.1	29.4	30.6	28.8		MW
Qout	9.9	9.3	9.7	9.1		MW
	160 bar 600 C	180 bar 600 C	200 bar 600 C	220 bar 600 C		
Tin	147.6	145.6	148.6	144.6		C
Qin	30.4	29.0	30.3	27.9		MW
Qout	9.6	9.2	9.6	8.8		MW

Table 58: Cooling Power Output for the Torrefied EFBs with COP = 0.3168

	160 bar 540 C	180 bar 540 C	200 bar 540 C	220 bar 540 C	230 bar 540 C	
T_{in}	145.8	147.8	147.4	148.2	144.57	C
Q_{in}	28.9	29.6	29.1	29.4	26.8	MW
Q_{out}	9.1	9.4	9.2	9.3	8.5	MW
	160 bar 560 C	180 bar 560 C	200 bar 560 C	220 bar 560 C		
T_{in}	148.5	147.5	144.9	147.4		C
Q_{in}	30.2	29.3	27.7	28.8		MW
Q_{out}	9.6	9.3	8.8	9.1		MW
	160 bar 580 C	180 bar 580 C	200 bar 580 C	220 bar 580 C		
T_{in}	147.6	150.4	147.5	146.4		C
Q_{in}	29.6	30.7	28.9	28.1		MW
Q_{out}	9.4	9.7	9.1	8.9		MW
	160 bar 600 C	180 bar 600 C	200 bar 600 C	220 bar 600 C		
T_{in}	146.7	153.3	147.4	147.1		C
Q_{in}	29.0	32.1	28.6	28.3		MW
Q_{out}	9.2	10.2	9.1	9.0		MW

As shown in the figures and tables above, the ECC has a lower COP than the absorption chiller, but it can operate with higher inlet temperatures of heat sources. It is noted that the flue gas temperature exiting the power plant models with the dried fuels is 85 °C, while the flue gas temperature exiting the power plant models with the torrefied fuels is 90 °C. So even though the heat offered by the flue gases is almost identical in all of the fuel scenarios, the cooling capacity of the torrefied fuels power plant is significantly lower.

5. Conclusions and Further Research

In this thesis, the importance of biomass as a renewable fuel was presented, together with processes which promote the use of biomass fuels in Combined Heat and Power plants, as well as the upgrade, in terms of chemical and thermodynamic properties, these processes offer.

At first, a modification was made to the existing Combined Cycle near the Aluminum plant in Aspra Spitia, Viotia, Greece. Instead of having a Rankine cycle receiving heat from gas turbine exhaust gases, this modification implements a fluidized bed boiler, fueled with biomass. Four different biomass fuels were used in the full and part load simulations of the modified CHP plant. These fuels are raw Spruce wood, raw Empty Fruit Bunches, wet Torrefied Spruce Wood and dry Torrefied Empty Fruit Bunches.

The simulations of all the different case studies were conducted by commercial software named GateCycle, which is developed by General Electric. GateCycle simulates steady state operations. The results of the modified Combined Cycle power plant, indicated that the Combined Heat and Power plant can operate in satisfying overall and electrical efficiencies, meaning that biomass could be used for a base load plant fuel. The overall efficiencies of the pretreated fuels stand higher, close to 70%, than those of the raw fuels, which stand somewhere near 65%. So the pretreated fuels undoubtedly are better fuels, something also shown by their chemical composition and LHV. Their superiority is shown as well by the exergetic efficiencies, whose value is correlated with the chemical exergy of the fuel, which in turn depends on the chemical composition.

After the modifications, an improved model was created, having the same configuration with an addition of one more high pressure turbine stage. In this modified Combined Heat and Power plant, high pressure and temperatures are simulated. These pressures commence at 160 bar, up to 220 bar with a step of 20 bar, while the temperatures amount from 540 °C to 600 °C with a step of 20 °C. As an addition, one more simulation was performed for the four case studies at 230 bar and 600 °C, namely operation in supercritical conditions. The simulations of these four case studies indicated the impact of the temperature is smaller compared to the impact the pressure rise inflicts. For each 20 bar of increase, the increase in all of the efficiencies is way more significant than the rise of 20 °C.

Lastly, one more thing to note is the impact supercritical conditions of steam incur. On the simulation charts, one can observe the rate of increase diminishes as the pressure or the temperature rises, but remaining in subcritical conditions, but once the plant operates on supercritical conditions, the rate increases, meaning that supercritical conditions should be examined thoroughly because, as other sources and papers suggest, they provide much higher energetic and exergetic efficiencies.

As far as the further research is concerned in this thesis, a possible research would be the simulation of strictly supercritical cycles and several configurations of cycles. Those simulations shouldn't only focus on steady state operations, but rather in dynamic conditions, such as start up operations or fluctuations in load.

1. Fagnäs, L., et al., *Bioenergy in Europe*. Opportunities and Barriers. VTT Tierdotteita Research Notes, 2006. **2352**.
2. Commission, E., *EU Energy in figures 2016*. 2016.
3. IEA, August 2016.
4. Agency, E.E. *Renewable Energy in Europe 2016* Recent growth and knock-off effects, 2016.
5. AEBIOM, *AEBIOM STATISTICAL REPORT 2016*. 2016.
6. reports), E.b.o.d.f.E.a.N.
7. Fortum *More sustainable, less subsidised Biomass*. 2016.
8. UNFCCC, *Clarifications of definition of biomass and consideration of changes in carbon pools due to a CDM project activity*. 2005.
9. Koppejan, J. and S. Van Loo, *The handbook of biomass combustion and co-firing*. 2012: Routledge.
10. Κακαράς, E. and Σ. Καρέλλας, *Αποκεντρωμένα Θερμικά Συστήματα*. 2015: Εκδόσεις Τσιότρας.
11. Koçar, G. and N. Civaş, *An overview of biofuels from energy crops: Current status and future prospects*. Renewable and Sustainable Energy Reviews, 2013. **28**: p. 900-916.
12. Fillaudeau, L., P. Blanpain-Avet, and G. Daufin, *Water, wastewater and waste management in brewing industries*. Journal of cleaner production, 2006. **14**(5): p. 463-471.
13. Aliyu, S. and M. Bala, *Brewer's spent grain: a review of its potentials and applications*. African Journal of Biotechnology, 2011. **10**(3): p. 324-331.
14. Himmel, M., *Biomass Recalcitrance: Deconstructing the Plant Cell Wall for Bioenergy*. 2008.
15. Ezeonu, F. and A. Okaka, *Process kinetics and digestion efficiency of anaerobic batch fermentation of brewer's spent grains (BSG)*. Process Biochemistry, 1996. **31**(1): p. 7-12.
16. Mussatto, S.I. and J. Teixeira, *Lignocellulose as raw material in fermentation processes*. Current Research, Technology and Education Topics in Applied Microbiology and Microbial Biotechnology (Méndez-Vilas, A., Ed.), 2010. **2**: p. 897-907.
17. Čater, M., et al., *Biogas production from brewery spent grain enhanced by bioaugmentation with hydrolytic anaerobic bacteria*. Bioresource technology, 2015. **186**: p. 261-269.
18. Huang, Y., et al., *Biofuel pellets made at low moisture content—Influence of water in the binding mechanism of densified biomass*. Biomass and Bioenergy, 2017. **98**: p. 8-14.
19. Lehtikangas, P., *Quality properties of pelletised sawdust, logging residues and bark*. Biomass and bioenergy, 2001. **20**(5): p. 351-360.
20. Zhou, H., et al., *Formation and reduction of nitric oxide in fixed-bed combustion of straw*. Fuel, 2006. **85**(5): p. 705-716.
21. Jyske, T., et al., *Yield of stilbene glucosides from the bark of young and old Norway spruce stems*. Biomass and Bioenergy, 2014. **71**: p. 216-227.
22. Chong, J., A. Poutaraud, and P. Huguene, *Metabolism and roles of stilbenes in plants*. Plant Science, 2009. **177**(3): p. 143-155.
23. Chang, S.H., *An overview of empty fruit bunch from oil palm as feedstock for bio-oil production*. Biomass and Bioenergy, 2014. **62**: p. 174-181.
24. Sulaiman, F., et al., *A perspective of oil palm and its wastes*. J Phys Sci, 2010. **21**(1): p. 67-77.
25. Kerdsuwan, S. and K. Laohalidanond, *Renewable energy from palm oil empty fruit bunch*. 2011: INTECH Open Access Publisher.
26. Jacobson, K., K.C. Maheria, and A.K. Dalai, *Bio-oil valorization: a review*. Renewable and Sustainable Energy Reviews, 2013. **23**: p. 91-106.
27. Sreekala, M., M. Kumaran, and S. Thomas, *Oil palm fibers: Morphology, chemical composition, surface modification, and mechanical properties*. Journal of Applied Polymer Science, 1997. **66**(5): p. 821-835.

28. ; Available from: https://gettotalplant.com/GateCycle/docs/assets/pdf/GateCycle%20fact_sheet%20GEA-14291C.pdf.
29. Barten, T.J., *Evaluation and prediction of corn stover biomass and composition from commercially available corn hybrids*. 2013.
30. Shinnors, K.J. and B.N. Binversie, *Fractional yield and moisture of corn stover biomass produced in the Northern US Corn Belt*. Biomass and Bioenergy, 2007. **31**(8): p. 576-584.
31. Turhollow, A., et al., *The updated billion-ton resource assessment*. biomass and bioenergy, 2014. **70**: p. 149-164.
32. Carriquiry, M.A., X. Du, and G.R. Timilsina, *Second generation biofuels: Economics and policies*. Energy Policy, 2011. **39**(7): p. 4222-4234.
33. Golecha, R. and J. Gan, *Effects of corn stover year-to-year supply variability and market structure on biomass utilization and cost*. Renewable and Sustainable Energy Reviews, 2016. **57**: p. 34-44.
34. Bauen, A., et al., *Bioenergy: a sustainable and reliable energy source. A review of status and prospects*. Bioenergy: a sustainable and reliable energy source. A review of status and prospects., 2009.
35. McKendry, P., *Energy production from biomass (part 1): overview of biomass*. Bioresource technology, 2002. **83**(1): p. 37-46.
36. Searcy, E., et al., *The relative cost of biomass energy transport*. Applied biochemistry and biotechnology, 2007: p. 639-652.
37. Kostas, E.T., D. Beneroso, and J.P. Robinson, *The application of microwave heating in bioenergy: A review on the microwave pre-treatment and upgrading technologies for biomass*. Renewable and Sustainable Energy Reviews, 2017. **77**: p. 12-27.
38. Agbor, V.B., et al., *Biomass pretreatment: fundamentals toward application*. Biotechnology advances, 2011. **29**(6): p. 675-685.
39. Alvira, P., et al., *Pretreatment technologies for an efficient bioethanol production process based on enzymatic hydrolysis: a review*. Bioresource technology, 2010. **101**(13): p. 4851-4861.
40. Alfani, F., et al., *Comparison of SHF and SSF processes for the bioconversion of steam-exploded wheat straw*. Journal of Industrial Microbiology & Biotechnology, 2000. **25**(4): p. 184-192.
41. Mosier, N., et al., *Features of promising technologies for pretreatment of lignocellulosic biomass*. Bioresource technology, 2005. **96**(6): p. 673-686.
42. Ciolkosz, D. and R. Wallace, *A review of torrefaction for bioenergy feedstock production*. Biofuels, Bioproducts and Biorefining, 2011. **5**(3): p. 317-329.
43. Paoluccio, J.A., *Method and apparatus for biomass torrefaction, manufacturing a storable fuel from biomass and producing offsets for the combustion products of fossil fuels and a combustible article of manufacture*. 2011, Google Patents.
44. Bergman, P.C. and J.H. Kiel. *Torrefaction for biomass upgrading*. in *Proc. 14th European Biomass Conference, Paris, France*. 2005.
45. Reza, M.T., *Hydrothermal carbonization of lignocellulosic biomass*. 2011, University of Nevada, Reno.
46. Xiao, L.-P., et al., *Hydrothermal carbonization of lignocellulosic biomass*. Bioresource Technology, 2012. **118**: p. 619-623.
47. Libra, J.A., et al., *Hydrothermal carbonization of biomass residuals: a comparative review of the chemistry, processes and applications of wet and dry pyrolysis*. Biofuels, 2011. **2**(1): p. 71-106.
48. Bach, Q.-V. and Ø. Skreiberg, *Upgrading biomass fuels via wet torrefaction: A review and comparison with dry torrefaction*. Renewable and Sustainable Energy Reviews, 2016. **54**: p. 665-677.

49. Skorek-Osikowska, A., et al., *The influence of the size of the CHP (combined heat and power) system integrated with a biomass fueled gas generator and piston engine on the thermodynamic and economic effectiveness of electricity and heat generation*. Energy, 2014. **67**: p. 328-340.
50. Miller, B.G., *Clean coal engineering technology*. 2010: Elsevier.
51. Yang, Y., et al., *Comprehensive exergy-based evaluation and parametric study of a coal-fired ultra-supercritical power plant*. Applied energy, 2013. **112**: p. 1087-1099.
52. Suojanen, S., *Development of concentrated solar power and conventional power plant hybrids*. 2016.
53. Kuronen, J., *Improving transient simulation of pulverized coal-fired power plants in dynamic simulation software*. 2016.
54. Tziritas, D., *Energetic, exergetic and techno-economic comparison of thermal cooling technologies powered by waste heat*. 2017.